# ST. ANTHONY FALLS LABORATORY

Engineering, Environmental and Geophysical Fluid Dynamics

**SAFL Project Report No. 600**

# *A Field Study of Maximum Wave Height, Total Wave Energy, and Maximum Wave Power Produced by Four Recreational Boats on a Freshwater Lake*

By:

Jeffrey Marr[1], Andrew Riesgraf[1], William Herb[1], Matthew Lueker[1], Jessica Kozarek[1], Kimberly Hill[1, 2]

[1] St. Anthony Falls Laboratory, University of Minnesota, 2 Third Ave SE, Minneapolis, MN 55414

[2] Department of Civil, Environmental, and Geo- Engineering, 500 Pillsbury Drive S.E., Minneapolis, MN 55455-0116

Prepared for:

St. Anthony Falls Laboratory, Healthy Waters Initiative

**February 2022**

**Minneapolis, Minnesota**

(This page intentionally left blank)

## ACKNOWLEDGEMENTS

The research reported here was fully supported through contributions made to SAFL's Healthy Waters Initiative. We are grateful for the trust these donors placed in the University of Minnesota to carry out independent research on boat-generated waves. To ensure our ability to perform independent research, donors had no input in the design, data collection, or analysis of this research.

The authors would like to thank Three Rivers Park District for allowing us the use of facilities at Baker Park Reserve as home base for this study. We thank the McLaughlin family for providing access to their shoreline, dock, lifts, and property on Lake Independence during the study. We thank the individual boat owners for their generosity in providing the test boats, as well as their time and effort in planning and preparing the boats. We thank the Christmas Lake Homeowners Association for the use of their work pontoon for the duration of the field study. We are grateful to Dr. Omid Mohseni of Barr Engineering Company for officiating the independent technical review process and two external reviewers, Dr. Gregory Cox and Dr. Gregor MacFarlane, who provided thorough and constructive comments that greatly improved this report.

(This page intentionally left blank)

# TABLE OF CONTENTS

(Page intentionally left blank)

# EXECUTIVE SUMMARY

The lakes in Minnesota are considered among the state's most valuable natural resources and are utilized by many visitors and citizens throughout the year. The protection and preservation of surface water resources, lake and shoreline ecosystems, and lakeshore property are shared goals for many in Minnesota. Recreational boating is a highly popular activity and includes motorized and non-motorized watercraft. In recent years, with the growth of recreational activities including the emergence of the sport of wakesurfing, there has been growing concern over the impacts of boat-generated waves and propeller wash on these natural resources. The research reported here was motivated by a need to better understand the characteristics of wakes and waves produced by recreational boats common on lakes and rivers, in particular, in the state of Minnesota.

In the summer of 2020, the University of Minnesota (UMN) launched a program titled "Healthy Waters Initiative" through the St. Anthony Falls Laboratory, an interdisciplinary research laboratory associated with the College of Science and Engineering. The mission of the initiative is to establish multi-year research efforts focusing on issues that have the potential to adversely affect Minnesota lakes and rivers. The Initiative is an independent research program focused on producing targeted, unbiased, peer-reviewed publications of data and research findings.

The initial research performed under the Healthy Waters Initiative was focused on the characterization of boat-generated waves. Funded by a crowdfunding campaign launched in the summer of 2020, the program carried out a six-week, field-based research study examining the wake characteristics of four boats. This report is the first product of the Healthy Waters Initiative.

The field component of the research was conducted in September and October 2020 on Lake Independence, Maple Plain, MN. A study site was selected on the north-eastern shoreline of the lake that provided ideal conditions for a field study of this magnitude. The lake depth increased gradually with distance from shore and was easily accessible from the lake's boat launch. Five, fixed-sensor positions were established at the site to measure wave height – two of these sensors

were submerged Acoustic Doppler Current Profilers attached to pads that rested on the bottom of the lake and three were submerged pressure sensors fixed to masts.

Four boats were evaluated. Two of the boats were typical recreational boats (i.e., non-wakesurf) that are commonly operated (e.g., tubing, waterskiing, wakeboarding) on Minnesota lakes and the two additional boats were wakesurf boats designed specifically for the sport of wakesurfing.

Testing involved operating each boat at four distances from the shoreline (225 ft, 325 ft, 425 ft, and 625 ft) under various conditions (e.g., speed, ballast weight, trim setting, etc.). Test boats were selected based on their size, operational characteristics, typical usage, and availability, and were evaluated under three operating conditions - Condition 1a, Condition 1b, and Condition 2. Conditions 1a and 1b included boat speeds of 10-11 mph and boat configurations that yielded either the largest wake wave possible or settings that are typically used for wakesurfing. Condition 2 included speeds of 20 mph and configurations that resulted in the boat planing on the water surface. Each condition and distance were repeated four times and average wake wave characteristics (i.e., maximum wave height, total wave energy, and maximum wave power) were computed.

An on-board Inertial Navigation System (INS) with an integrated Global Navigation Satellite System (GNSS) was mounted to each test boat and recorded boat attitude (i.e., roll, pitch, and yaw), location, and speed during each pass. The boat positions and mast/pad locations were analyzed to determine the precise location of boat passes and their associated operational distances.

Maximum wave height and maximum wave power within each wake wave packet and the total wave energy content within the packet were calculated for each sensor location and for each boat pass. The wake wave packet is defined as the series of individual waves produced by a single boat pass. These wake wave characteristics were computed for each boat condition at each of the four distances from shoreline. The data from the sensors at each mast/pad location were aggregated and evaluated. The results from this research provide new information on the characteristics of boat-generated waves and reveal interesting and potentially important differences between non-wakesurf and wakesurf boats. The key findings are summarized here:

- The two Malibu Wakesetter (wakesurfing) boats produced the largest waves under all the conditions studied- Condition 1a (largest wave/surfing) and Condition 2 (planing). The longer and heavier of the wakesurf boats, the Malibu Wakesetter MXZ, produced the highest waves with the greatest total wave energy and maximum wave power.
- The smallest maximum wave heights, lowest total wave packet energies and lowest wave powers occurred when boats were planing on the water surface (Condition 2). This was true for all four test boats.
- For an individual boat, the difference in maximum wave height, total wave energy, and maximum wave power between Condition 1a (largest wave/surfing) and Condition 2 (planing) was largest for the wakesurf boats. The Larson LXI 210 and the Malibu Response LX also showed increases in these wave characteristics, however, the magnitude of the changes was smaller for these boats. This is attributable to the large and energetic waves produced by the wakesurf boats under Condition 1a, which is the primary design feature of these boats.
- The decrease (attenuation) in maximum wave height, total wave energy, and maximum wave power over distance was well-characterized by the data and indicate longer operational distances (e.g., distances from shore, other boats, etc.) are required for larger and more energetic wakes to reach the same heights, energies, and powers of smaller wakes.
- Operating with full ballast tanks (Condition 1a) versus empty ballast tanks (Condition 1b) had little impact on maximum wave height, total wave energy, and maximum wave power for the two Malibu Wakesetter boats at operational distances greater than 100 ft.
- The aftermarket wake shaper attached to the Malibu Response LX had a measurable impact on the wave characteristics, resulting in increased maximum wave height, total wave energy, and maximum wave power. This suggests aftermarket products installed on non-wakesurfing boats can create wake waves similar to wakesurfing boats.
- Based on the data and our example method for determining recommended operational distance, we show that when operating under typical wakesurfing conditions, wakesurf boats required distances greater than 500 ft to attenuate wake wave characteristics

(height, energy, and power) to levels equivalent to non-wakesurf boats operating under typical planing conditions. A second example, in which the largest wave was used as reference for the non-wakesurf boats (Condition 1a), an operational distance of 425 ft or greater was required. These results are summarized in the table below.

**Results for required operational distance illustrating how data from this study may be used**

| Reference condition | Operational distance required by wakesurf boat to attenuate to reference condition levels |
|---|---|
| Example 1<br>non-wakesurf boat planing at an operational distance of 200 ft (Condition 2 - planing) | Maximum Wave Height: >500 ft.<br>Total Wave Energy: >575 ft.<br>Maximum Wave Power: >600 ft. |
| Example 2<br>non-wakesurf boat transition to planing at an operational distance of 200 ft (Condition 1a - largest wave) | Maximum Wave Height: >425 ft.<br>Total Wave Energy: >425 ft.<br>Maximum Wave Power: >425 ft. |

In addition to these conclusions, this document offers a summary of research priorities pertaining to the topic of boat-generated waves on lakes and rivers.

## INDEPENDENT TECHNICAL REVIEW PROCESS

This report has undergone an independent technical review by subject matter experts not affiliated with the University of Minnesota. The review was facilitated by Dr. Omid Mohseni of Barr Engineering Company, Minneapolis, Minnesota. Two independent experts with backgrounds in naval architecture and vessel wake waves reviewed this work and provided detailed feedback to the review facilitator and authors. The reviewers were Dr. Gregory Cox and Dr. Gregor MacFarlane.

The authors addressed all comments provided by the reviewers and incorporated recommended changes into the final version presented here. UMN responses were shared with the review facilitator who concurred that the updated final report has sufficiently considered and incorporated feedback from the reviewers. UMN responses have also been shared with the reviewers. A draft of this report was submitted for external review on September 29, 2021 and the final version was produced and published through the University of Minnesota's Digital Conservancy on February 1, 2022.

(This page intentionally left blank)

## TERMINOLOGY

**Acoustic Doppler Current Profiler (ADCP)** – sensor system that uses pulsed, high-frequency sound to measure the velocity field in the water column and vertical position of the water surface.

**Boat Wake** – surface water waves produced by a boat as it travels on the water surface.

**Crest** – highest water surface elevation of a single wave.

**Dispersion** – spreading out or lengthening of the wake wave packet with increasing distance from the source (boat).

**Mast** – rigid structure used to deploy submerged pressure sensors during testing. Above the water surface, the masts held a datalogger, 12v battery, charge controller, solar panel system, GPS receiver, and wind speed and direction sensors.

**Operating Condition** – set of boat parameters selected and used within a test. The parameters included: speed, trim setting, ballast setting, hydrofoil setting, wake shaper setting, and number of people aboard.

**Operational Distance** – distance maintained between the boat and another watercraft, shoreline, dock, lift, raft, or person(s)/animal(s) in the water. For this study, operational distance is the perpendicular distance measured from the boat track line to the object/sensor.

**Pad** – Acoustic Doppler Current Profiler (ADCP) deployment structure, which sat on the bottom of the lake during testing.

**Pass** – single instance of a test boat driven along a track line (e.g., 225 ft from shore) under one of the operating conditions.

**Trough** – lowest water surface elevation of a single wave.

**Track Line** – line marked by two buoys that ran parallel to the shoreline and perpendicular to the masts/pads. There were four track lines distanced at 225 ft, 325 ft, 425 ft, and 625 ft from shore, that the test boat followed while making a single pass.

**Trim** – angle of the boat in relation to the water surface measured in the direction of travel.

**Wake Wave Packet** – series of individual waves generated by a single boat pass. The group of waves within the packet moves outward from the boat track line.

**Wave attenuation** – decrease in wave height, energy, and power as the operational distance increases from the boat track line.

**Wave Energy** – a quantifiable attribute of a single wave or series of waves that represents the ability of the wave(s) to do work or make change. In physics, work is often quantified as force applied over a distance.

**Wave Height** – vertical distance measured from trough to crest of a wave.

**Wave Power** – the rate at which energy is transferred or used. For wake waves, it is the rate at which energy is transferred away from the track line.

## 1.0 INTRODUCTION

The state of Minnesota, located in the north central United States, is recognized for having the largest number of natural, inland freshwater lakes and pristine river systems of any state in the lower 48 states of the US (MNDNR 2021). It follows that access, usage, and management of surface waters are highly important subjects within the state. This report is motivated by a need for science-based information on the impacts of motorized recreational boats on surface water resources.

Motorized recreational boats (referred to hereafter as boats) are prevalent on Minnesota waters. In all its forms, including cruising, tubing, waterskiing, wakeboarding, wakesurfing, fishing, or just anchoring to sunbathe and swim, recreational boating is enjoyed by young and old, state residents and visitors, individuals and groups, families, neighbors and friends. Boating and associated activities also represent measurable components of the state's economy.

Those tasked with managing the state's public surface waters face the difficult challenges of balancing public access, long-term protection and preservation of the resources, ensuring protection of property, and public safety. As the popularity of recreational boating continues to grow in Minnesota, so too does the size of boats and their motors. Moreover, new designs of watercraft, specifically, boats engineered to create large wakes for the primary purpose of wakesurfing, are elevating concerns around impacts to safety, lake and river health, shared-use accessibility, and degradation of property. Research to address these concerns is currently lacking or difficult for managers/practitioners to access and apply.

All boats generate wakes associated with the displacement of water by the boat hull. The wake and associated waves produced by a boat are complex hydrodynamic phenomena that have been the subject of research for over a century and have been examined from both fundamental and applied perspectives (see Section 2.0). In this report, we include a brief overview of the salient aspects of boat-generated waves, referred to hereafter as wake waves, however our main focus is on a more pragmatic investigation of common recreational boats operated under typical usage conditions.

(This page intentionally left blank)

## 2.0 BACKGROUND

Many books, research reports, theses, and journal papers have been published examining various aspects of boat-generated wake waves. This section provides a summary of the relevant literature on boat wake waves.

### 2.1 Fundamental research on surface waves, wave energy and power, coastal engineering, and marine architecture

Fundamental research on surface waves and wave attenuation extends back 150 years including fluid mechanics, analytical model development, field investigations, laboratory experiments, and numerical simulations (Lord Kelvin (Thomson) 1887; Stoker 1957; Lighthill 1978; Dingemans 1997; Madsen et al. 2006). This body of fundamental research and theory yields physics-based understanding and mathematical relationships that have enabled practical fields such as naval architecture and coastal and marine engineering. Development of linear wave theory, for example, elements of which are employed in this project, as well as more complex, non-linear wave theories and advanced numerical simulation of waves, continue to be expanded upon today by researchers across the world. In addition, technical guides for the management of coastal areas, such as the Shore Protection Manual (USACE 1984) and Coastal Engineering Manual (USACE 2012) provide useful information and practical equations for computing and modeling surface water waves and applying these to coastal and shoreline engineering problems.

Our study utilized two published doctoral theses in the design of the project (i.e., MacFarlane 2012 and Cox 2020). MacFarlane (2012) is a comprehensive document that provides important and clear summaries of the fundamental theories to the problem of vessel-generated wake waves and the impacts of waves on shoreline environments. This thesis provides insights, among other topics, into the treatment of wave height and practical methods for calculating total wave energy, as well as guidance on proper field deployment of sensors and post-processing methods to field data. Similarly, Cox (2020) offers a wealth of information relevant to this study, such as vessel characterizations, description of surface wave dynamics and classifications, and wave energy dispersion and attenuation.

## 2.2 Field studies on the impacts of boat-generated wake waves on water quality and shorelines

There are a significant number of published reports and journal articles examining the impacts of boat-generated wake waves on shorelines and near-shore environments. We focused on papers examining transportation vessels, like high-speed or conventional ferries, and on papers examining recreational watercraft. For research published prior to about 2014, wakesurf boats and the sport of wakesurfing were not specifically identified. Several reports and papers after 2014 focused on wakesurfing, which will be discussed in Section 2.3.

The University of New South Wales, Water Research Laboratory, developed a management support tool for boat wake impacts on shoreline zones using standardized field-based measurements of boat-generated wake waves and assessment of impacts on shorelines (Glamore 2008; Glamore and Badenhop 2013). The papers summarized field experience and detailed data collection conducted by the authors and outlined a standardized approach to conduct wake wave assessments including post processing of wave height measurements and calculation of wave energy. Glamore et al. (2013) extended the work to riverbank erosion as well.

We reviewed many field-based studies that focus on assessing boat wave impacts on specific lakes or water bodies. Many of these projects were motivated by anecdotal observations that: 1) boat activity appeared to be increasing, and 2) the increased activity was associated with shoreline erosion and reduction in water quality. A study commissioned by the Maryland Department of Natural Resources (Zabawa and Ostrom 1980) used measurements of wave height and wave energy density for wind-driven and boat-generated waves at five popular boating sites within the project area. The work was performed long before the invention of wakesurfing and wakesurfing watercraft; however, impacts from recreational boating were a concern. In this study, wind wave and storm events appeared to have larger impacts on shoreline erosion than boat wave impacts; however, erosion from boat waves was determined to be significant where wake waves were large and the boats consistently passed within 200 ft or less of the shorelines.

Gourlay (2010) is a similar site-specific field study on the boat waves produced by nine different watercrafts measured at three locations on the Swan River in Perth, Western Australia. The report detailed an approach to wave characterization that was largely adopted in our project. Details on the relationships for correcting attenuation in pressure measurements and computing wave energy in deep water and transitional depths were also provided.

Recent research on boat wake wave impacts within the Chesapeake Bay utilized surveys and existing data to analyze boat wake wave impacts (Bilkovic et al. 2017, 2019). While the research did not involve direct measurement of wave height or wave energy, the authors provided novel approaches to estimating boat activity and locating where impairment/mitigation of shoreline erosion was occurring. Long records of turbidity (a surrogate for suspended sediments) were used to correlate against weekend and holiday lake usage (high boater usage) and weekday usage (low boater usage). The research concluded that boat activity was linked to elevated turbidity and shoreline erosion and this was especially true in regions that were not armored or were not subject to long-fetch wind waves.

While our study focuses on wake waves from recreational boats, observations from studies on wake wave impacts from commercial ferries operating on large marine bays can provide context. Parnell et al. (2007) summarizes research of ferry wave impacts in New Zealand with propagation distances of over 7 km. The authors demonstrated linkages to geomorphic changes on regions they defined as “low wave energy shorelines” meaning shorelines that had not experienced large wind-driven waves and had not become self-armored. Self-armoring refers to a natural process where the waves, over time, mobilize and wash away clays, sands, and gravels up to a certain grainsize. Eventually, only larger grainsizes that are not easily eroded by the waves remain, which serve to protect or ‘armor’ the shoreline. Several papers examined the wave impacts in Tallin Bay, Estonia, which is located within the Gulf of Finland (Parnell et al. 2008; Kurennoy et al. 2009; Kelpšaite et al. 2009). This body of research examined the role of boat operational characteristics, vessel type, wave height, and wave energy on sediment resuspension. The approaches and methods described in these papers informed our research methods.

Boat-generated wake wave impacts on river banks were explored in a number of studies from around the globe and several were informative for this project. USACE (1994) is a final report for a larger research study that provided a comprehensive look at a specific surface water system -

the Fox River and Chain O'Lake public waterway. The findings from the study indicated a nearly instantaneous response in water quality to high boating activity. MacFarlane and Cox (2003a, 2003b, 2005) describe detailed investigations of vessel wake wave characteristics and impacts on bank erosion on the Brisbane, Noosa, and Maroochy Rivers in southeast Queensland, Australia. The authors utilized field measurements of wave height and period to establish threshold criteria that can be used to inform management decisions on these systems. Shoreline erosion was studied on the Waikato River in New Zealand for two recreational watercraft and a personal watercraft (McConchie 2003). The study relied on field measurements of wave height using submerged pressure sensors and the data were used to calculate wave energy. Suspended sediment samples were also collected in an attempt to link wave characteristics to bank erosion. Similarly, Maynord et al. (2008), studied boat-generated wave erosion on the river banks of the Kenai River, Alaska. Here, wave heights were measured with a capacitance-based system but the approach for determining wave heights and energy were the same approaches adopted in our study.

## 2.3 Field studies on the impacts specific to wakesurf boats

We identified a small number of research reports that specifically focus on wakesurfing conditions (e.g. relatively slow speeds ~10-12 mph, internal ballast tanks and wake enhancing technologies). We were not able to find any journal articles within the peer-reviewed literature. Ruprecht et al. (2015) is a conference paper that compared measured wake height and energy of a boat described as a "wakeboarding vessel" that was operated under wakesurfing, wakeboarding, and waterskiing conditions. The research reported a four-fold increase in wave energy under wakesurfing conditions. In addition, the authors offered an approach for developing empirical equations relating maximum wave height to wake wave energy, which may be a useful and practical approach to adopt in upper Midwest US lakes and rivers. Wakeboarding and waterskiing operational conditions yielded similar wave heights and energy, but were both lower than wakesurfing conditions.

Two research reports from Canada examine impacts from the wake wave and propeller wash of wakesurf boats. Mercier-Blaise and Praire (2014) is a research report from the University of

Québec, Montreal, that details a field-based study of wake wave impacts on shorelines. The researchers used a single wakeboarding boat operated at various speeds and ballast conditions. The report defined 10 mph speed and biased ballasting to be the wakesurfing condition. A unique aspect of the project involved using an Acoustic Doppler Velocimeter (ADV) to record turbulent wave energy (turbulence kinetic energy or TKE) at a specific location in the nearshore environment. The researchers also collected water samples during testing and analyzed for suspended solids concentration. Results from the work showed an increase in TKE from boat-generated waves with the largest impacts resulting from the 10 mph wakesurf boat conditions. Raymond and Galvez-Cloutier (2015) was published by Laval University, Quebec, and focused on the impacts of wakeboat propeller wash on velocities and turbidity. As in Mercier-Blaise and Praire (2014), a single wakeboarding boat was used and operated under three conditions to simulate wakesurfing, wakeboarding, and waterskiing. An Acoustic Doppler Current Profiler (ADCP) was deployed on the lake bottom at a water depth of approximately 16 ft (5 meters) and recorded the velocity field within the water column as the boat traversed over the sensor. The effects of propeller wash appeared to have penetrated up to 16 ft (5 meters) deep for the condition associated with 10 mph and biased ballasting (i.e., wakesurfing). It should be noted that both Mercier-Blaise and Praire (2014) and Raymond and Galvez-Cloutier (2015) were pilot studies and the authors suggest more research is required. Regardless of the preliminary nature of the work, the two projects introduce the use of advanced sensors (ADV and ADCP) and incorporate environmental monitoring (turbidity), which are important for future research in this area.

(This page intentionally left blank)

# 3.0 MATERIALS AND METHODS

## 3.1 Study location and site

This study took place on Lake Independence, Maple Plain, Minnesota, USA (45°1'37"N 93°38'53"W) (Figure 1). Lake Independence is 832 acres (425 littoral acres) with a shoreline length of 7.47 miles. The main basin of the lake is bowl shaped with water depths gradually increasing to the lake's maximum depth of 58 ft. The lake is a popular recreational destination. For example, Baker Park Reserve, owned and operated by Three Rivers Park District, offers 2,700 acres of natural landscape that abuts to the lake via 4,000 ft of southeast shoreline (Figure 1). The park includes a swimming beach, boat launch, RV park, and hiking trails that attract many people to the lake to recreate. Having Baker Park Reserve on the southeast shoreline was integral to the success of this study because it was near our study site and Three Rivers Park District allowed us to use the park's boat rental facility and docks, which drastically increased our efficiency. Our study site was located along the northern shoreline of the lake's southeast quadrant (Figure 1). In addition to having Baker Park Reserve nearby, this site was chosen because a lake property owner graciously granted our team access to their dock and shoreline. The lake bathymetry at the study site had a moderately gradual slope 5.1% (Figure 2) and bottom substrate was measured to be primarily sand and gravel. The shoreline directly abutting the study site was protected with large riprap stones with minimal vegetation present.


**Figure 1. Lake Independence, Maple Plain, Minnesota, USA. The red box depicts the study site located along the northern shoreline of the lake's southeast quadrant.**

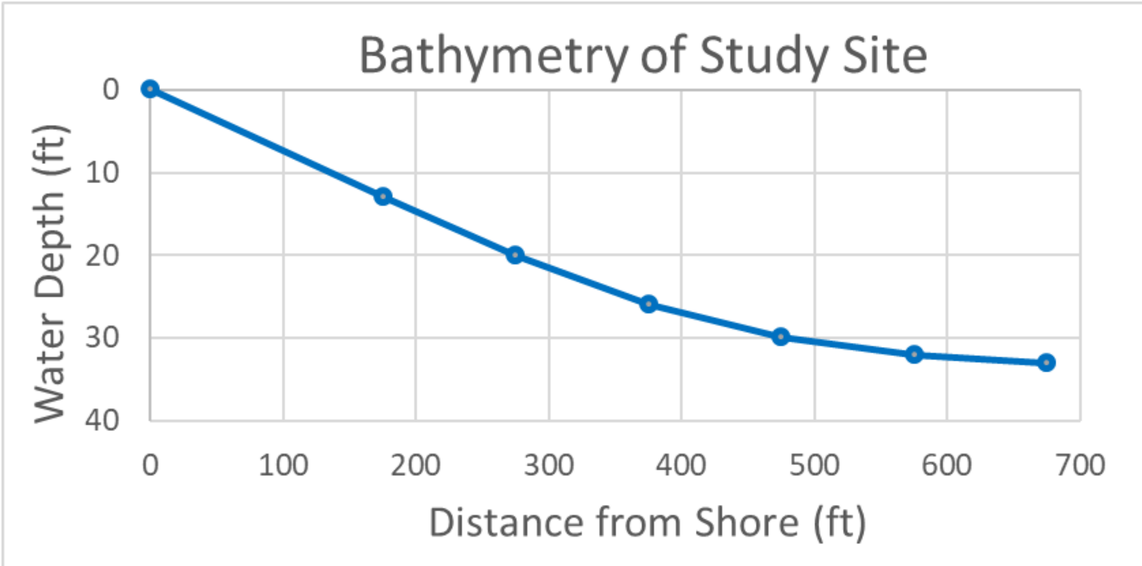


**Figure 2. Typical bathymetry at the study site showing a gradual increase in water depth with distance from shore. The maximum depth was 33 ft at 675 ft from shore.**

## 3.2 Layout of the study site

Figure 3 illustrates the layout of the study site and is described hereafter. Using bathymetric and Global Position System (GPS) data, three masts (Section 3.4) and two pads (Section 3.5) that held data sensors, were installed in a straight line approximately perpendicular to the shoreline at known depths and distances (Table 1). The line of masts/pads was also in an alignment that was roughly perpendicular to local bathymetric contour lines.

Four boat tracks were defined in a straight line approximately parallel to the shoreline and perpendicular to the masts and pads at approximately 225, 325, 425, and 625 ft from shore. Each track line was marked by a pair of taut-moored inflatable buoys that helped to visually guide the boat operator during testing (see Section 3.8 for more detailed description).

**Table 1. The distances of masts and pads from shore and their respective water depths.**

| Station | Distance From Shore | Water Depth |
|---|---|---|
| Mast A | 16 ft (5 m) | 1.8 ft (0.6 m) |
| Mast B | 114 ft (35 m) | 6.1 ft (1.9 m) |
| Mast C | 142 ft (43 m) | 8.5 ft (2.6 m) |
| Pad 1 | 219 ft (67 m) | 14.0 ft (4.3 m) |
| Pad 2 | 311 ft (95 m) | 22.0 ft (6.7 m) |

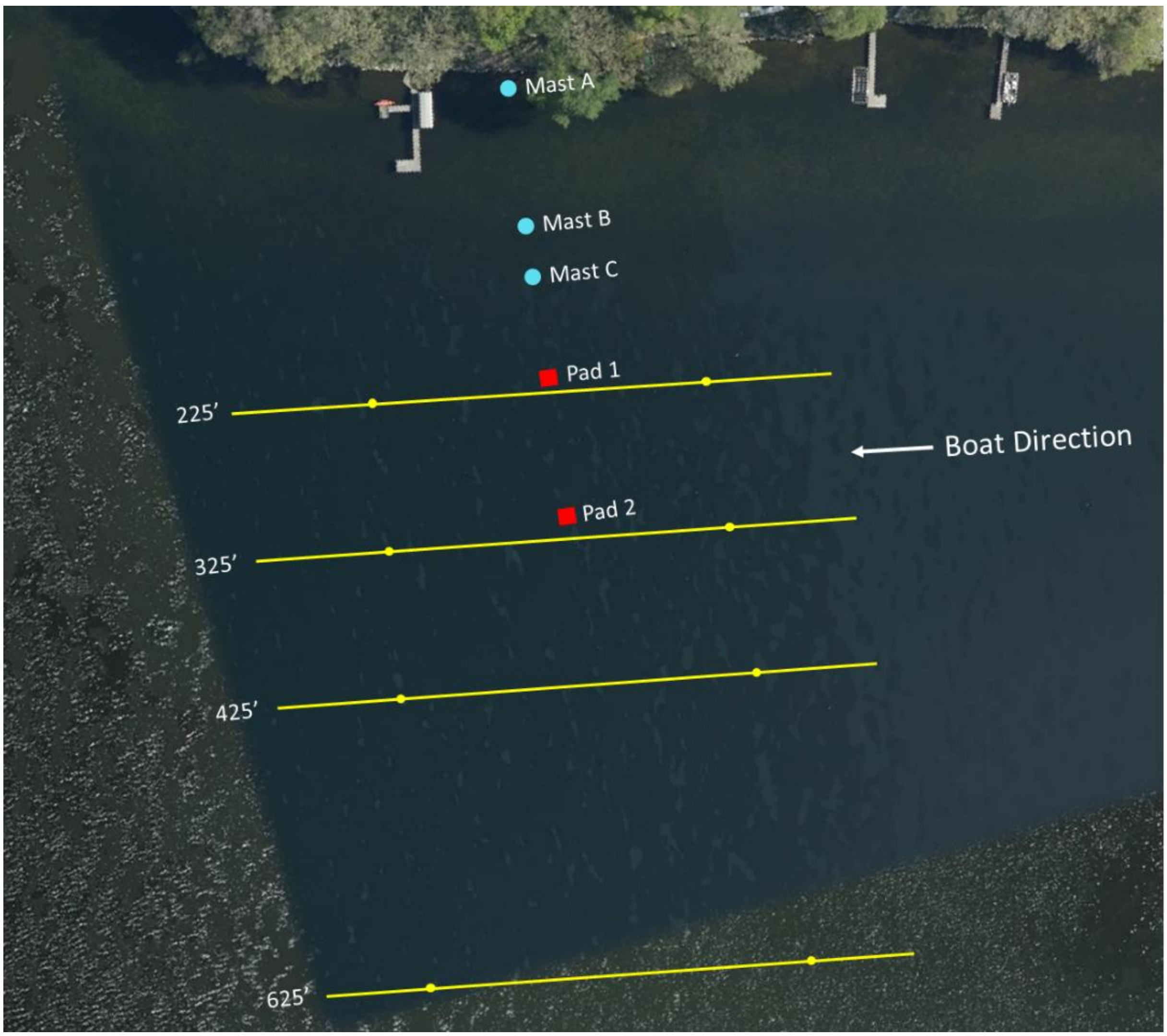


**Figure 3. Layout of the study site. The three blue circles and two red squares indicate the locations of the masts and pads, respectively. The yellow lines show the distance of the boat track lines from the shoreline.**

## 3.3 Description of masts and attached data sensors

The three masts were designed and fabricated to hold various types of data sensors. The masts were tripod structures composed of 2 in steel pipe (Figure 4a). To increase sturdiness, three 1-5/8 in steel struts along with three 3/16 in cable wires (made taut via turnbuckles) connected the legs to the center pipe. Because the masts were installed at different water depths, each mast was a different height. However, once deployed each mast had approximately 6 ft of center pipe emerging from the water surface, which was where equipment that needed to remain dry was attached (Figure 4b). With the assistance of a diver, the masts were installed, leveled, and secured to the lake bottom via 330 lbs of steel plate. The masts were installed in relatively shallow water (< 10 ft) and remained in their respective positions for the duration of the study (Table 1, Figure 3). Because Masts B and C were positioned further from shore in deeper navigable water, strobe lights were added to warn approaching watercraft of the hazard at night. Reflectors were also attached to all masts to further increase visibility.

Each mast was equipped with various data sensors, both above and below the water surface. Above the water surface, each was equipped with a water-resistant enclosure that housed a Campbell Scientific datalogger (CR1000X) powered by a 12v battery, charge controller, and solar panel system. A data acquisition program was written and installed on each data logger that collected data from various hardwired sensors. A GPS receiver with integrated antenna (GPS16x-HVS by Garmin International) that provided position, velocity, and timing information was fixed to each mast. Specifically, the GPS receiver allowed the data logger clocks to be synchronized to the highly accurate GPS time, and allowed post-processing synchronization between all sensor systems. Finally, Masts B and C were outfitted with wind speed and direction sensors. A single Campbell Scientific vented pressure transducer (CS431 PS9805 5PSI) was installed on each mast between 8-11 in (0.20-0.28 m) below the water surface. As the wake wave packet (i.e., series of waves produced by the boat) passed above the sensor, the water column height, and thus pressure at the sensor varied. This information was captured at 10 Hz (i.e., 10 samples per second) by the sensor and stored on the datalogger for later post-processing to determine maximum wave height, total wave energy, and maximum wave power of the wake wave packets.

Per the manufacturer's specifications, this model of pressure transducer has a repeatability of ± 0.1% FSO or ± 0.14 in of water.

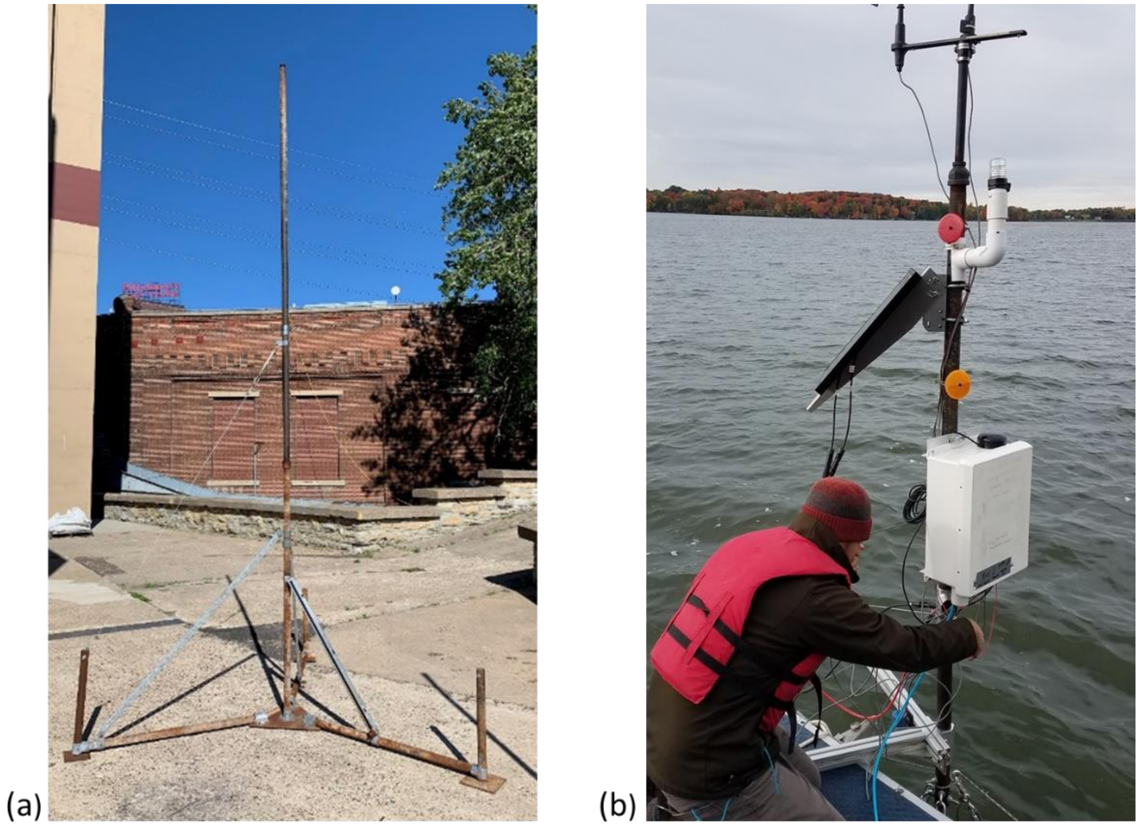

Figure 4. (a) Mast on land prior to being equipped with data sensors, (b) mast deployed and equipped with data sensors.

## 3.4 Description of pads and attached data sensor

Deployment of a mast system equipped with cabled data sensors was not practical in deeper waters (>10 ft). Instead, two pads were designed and custom-built to be easily deployed and retrieved from deeper waters (Table 1). The pads were rectangular structures made of 1-5/8 in steel strut with 12 in legs (Figure 5) that partially sunk into the substrate upon deployment and prevented the pad from moving. At each corner of the structure, a 4 ft x 3/16 in wire rope was secured. The four wire ropes were joined at a single lifting point and a nylon rope was attached to the lifting point and used to lower and lift the pad during deployment. The other end of the nylon rope was secured to a small buoy at the water surface. Because of the simplicity of this system, we were able to easily retrieve the pads and detach the data sensor and download data after each day of testing.

An Acoustic Doppler Current Profiler (ADCP; Nortek Signature 1000), capable of collecting data on the velocity fields within the water column, was secured to the center of each pad (Figure 5). Specifically, the ADCPs were used to collect high-resolution data on surface wave height. For water surface elevations (referred to as altimeter data by Nortek), the device records the two-way travel time of a single "ping" that is reflected off the water surface. The ADCPs are autonomous units with an internal clock, battery, and data logger. The clock on the ADCPs were set to match the internet time via a tethered laptop prior to deployment. The sampling rate of the ADCPs were set to 4 Hz for all tests.

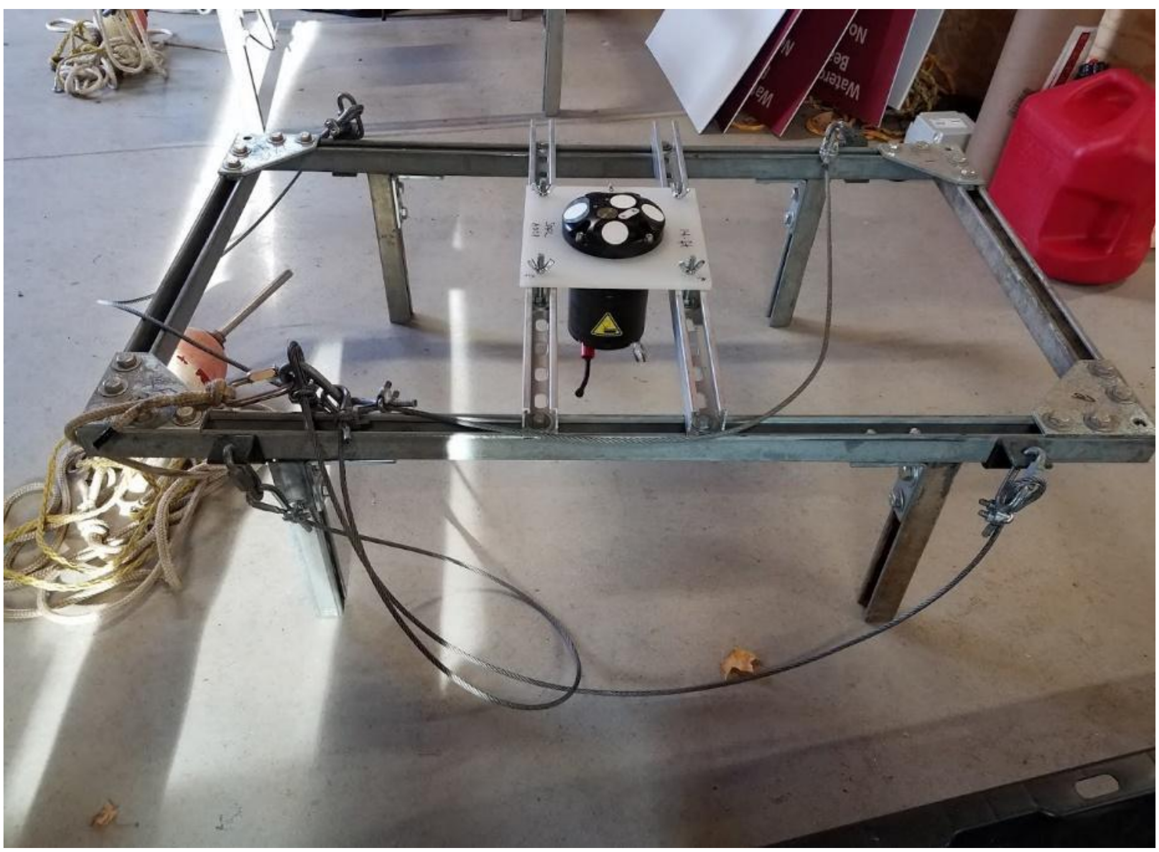

**Figure 5. An ADCP secured to the custom-built pad and ready for deployment. The four lifting cables and lift rope can also be seen in the image.**

## 3.5 Summary of test boat characteristics

The wake waves generated by four boats were evaluated in this field study (Table 2). The 2004 Larson LXI 210 is a common recreational boat powered by a 260 horsepower inboard/outboard (I/O) engine, otherwise known as a sterndrive. The engine is positioned at the stern of the boat, with the drive unit protruding through the transom. The boat operator can trim the drive unit up or down to change performance during various operating conditions. Moreover, when the steering wheel is turned the entire drive unit turns, making the boat more responsive to maneuvering at slower speeds than boats steered by a rudder.

There are two primary types of inboard powertrain configurations, D-Drive (direct drive) and V-Drive, and both were tested in this study. These powertrains are equipped with a system that includes a propeller that protrudes through the hull (i.e., under the boat) via a shaft and rudder that provides the steering. These types of powertrains are presently preferred for many tow sports because of increased safety with the propeller set forward of the transom. As the propeller pushes water past the rudder, the boat direction responds in accordance with the rudder position, which is controlled by the steering wheel. The 2004 Malibu Response LX had a 310 horsepower D-Drive inboard engine, meaning the engine was housed in the center of the boat. The D-Drive powertrain is mechanically simpler and also places the boat's center of mass forward, which allows the boat to transition to planing more efficiently. D-Drive inboards are popular among waterskiing enthusiasts because of this attribute.

Both the 2019 Malibu VLX and 2019 Malibu MXZ had 450 horsepower V-Drive inboard powertrains, meaning the engines were positioned at the rear of the boat beneath the transom seating. Having the weight of the large engine at the back of the boat creates greater aft trim for the boat, thus creating the bigger wakes needed for watersports like wakesurfing. In addition to the type of powertrain, boat manufacturers and independent businesses have developed methods to manipulate boat-generated wakes (e.g., height, length, shape, direction) that include: boat size and weight, hull design, ballast systems, and surf systems (e.g., hydrofoils and wake shapers).

It is important to state that this study was limited to examining only four boats. We selected watercraft that were representative of non-wakesurfing and wakesurfing boats; however, there are many other boat manufacturers and models not considered. The boat selection was based on the boats that were available to us within the short window of field work for this study. This research is not intended to highlight any specific watercraft manufacturer, but recreational boats in general.

In the next sections, we discuss specifics of the four boats tested in this study.

### 3.5.1 Larson LXI 210

The 2004 Larson LXI 210 had a length of 21 ft, a beam of 8.25 ft, and weighed 2,925 lbs dry (Table 2). The size, weight, and modified V hull design of this boat are common among all-purpose recreational boats (i.e., cruising, fishing, boat watersports). The boat used did not have any additional wake manipulating systems and created a symmetrical wake, meaning the wake waves produced was similar off both sides of the boat.

### 3.5.2 Malibu Response LX

The 2004 Malibu Response LX was the smallest and lightest of the test boats with a length of 20 ft, a beam of 7.5 ft, and a dry weight of 2,450 lbs (Table 2). Again, the hull design was a modified V shape. This boat was equipped with a manually operated transom mounted hydrofoil. When not in use the hydrofoil gets locked in the stow position (Figure 6a). When in use the hydrofoil is lowered to a single fixed position (Figure 6b). The principle of operation of this hydrofoil is to provide a downward force at the stern of the boat, creating greater aft trim. According to the manufacturer, the hydrofoil produces up to 1,000 lbs of equivalent aft ballast to the stern of the boat.

An aftermarket wake shaper (Wakesurf Creator 2.0 by Swell Wakesurf) was attached to the boat during one of the test conditions (i.e., Condition 1a, see Section 3.6.2). The wake shaper is a paddle-like baffle that was attached via suction cups to the port quarter of the hull just below the water surface (Figure 6c). When installed, the wake shaper increases the size and smoothness of the wake on the opposite side of the boat, making an asymmetric wake that is surfable on one side. The hydrofoil and wake shaper can be used in tandem to create wake conditions that are suitable for wakesurfing.

### 3.5.3 Malibu Wakesetter Boats: VLX and MXZ

Malibu's line of Wakesetter boats are specifically designed for wakesurfing. The 2019 Malibu VLX Wakesetter was the smaller of the two Wakesetters with a length of 21 ft, a beam of 8.2 ft, and an approximate dry weight of 4,200 lbs (Table 2). To make the wake larger by displacing more water, the boat can be made heavier via its ballast system that can hold up to an additional 3,690 lbs of water weight. The larger 2019 Malibu Wakesetter MXZ was 24.5 ft long, 8.5 ft beam, and weighed approximately 5,500 lbs dry (Table 2). This boat also had a ballast system that could hold up to an additional 4,885 lbs of water weight.

Both boats were equipped with Malibu's proprietary control system called the Integrated Surf Platform. The system combines an array of technologies to create and maintain a desired wake condition. The hydrofoil, termed Power Wedge III by Malibu, functions in the same principle manner as the aforementioned hydrofoil, where according to the manufacture, the Power Wedge III can produce up to 1,500 lbs of downward force, which is equivalent to 1,500 lbs of equivalent aft ballast (Malibu Boats 2020). The Power Wedge III had adjustable settings that range from "lift" to "stow" (Figure 8a). When in lift mode the Power Wedge is in position #1 and fully deployed down (Figure 7a). In this position, the foil creates an upward lift force that allows the boat to reach planing quickly. As the Power Wedge is raised from lower numbered settings to higher numbered settings (Figure 8a), the size, shape, and surface roughness of the wake changes. This control over the wake is desirable because it allows surfing conditions to be adjusted to the skill and preference of the surfer. Finally, when in stow mode, the Power Wedge is not in use (Figure 7b).

The Wakesetters also have factory installed wake shapers (Malibu Surf Gate) on either side of the transom, just below the water surface (Figure 7c). When deployed on one side, the wake shaper produces an asymmetric wave with a larger and smoother surfing wave on the opposite side of the boat.

**Table 2. Summary of the four test boats.**

| Manufacturer | Model | Year | Drive | Horsepower | Beam (ft) | Length (ft) | Dry Weight (lbs) | Ballast (lbs) | Hydrofoil | Wake Shaper |
|---|---|---|---|---|---|---|---|---|---|---|
| Larson | LXI 210 | 2004 | Sterndrive (I/O) | 260 | 8.3 | 21 | 2925 | No | No | No |
| Malibu | Response LX | 2004 | Direct Drive (I) | 310 | 7.5 | 20 | 2450 | No | Yes | Yes -aftermarket |
| Malibu | Wakesetter VLX | 2019 | V-Drive (I) | 450 | 8.2 | 21 | 4200 | 3690 | Yes | Yes |
| Malibu | Wakesetter MXZ | 2019 | V-Drive (I) | 450 | 8.5 | 24.5 | 5500 | 4885 | Yes | Yes |

*Notes:*
*(I/O) - inboard outboard or sterndrive powertrain*
*(I) - inboard powertrain*


**Figure 6. Malibu Response LX hydrofoil in the (a) stow position and (b) deployed down position. (c) Installed aftermarket wake shaper (Swell Wakesurf- Wakesurf Creator 2.0).**

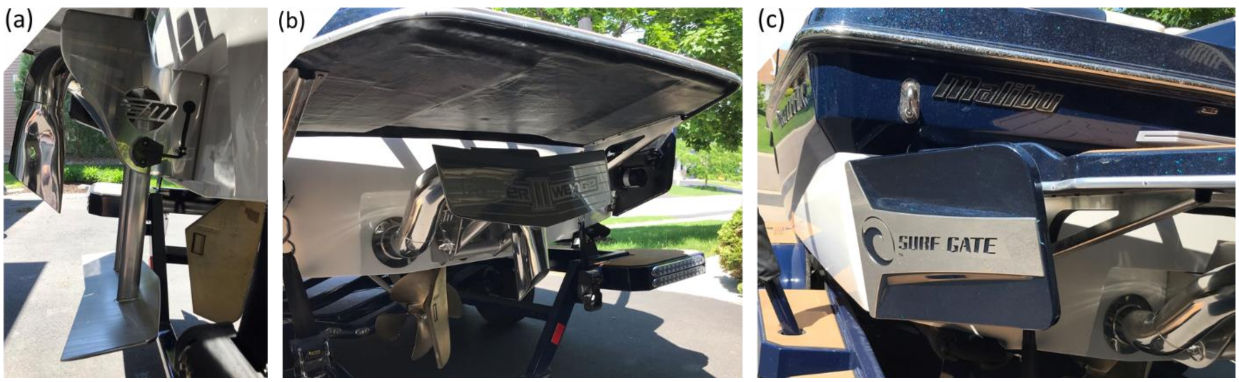


**Figure 7. Malibu Wakesetter hydrofoil (Power Wedge III) set to (a) lift and (b) stow. (c) Malibu Wakesetter wake shaper (Surf Gate) in the off position.**

## 3.6 Summary of operating conditions tested for each boat

The operating conditions used during testing of the four watercrafts are summarized in Table 3 and were defined by weight, operating speed, ballast condition (if applicable), hydrofoil (if applicable), and wake shaper (if applicable), and sought to represent typical recreational boating activities.

### 3.6.1 Larson LXI 210 operating conditions

During testing of the Larson LXI 210, two people were aboard the watercraft that added a combined weight of approximately 330 lbs. The passenger sat in the seat next to the boat operator to keep weight evenly distributed. Condition 1a created the largest wake wave possible without the addition of wake manipulating methods (Table 3). The boat speed was held at 10 mph and the propeller trim was adjusted to achieve the greatest aft trim possible. This propeller trim position was found to be the 50% position.

Condition 2 modeled typical operating conditions of the boat for tow sports like tubing, waterskiing, and wakeboarding (Table 3). The boat traveled at 20 mph with the propeller trim set to 100% (i.e., completely down) and was in a planing condition. Because no wake manipulating methods or technologies were used, the wake waves were symmetrical for both Condition 1a and 2.

### 3.6.2 Malibu Response LX operating conditions

During testing of the Malibu Response LX, two people were aboard the watercraft, which added approximately 330 lbs of weight. Condition 1a created the largest wake waves possible with the operating conditions tested (Table 3). The boat traveled at 10 mph. The hydrofoil was in the down position, which created an estimated downward force of 1,000lbs, equivalent to 1,000 lbs of equivalent aft ballast (Section 3.5.2, Figure 6b). To increase aft trim further, the passenger (175 lbs) sat in the stern seating area. The aftermarket wake shaper was installed on the outside surface of the port quarter of the hull, just beneath the water surface (Section 3.5.2, Figure 6c), which produced an asymmetric wake with the larger and less turbulent side forming starboard. We chose to have the larger wake on the starboard side because, during testing, the boat traveled from east to west and approximately parallel to the shoreline, which directed the wake towards shore where our data sensors were installed (Figure 3).

For Condition 1b (Table 3), the aftermarket wake shaper was removed so its effects on the wake characteristics (e.g., height, energy, power) could be measured (i.e., device on vs. device off).

The Condition 2 variables were set to model conditions commonly used during tubing, waterskiing, and wakeboarding (Table 3). The boat traveled in a planing condition at 20 mph with no wake shaper attached (symmetric wake). The passenger sat in the middle of the boat next to the boat operator to evenly distribute weight. The hydrofoil was placed in the downward position creating downward force and additional aft trim.

### 3.6.3 Malibu Wakesetter Boats: VLX and MXZ operating conditions

Both the Malibu VLX Wakesetter and Malibu MXZ Wakesetter were tested using the same two conditions (Table 3), with the only difference being the manufacturer's boat characteristics (Section 3.5.3, Table 2). Four people were aboard with a combined weight of approximately 740 lbs. To keep the weight in the back half of the boat and evenly distributed, one passenger sat in the passenger seat next to the boat operator and the other two passengers sat in the rear transom seating area. Condition 1a modeled the conditions and settings commonly used by the boat owners when they wakesurf (Table 3). During this condition, the boats traveled at 11 mph with the ballast tanks 100% full. The Power Wedge III was set to setting #3 (Figure 8), with the portside Surf Gate on (asymmetrical wake). Again, this formed a large surf wake on the starboard side of the boat that traveled towards the shoreline and our data sensors (Figure 3).

All variables remained the same for Condition 1b, except for the ballast tank setting (Table 3). The ballast water was completely drained so its effects on the wake characteristics (e.g., height, energy, power) could be compared (i.e., full vs. empty).

The variables in Condition 2 were set to model conditions commonly used during tubing, waterskiing, and wakeboarding (Table 3). The boat traveled at 20 mph with the ballast tanks empty, the Power Wedge III remaining in setting #3, and the Surf Gate off (symmetric wake).

(a)

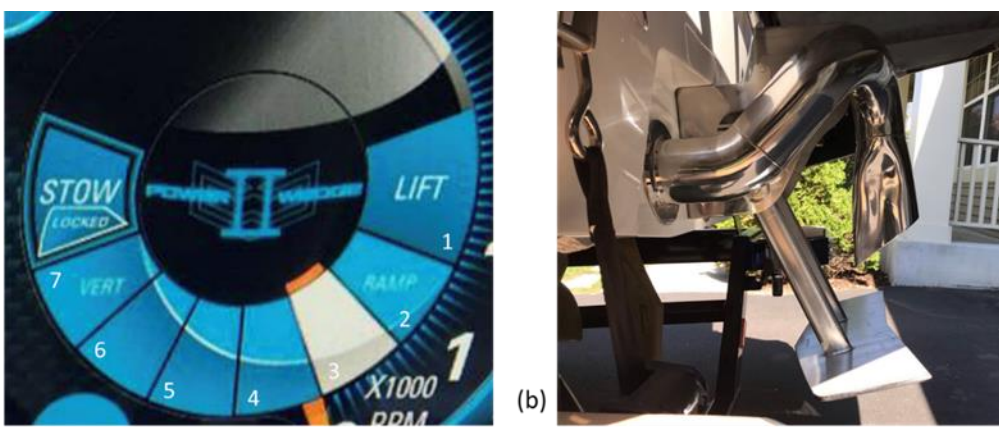


(b)

**Figure 8. (a) Power Wedge III settings that range from lift to stow. Lift is noted as position #1, with the white highlight indicating that setting #3 is selected. (b) Power Wedge set to setting #3.**

**Table 3. Summary of the operating conditions for each boat tested. The only difference between Conditions 1a and 1b for the Malibu Response LX was the wake shaper setting (i.e., on vs off). The only difference between Conditions 1a and 1b for each Malibu Wakesetters was the ballast setting (i.e., full vs empty).**

| Boat | Condition # | Speed (mph) | Trim Setting (%) | Ballast (% filled) | Hydrofoil/Power Wedge III | Wake Shaper/Surf Gate | People Aboard | Approx. People Weight (lbs.) |
|---|---|---|---|---|---|---|---|---|
| **Larson LXI 210** | 1a | 10 | 50 (middle) | N/A | N/A | N/A | 2 | 330 |
| | 2 | 20 | 100 (down) | N/A | N/A | N/A | 2 | 330 |
| **Malibu Response LX** | 1a | 10 | N/A | N/A | Down | On – Port Side | 2 | 330 |
| | 1b | 10 | N/A | N/A | Down | Off | 2 | 330 |
| | 2 | 20 | N/A | N/A | Down | Off | 2 | 330 |
| **Malibu VLX Wakesetter** | 1a | 11 | N/A | 100 | Down – Setting #3 | On – Port Side | 4 | 740 |
| | 1b | 11 | N/A | 0 | Down – Setting #3 | On – Port Side | 4 | 740 |
| | 2 | 20 | N/A | 0 | Down – Setting #3 | Off | 4 | 740 |
| **Malibu MXZ Wakesetter** | 1a | 11 | N/A | 100 | Down – Setting #3 | On – Port Side | 4 | 740 |
| | 1b | 11 | N/A | 0 | Down – Setting #3 | On – Port Side | 4 | 740 |
| | 2 | 20 | N/A | 0 | Down – Setting #3 | Off | 4 | 740 |

## 3.7 Generating boat wake waves

Test boats were driven approximately from east to west along designated track lines set at 225, 325, 425, and 625 ft from shore, with the shoreline on the starboard side of the boat (Figure 3). The track lines were deployed in a straight line approximately parallel to the lake's measured bathymetry contours, which were also approximately parallel to the shoreline, and perpendicular to the mast/pad alignment. Using GPS coordinates, each track line was marked by a pair of taut-moored inflatable buoys that helped to visually guide the boat operator during testing. Moreover, the buoy locations were marked as waypoints on an onboard GPS unit (Humminbird Helix 10) that charted real-time boat position, further helping the boat operator navigate consistent and repeatable passes along the track lines. To ensure the wake waves that reached the mast/pad sensors were generated under steady conditions, the boat operator maintained test speed and alignment with the track line well before and after the track line buoys.

For each operating condition evaluated (Section 3.6, Table 3), the test boat made four passes along each track line. An observer was stationed onshore to notify the boat operator (via two-way radios) when it was clear to make the next pass, which was made only after the previous wake wave packet had made landfall in its entirety. This ensured that the wake wave packet generated by a single pass would be easily identifiable (i.e., clear start and end of each wake packet) during data post-processing.

## 3.8 Boat positional data

Instrumentation was mounted on each of the test boats to continually measure the boat's GPS position, velocity, yaw, pitch (trim) and roll. The on-board instrumentation utilized a mobile Raspberry Pi-based interface running Python to query the data from a VectorNav VN-200 inertial navigation sensor (INS)[1], which was positioned mid-boat. The sensor system included a L1 global navigation satellite system (GNSS) module, 3-axis accelerometers, 3-axis gyros, 3-axis magnetometer, barometric pressure, and an on-board processor. An INS Kalman filter reported position, velocity, and orientation at high frequencies after coupling GNSS location information with other on-board sensors used to record hull submergence (not discussed in this report). The

[1] (https://www.vectornav.com/)

stated accuracies of the VN-200 system after coupling with GNSS data are 1.0 m root mean square (RMS) for horizontal position, <0.05 m/s for velocity accuracy, 0.2-degree RMS for heading, and 0.03-degree RMS for pitch and roll. Additionally, the system data continuously reported uncertainties for attitude, position, and velocities, which included measured outliers in those reported values. The data were recorded at ~5Hz and collected within a single data file. To eliminate any potential velocity inconsistency between boats (e.g., different speedometer accuracies), we used the real-time velocity readings of this system during passes. The positional data for each pass were later imported into AutoCAD and used to estimate operational distance (Section 4.1).

(This page intentionally left blank)

# 4.0 DATA ANALYSIS

## 4.1 Computing operational distances

The boat positional data (Section 3.8) were imported into AutoCAD and plotted (Figure 9). The perpendicular distances between each boat pass and each of the masts/pads (i.e., measurement sensors) were then calculated; these distances were defined as operational distances (Figure 9). For each of the four passes along a track line, an operational distance average and standard deviation were calculated. The passes along the track lines were highly repeatable, as the standard deviations for the averaged operational distances were <4 ft. The data and results presented in Section 5.0 are plotted against operational distance.

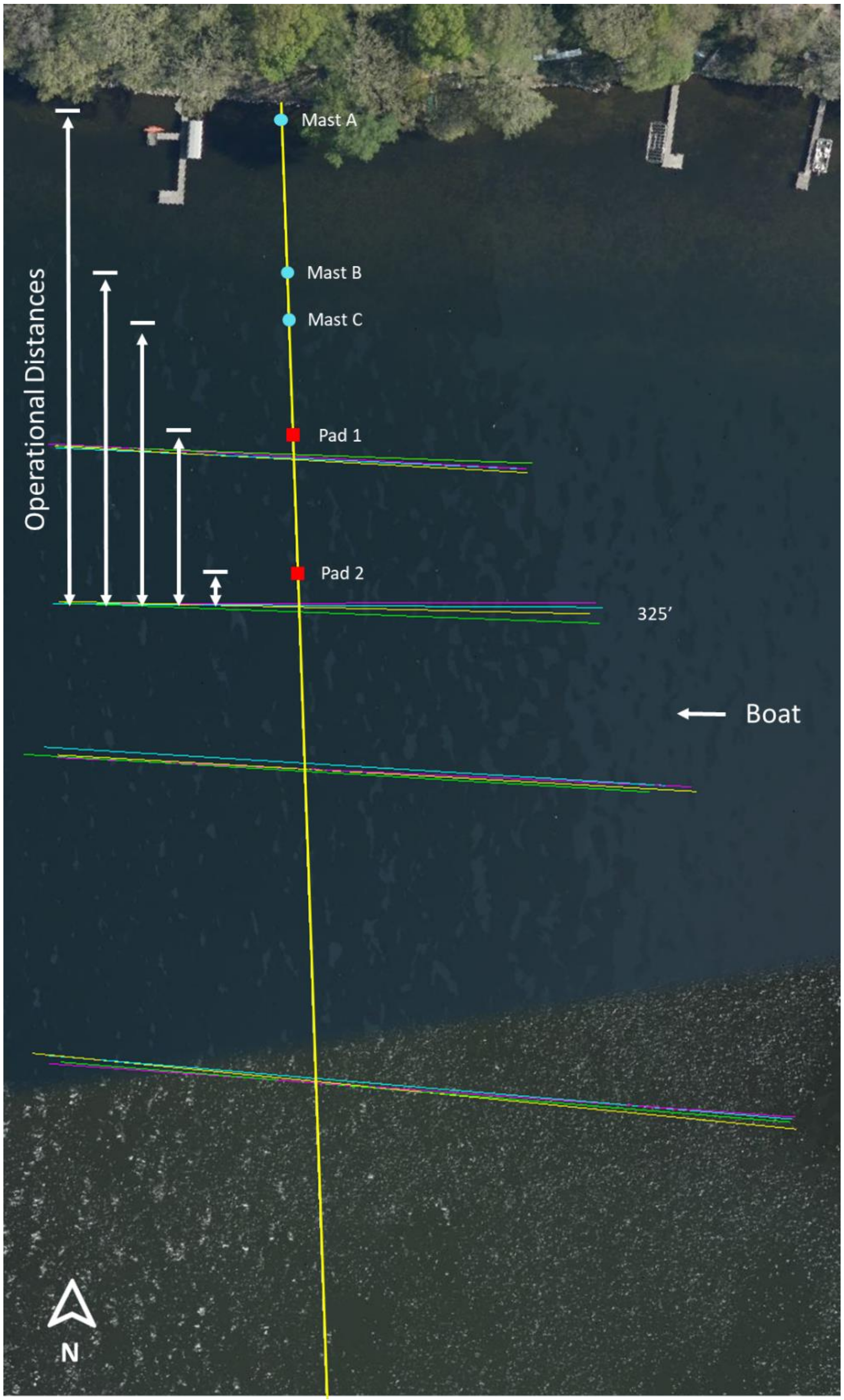


**Figure 9. Example of the boat position data imported into AutoCAD for each of the four passes along the four track lines of the Malibu Response LX under operating Condition 1a (colored lines). The operational distance measurements were taken along the yellow line between each track line pass and each mast/pad. The white arrowed lines illustrate the various operational distances from the 325 ft track line.**

## 4.2 Wave Height, Energy and Power

The primary wake wave parameters evaluated in this report are maximum wave height, total wave energy, and maximum wave power produced by the various test boats and how these varied with test conditions and operational distances. This section discusses our approach for collecting and analyzing these data.

### 4.2.1 Experimental time and wave height data collection – raw data

As previously discussed in Sections 3.3 and 3.4, the change in the water surface elevation was measured at the masts and the pads and was used to record the wave height as a function of time. Time zero (t=0.0) was set as midnight of the day tests were performed and all recorded times were converted to minutes from midnight.

The collected wave height time series data were the raw data sets that served as the bases for further calculations. The first post-processing step was to isolate the wake wave packets of each individual boat pass by manually identifying the first wave peak within the wake wave packet and noting the experimental time that this occurred. We then selected a window 0.3 minutes ahead and 2.0 minutes after this time (2.3 minutes total duration). Selection of these up-time and down-time duration windows was based on trial and error and was set based on the durations needed to fully capture the longest wake wave packet event. From this method, each boat pass yielded three, 2.3-minute duration data clips from the three masts and two, 2.3-minute clips from the two ADCP pads. These data clips were the inputs to further analyses of maximum wave height, total wave energy, and maximum wave power.

### 4.2.2 Attenuation correction of the mast pressure sensors

Because the pressure sensors were mounted a discrete distance below the water surface (i.e., 8-11 in (0.20-0.28 m)), it was necessary to apply a correction for attenuation of the pressure fluctuations (Tucker and Pitt 2001; Gourlay 2010; Shuster 2017). In many published applications, the pressure sensors were mounted near the bottom of the water body and in deep-water settings where the attenuation corrections were quite large. In our deployment however, the sensors were placed near the water surface slightly below the minimum wave trough elevation and so the correction was fairly minor (<22%). The attenuation correction method used was based on the approach described by Tucker and Pitt (2001) and coded into MATLAB by Neumeier (2020). The formulation applies an attenuation correction over a defined range of wave frequencies (0.05 – 0.8 Hz) that we selected based on a spectral analysis of each boat pass time series. Figure 10 is an example of typical raw and corrected wave height data collected from the pressure sensors plotted against time.

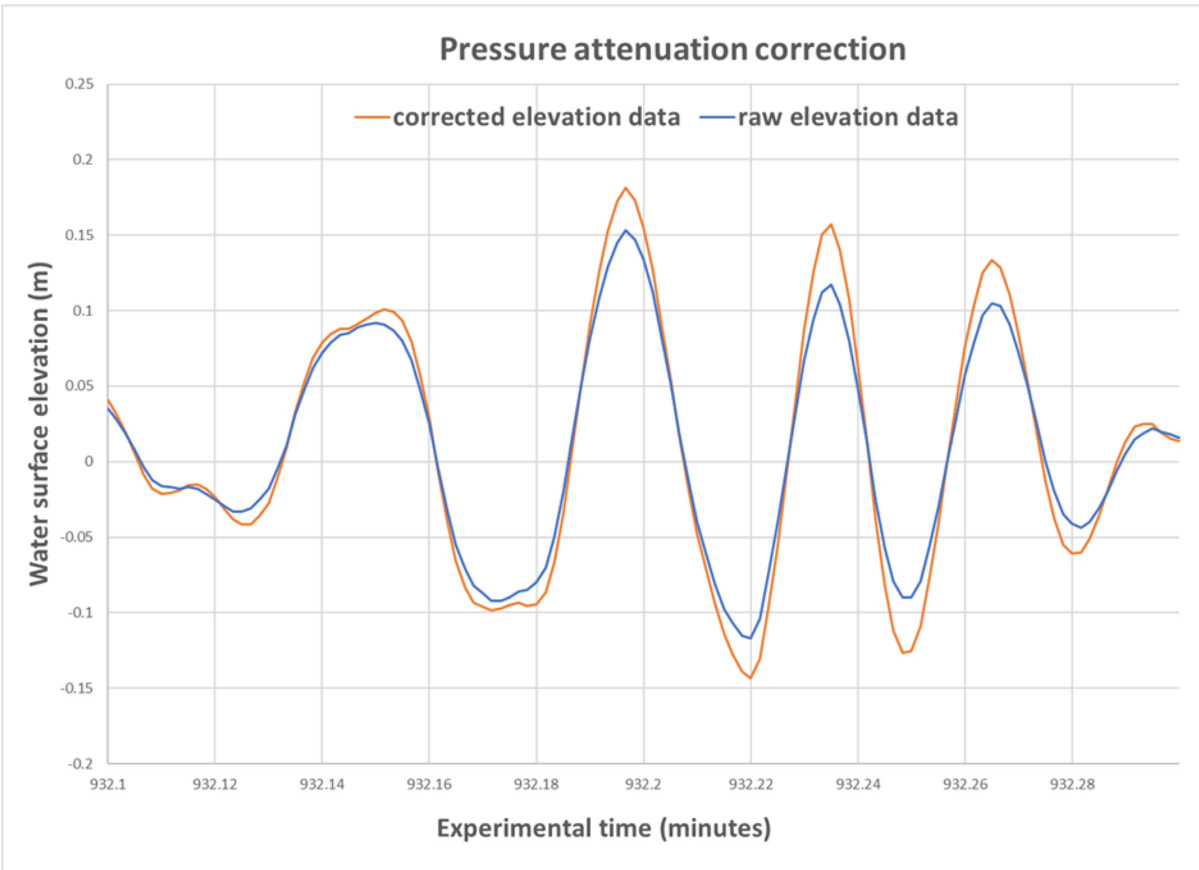


**Figure 10. Plot showing an example of pressure attenuation correction applied to raw data of wave height.**

### 4.2.3 Maximum Wave Height

Each corrected data clip was segmented into individual waves by locating the zero-crossing down locations within the 2.3-minute time series. Zero-crossing down refers to the point in time when the detrended water surface passed the zero or mean water surface elevation as it moved from crest to a trough (Figure 11). For each wave in the wake wave packet, the minimum and maximum water elevations were determined and the wave height, $H_i$, was calculated, where $i$ is an integer value representing the sequential number of a wave within the wake wave packet. The duration of a wave or wave period, $T_i$, was also calculated. In this way, each boat pass wake wave packet was broken down into its individual waves characterized by the $H_i$ and $T_i$ of each wave.

Maximum wave height was simply determined by locating the maximum wave height, $H_{max}$, that occurred during the pass. $H_{max}$ was the largest single wave that occurred within the wake wave packet.

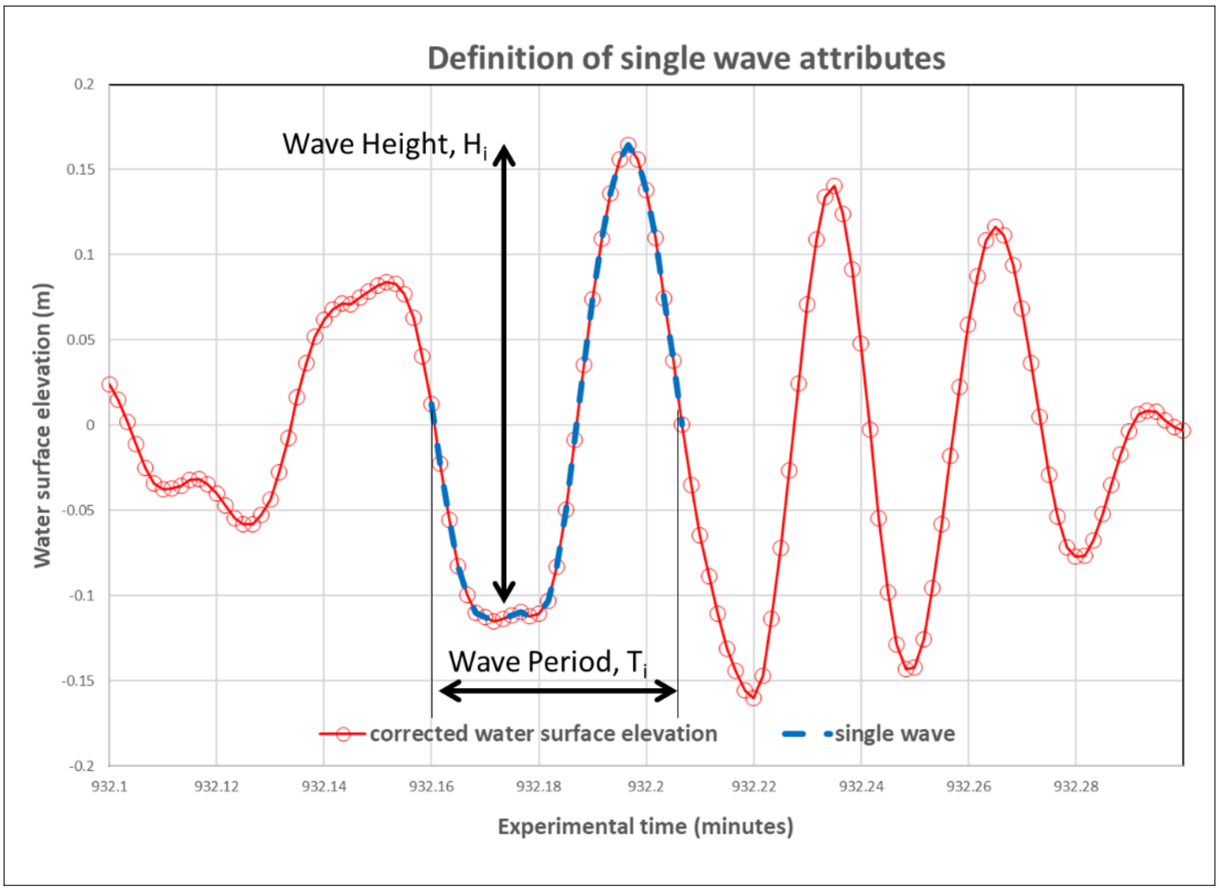


**Figure 11. Definitions of zero-crossing down (blue dashed line) as well as wave characteristics of wave height, $H_i$ and wave period $T_i$, where subscript *i* is an integer representing the sequential number of a wave within the packet.**

### 4.2.4 Total Wave Energy

Energy is a quantifiable attribute and, for waves, is a measure of the ability of the wave or packet of waves to do work such as apply force on the lake bottom or shoreline. The total wave energy within each wake wave packet was determined. Here, we document the formulation used in this calculation.

Equation (1) is the form of the total potential and kinetic energy within a water wave per unit crest length derived from linear wave theory or Airy wave theory (USACE 1984; Dingemans 1997; Stumbo et al. 1999).

$$E_i = \frac{\rho g {H_i}^2 \lambda_i}{8} \tag{1}$$

In this report, we adopt metric SI units for energy and power calculations where, $\rho$ is the density of water (kg/m$^3$), $g$ is the gravitational acceleration constant (m/s$^2$), $H_i$ is the wave height (m) and $\lambda_i$ is wavelength (m). Equation 1 indicates that the total energy per unit crest length within a single wave is related to the density of the water ($\rho$), the square of wave height, and the wavelength of the wave.

It is important to point out that the data collected in this study was wave height versus time. We did not collect direct measurements of wavelength, $\lambda_i$, so it was not possible to evaluate (1) directly; however, we have measurements of the wave period, $T_i$, which we used in combination with functional relationships between wavelength and wave period to estimate $\lambda_i$.

The wavelength and wave period have a complex relationship that required consideration of the local water depth and whether the wave's vertical extent interacted with the lake bottom or not. If the water depth is sufficiently deep, waves are not influenced by the bottom of the lake. Borrowing from the classification adopted by USACE (1984), deep water waves are defined as having wavelengths that are less than twice the water depth. For example, a single wave with a wavelength of 20 ft (6.1 m) is considered a deep wave in depths of 10 ft (3.0 m) or greater. The wave is considered an intermediate wave, meaning some interactions with the lake bottom, if depths are between ½ and $^1/_{25}$ of the wavelength. Below $^1/_{25}$ wavelength, the wave is considered a shallow water wave. For the example given, a wave with a wavelength of 20 ft would be an intermediate wave between 10 ft and 0.8 ft of depth and a shallow wave below 0.8 ft of depth. These definitions become important as the functional relationship between wave period and wavelength for intermediate and shallow waves are influenced by water depth (Dingemans 1997).

Equation (2) is a general form of a relationship for the phase velocity of a wave (Cp) and is applicable for deep and intermediate depths (USACE 2012). In Equations (3) and (4) we introduce standard definitions for angular frequency, ω, and wave number, *k*. Substituting (3) and (4) into (2) and rearranging terms, we derive Equation (5), which is a general relationship for the wave period, $T_i$, and wavelength, $\lambda_i$, at a specific water depth, $d_i$.

$$C_p = \frac{\omega}{k} = \sqrt{\frac{g}{k} tanh(kd_i)} = \sqrt{\frac{g\lambda_i}{2\pi} tanh(\frac{2\pi}{\lambda_i} d_i)} \quad (2)$$

$$\omega = \frac{2\pi}{T} \quad (3)$$

$$k = \frac{2\pi}{\lambda} \quad (4)$$

$$\left(\frac{2\pi}{T_i}\right)^2 = \left(\frac{2\pi\, g}{\lambda_i}\right) tanh\left(\frac{2\pi\, d_i}{\lambda_i}\right) \quad (5)$$

To utilize (5), recall that the data collection and initial analysis resulted in determining wave height, $H_i$, and wave period, $T_i$, for all waves in a wake wave packet for each boat pass. We also recorded the water depth at each mast ($d_{MastA}$ = 0.56 m; $d_{MastB}$ = 1.86 m; and $d_{MastC}$ = 2.63 m). Using this information in Equation (5), we solved for the wavelength, $\lambda_i$, for each of the waves measured in a wake packet (USACE 1984; MacFarlane 2012).

With the wavelength calculated for each wave, we then evaluated (1) and determined the total energy per unit crest width for each wave by summing all the waves in the wake wave packet generated by a single boat pass (Equation 6). The variable, *n*, represents the total number of individual waves within a wake wave packet.

$$E_{total} = \sum_{i=1}^{i=n} E_i = \sum_{i=1}^{n} \frac{\rho g {H_i}^2 \lambda_i}{8} \tag{6}$$

An important and likely obvious observation is that a single boat passage generated a series of waves that we refer to in this report as the wake wave packet. Because of wave dispersion, the number of individual waves occurring in a wake wave packet increases with distance. For example, at Mast A we observed 8 or 9 individual waves arriving from a ~225 ft pass distance, and greater than 20 individual waves from a ~625 ft pass distances. In addition to the increase in the number of individual waves, we also observed a longer duration of time for the wake wave packet to fully make landfall. Finally, the height of the waves decreased with distance from the boat, defined as wave attenuation. In general, closer to the boat, a smaller number of larger waves will reach the observation point and as the boat distance increases, a larger number of smaller waves will reach the same observation point over a longer duration of time.

The variation in wake wave packet duration with distance noted above had implications for how we determined the endpoint of the packet and calculations for total cumulative wave energy, $E_{total}$ for a boat pass. To determine this point in time, $t_{end}$, we established a threshold criterion, ε, defined as the point in time when the incremental change in total cumulative wave energy dropped below 1% of the total cumulative wave energy (Equations 7 and 8). Figure 12 shows an example of a cumulative total wave energy plot measured for one boat pass. The total duration of the analysis was ~130 seconds (2.3 minutes); however, in general, the main contribution of the wake wave packet occurred over 35-40 seconds from the start of the packet. Once $t_{end}$ was located, it was used to determine the total energy of the wake wave packet.

$$\varepsilon(t) = \left(\frac{E_{total(t)} - E_{total(t-1)}}{E_{total(t-1)}}\right) * 100 \tag{7}$$

$$t_{end} = \varepsilon(t) < 1.0 \quad \text{\{threshold criteria\}} \tag{8}$$

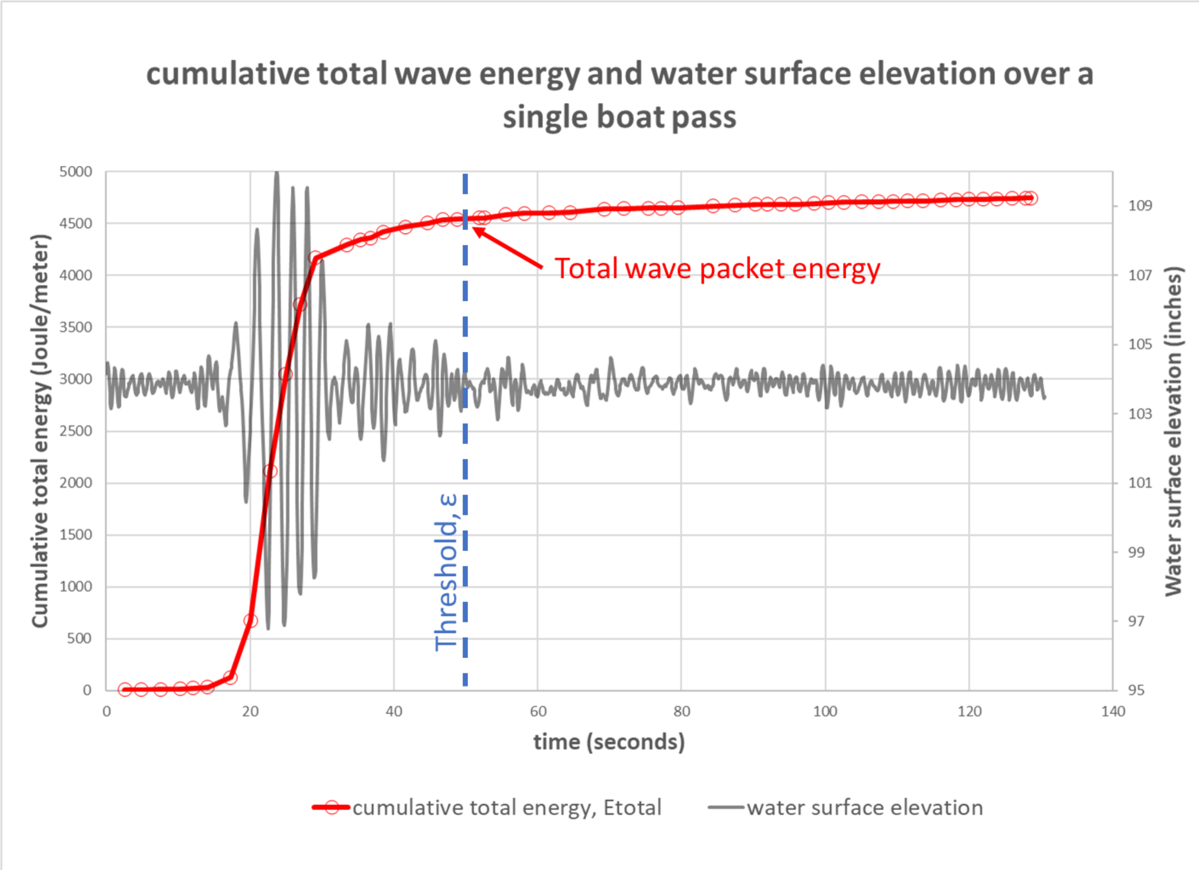


**Figure 12. Example of a wake wave packet measurement and equivalent cumulative wave energy computed for the packet. The blue dashed line represents the end of the wake packet as defined by the threshold criteria, ε.**

### 4.2.5 Maximum Wave Power

Another characteristic commonly computed for water waves is the wave power, also referred to as wave energy flux (Equation 9), which is calculated as the product of wave energy density, $\bar{E}$ (Equation 10) and group velocity, $C_g$ (Equation 11) (USACE 1984 and 2012, MacFarlane 2012). The wave power quantifies the rate at which energy within a wave is delivered to a shoreline or object, and is another measure of the ability of a wave to impact the near-shore environment. We estimated that the majority of wake waves produced in the study were deep-water waves and we therefore employed the deep-water formulation of group velocity (11).

$$\bar{P} = \bar{E} C_g \tag{9}$$

$$\bar{E} = \frac{\rho g H^2}{8} \tag{10}$$

$$C_g = \frac{g T_{max}}{4\pi} \tag{11}$$

Our analysis involved determining the wave energy flux associated with the largest wave within the wake wave packet and its associated wave period. Maximum power, $P_{max}$, was calculated using Equation 12.

$$P_{max} = \left(\frac{\rho g (H_{max})^2}{8} C_g\right) \tag{12}$$

# 5.0 RESULTS

The maximum wave height, total wave energy and maximum wave power were analyzed as a function of operational distance for each boat and operating condition. Each data point shown in the following figures is the mean value of the four passes at a given distance and under the same conditions, with the error bars depicting the standard deviation. Data points obtained from the masts (i.e., pressure transducers) and pads (i.e., ADCPs) and are represented as closed circles or squares and open triangles or diamonds, respectively. The vertical axis is either the maximum wave height (in), total wave energy (J/m), or maximum wave power (J/m-s). The horizontal axis is the operational distance (ft), which again is defined as the perpendicular distance from the boat track line to the masts/pads. A best fit power-law trendline is fit to all data points greater than one boat length from the track line (20-24-ft). The equation of this best-fit relationship and the corresponding $R^2$ correlation is provided on each graph. Data within one boat length had greater variability and was subject to influence from both transverse and divergent waves produced by the boat. We include these data points in the following figures, however, we do not include them in the regression analyses. Further, a power-law regression is adopted here based on the fact that it provides a reasonable fit to the observed data trends and also because of the long history of describing wave parameter decay using power law formulation. A thorough summary of many of these methodologies can be found in MacFarlane (2012). It should be noted that we were not able to collect data within the first 100 ft of operational distance for the Malibu Response LX because of technical issues with the ADCP sensors on the test day.

The results discussion relies heavily on the reader being familiar with the various test conditions (Conditions 1a, 1b and 2) for each boat tested. For convenience, we provide Table 3 again for quick reference.

(This page intentionally left blank)

**Table 3. Summary of the operating conditions for each boat tested. The only difference between Conditions 1a and 1b for the Malibu Response LX was the wake shaper setting (i.e., on vs off). The only difference between Conditions 1a and 1b for each Malibu Wakesetters was the ballast setting (i.e., full vs empty).**

| Boat | Condition # | Speed (mph) | Trim Setting (%) | Ballast (% filled) | Hydrofoil/Power Wedge III | Wake Shaper/Surf Gate | People Aboard | Approx. People Weight (lbs.) |
|---|---|---|---|---|---|---|---|---|
| **Larson LXI 210** | 1a | 10 | 50 (middle) | N/A | N/A | N/A | 2 | 330 |
| | 2 | 20 | 100 (down) | N/A | N/A | N/A | 2 | 330 |
| **Malibu Response LX** | 1a | 10 | N/A | N/A | Down | On – Port Side | 2 | 330 |
| | 1b | 10 | N/A | N/A | Down | Off | 2 | 330 |
| | 2 | 20 | N/A | N/A | Down | Off | 2 | 330 |
| **Malibu VLX Wakesetter** | 1a | 11 | N/A | 100 | Down – Setting #3 | On – Port Side | 4 | 740 |
| | 1b | 11 | N/A | 0 | Down – Setting #3 | On – Port Side | 4 | 740 |
| | 2 | 20 | N/A | 0 | Down – Setting #3 | Off | 4 | 740 |
| **Malibu MXZ Wakesetter** | 1a | 11 | N/A | 100 | Down – Setting #3 | On – Port Side | 4 | 740 |
| | 1b | 11 | N/A | 0 | Down – Setting #3 | On – Port Side | 4 | 740 |
| | 2 | 20 | N/A | 0 | Down – Setting #3 | Off | 4 | 740 |

(This page intentionally left blank)

## 5.1 Condition 1a

This section discusses the results of the data analyses for maximum wave height, total wave energy, and maximum wave power for each of the four boats tested under operating Condition 1a. Detailed descriptions of the boat operating conditions are provided in Section 3.6 and Table 3.

### 5.1.1 Maximum Wave Height

The maximum wave height is defined as the highest single wave measured within a wake wave packet and this value was computed for each pass. The average maximum wave height was then computed from these data and is presented in the following figures. For simplification, we refer to these values as maximum wave heights with the understanding that they are averages of all passes at a given distance.

All boats showed a nonlinear decrease in maximum wave height with operational distance (Figures 13 and 14). The most rapid decline in wave height occurred over the first 100 ft of operational distance where, for all boats, the maximum wave height decreased by half. The initial maximum wave heights recorded for the Larson LXI 210, Malibu VLX, and Malibu MXZ were 22 in, 34 in, and 39 in, respectively, which occurred within 4-6 ft of the boat track line.

All the data from Figures 13 and 14 are presented together in Figure 15 for easier comparison. The Larson LXI 210 attenuated from a maximum wave height of 22 in to 10 in at 84 ft of distance. The Malibu Response LX recorded a 10 in maximum wave height at 120 ft of distance. At 600 ft, both the Larson LXI 200 and Malibu Response LX had maximum wave heights of roughly 5 in. The Malibu VLX had a maximum height of 34 in that attenuated to 10 in after 210 ft. At 600 ft, the maximum wave height had decreased to approximately 5 in. Of the four boats tested, the largest boat in terms of length, total weight, and ballast water weight was the Malibu MXZ. The Malibu MXZ’s maximum wave height attenuated from 39 in to 8 in after 400 ft. Finally, by ~600 ft of operational distance the maximum wave height had decreased to roughly 6 in.

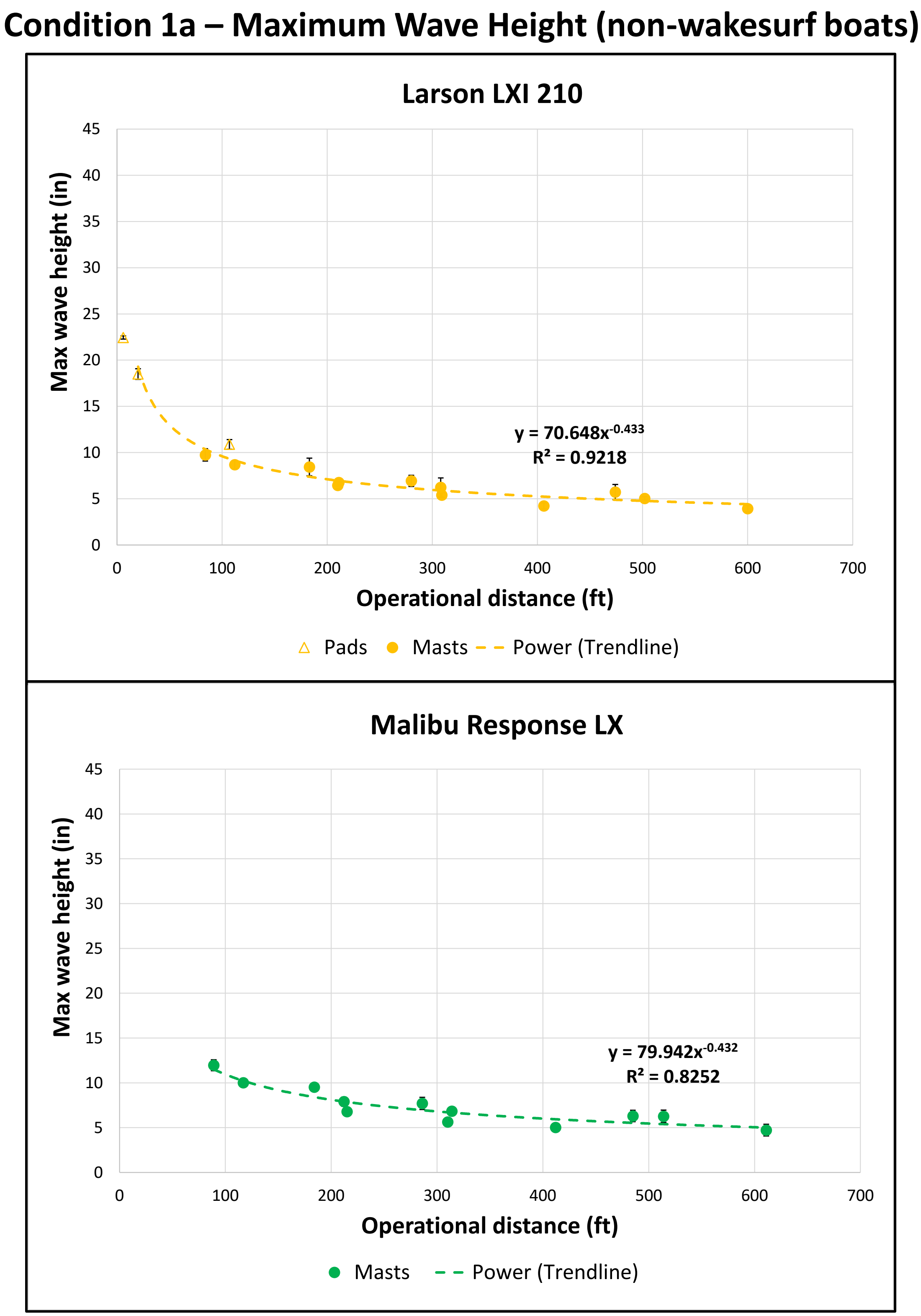


**Figure 13. Maximum wave height as a function of distance for the two non-wakesurf boats tested under Condition 1a. The error bars represent the standard deviation. There are no data for the Pads for the Malibu Response LX due to technical issues with the ADCP on test day. Data points less than one boat length from the track line were not included in the regression analysis.**

## Condition 1a – Maximum Wave Height (wakesurf boats)

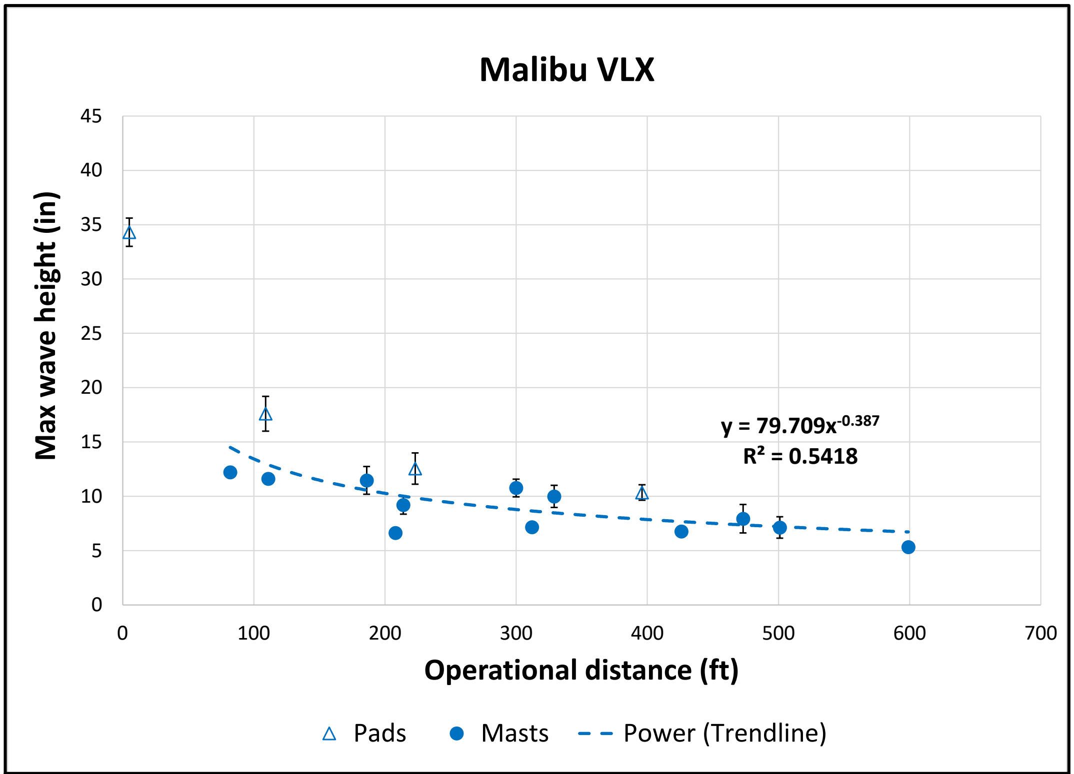


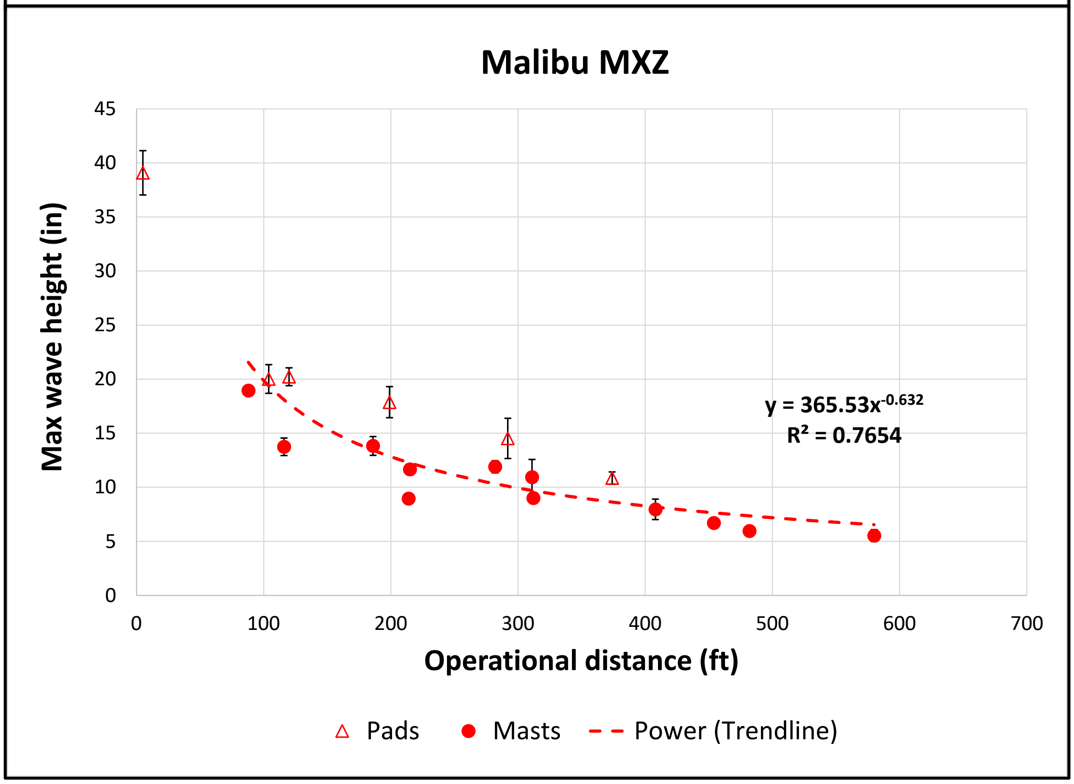


**Figure 14. Maximum wave height as a function of distance for the two wakesurf boats tested under Condition 1a. The error bars represent the standard deviation. Data points less than one boat length from the track line were not included in the regression analysis.**

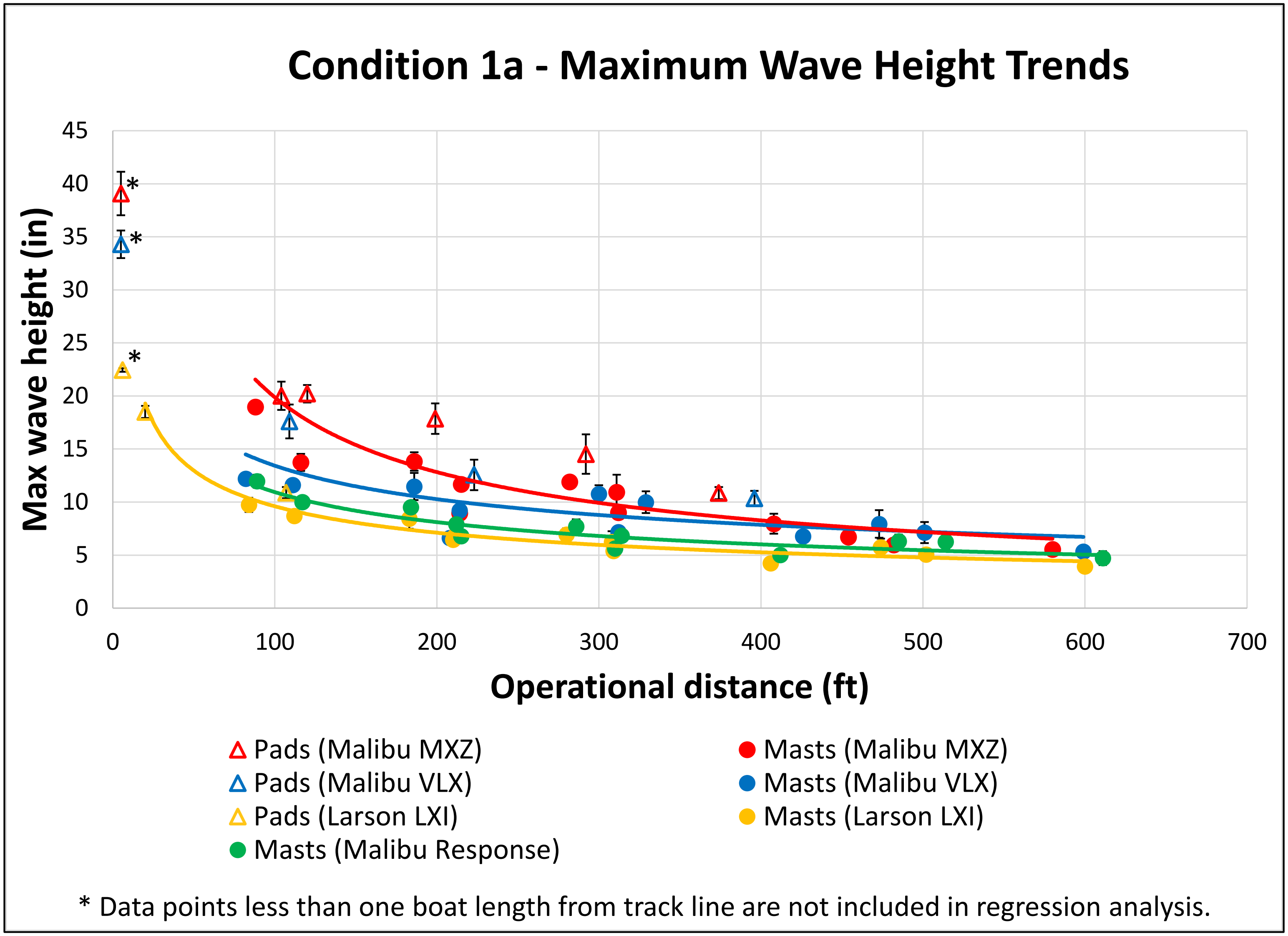


**Figure 15. Condition 1a best-fit power law trendlines of the four test boats showing maximum wave heights over operational distance.**

### 5.1.2 Total Wave Energy

All four test boats showed a nonlinear decrease in total wave energy with increasing operational distance (Figure 16 and 17). The maximum total wave energy recorded for the Larson LXI 210, Malibu VLX, and Malibu MXZ was 5,400 J/m, 12,200 J/m, and 16,300 J/m, respectively, which occurred within 4-6 ft of operational distance.

Figure 18 compares all the data and trendlines for the four boats. The Larson LXI 210 and Malibu Response LX had nearly identical total wave energies and attenuation rates. At 120 ft of operational distance, their total wave energies had attenuated to 2,000 J/m, and by 600 ft they had decreased to roughly 700 J/m. The Malibu VLX had the second greatest total wave energy at all distances, with a maximum level of 12,200 J/m that attenuated to 2,000 J/m around 400 ft of operational distance. At 600 ft, the total wave energy had decreased to around 1,000 J/m. Of all the boats tested, the Malibu MXZ produced the greatest total wave energy at all distances, with an initial maximum of 16,300 J/m that, like the Malibu VLX, decreased to 2,000 J/m around 400 ft. At 600 ft of operational distance, the total wave energy had attenuated to roughly 1,000 J/m.

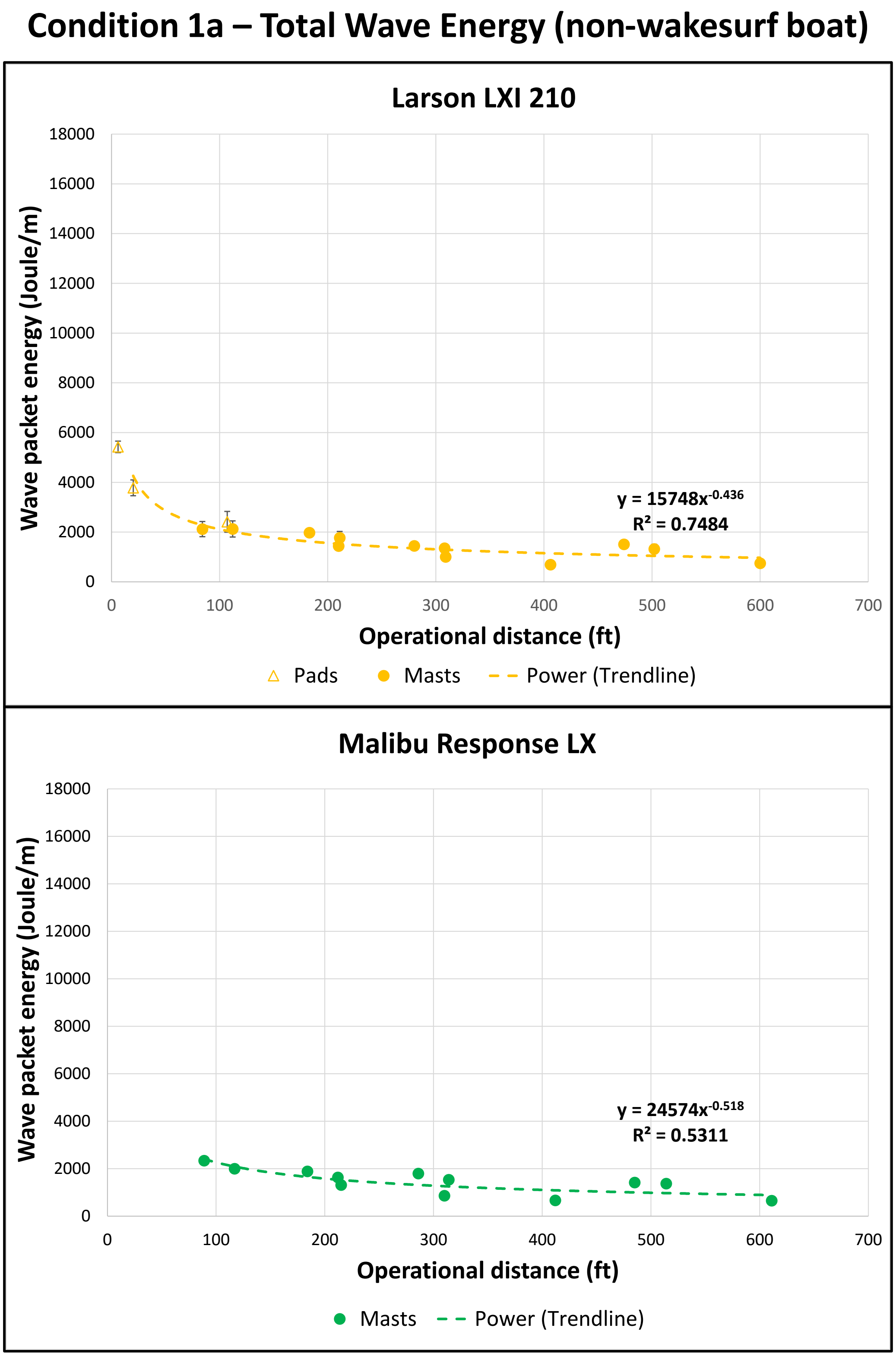


**Figure 16. Total wake packet energy as a function of operational distance for the two non-wakesurf boats tested under Condition 1a. There are no data for the Pads for the Malibu Response LX due to technical issues with the ADCP on test day. Data points less than one boat length from the track line were not included in the regression analysis.**

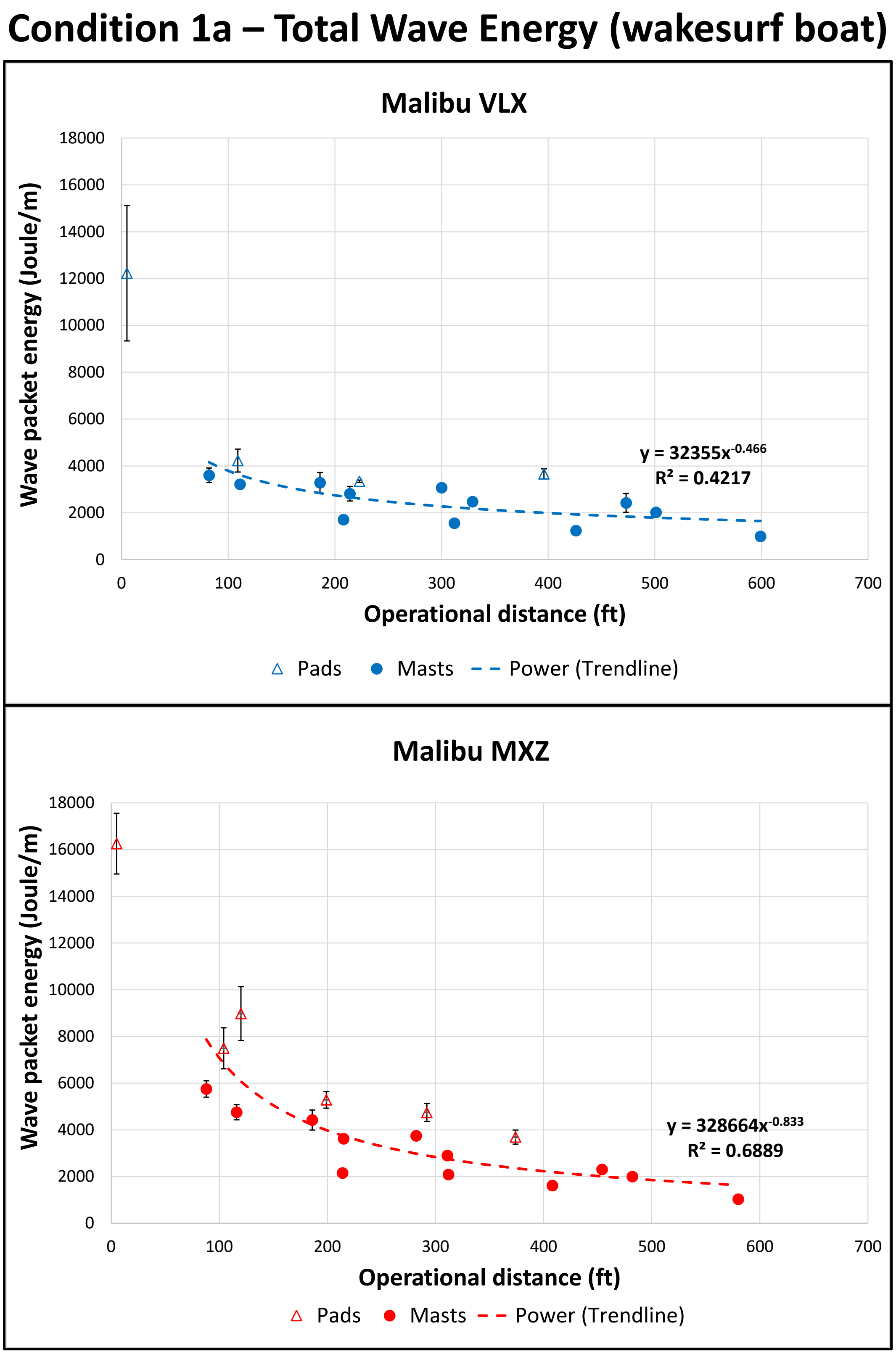


**Figure 17. Total wake packet energy as a function of operational distance for the two wakesurf boats tested under Condition 1a. Data points less than one boat length from the track line were not included in the regression analysis.**

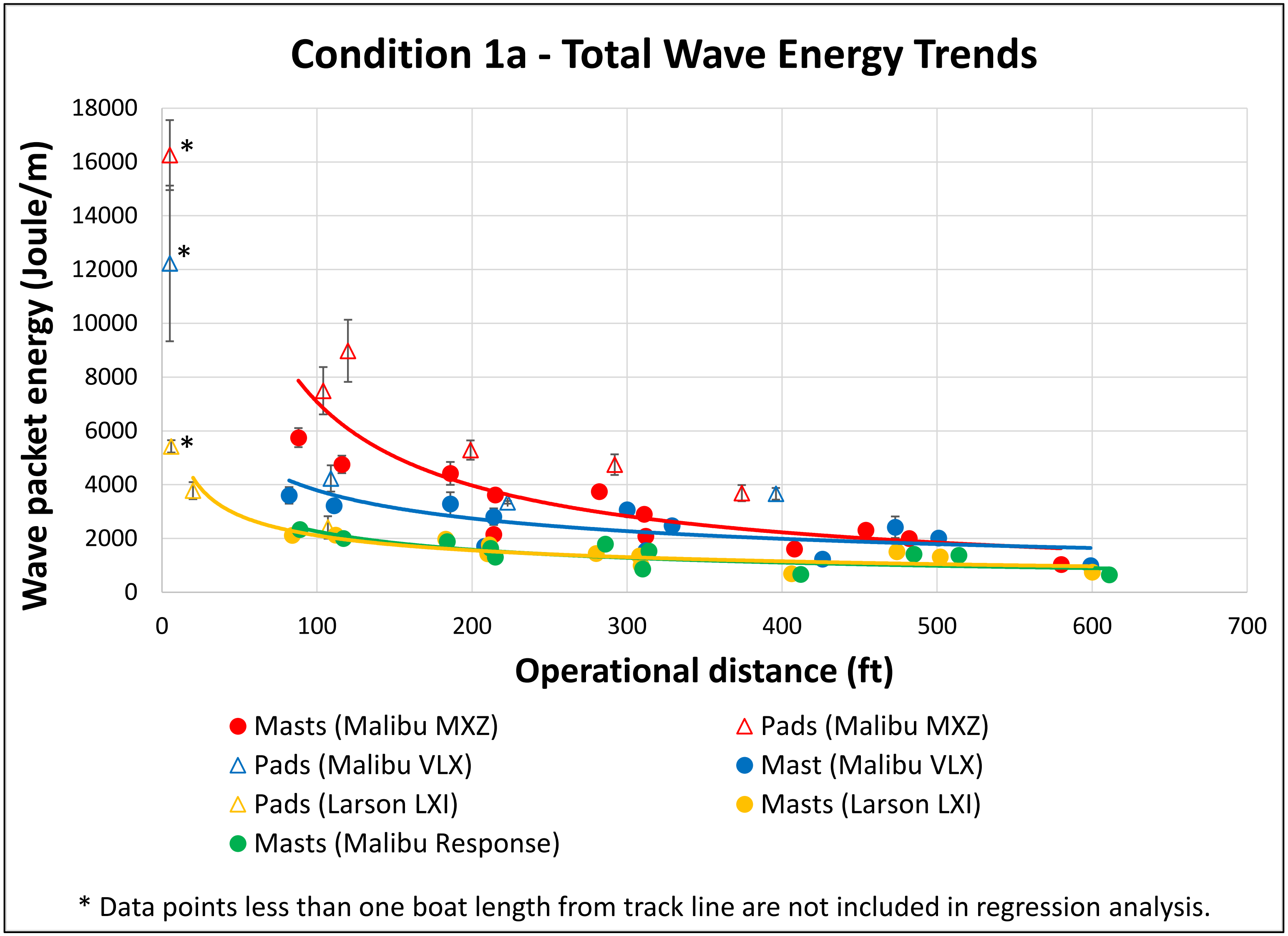


**Figure 18. Condition 1a trendlines for the four test boats showing total wave energy over operational distance.**

### 5.1.3 Maximum Wave Power

Like maximum wave height and total wave energy, the maximum wave power showed a well-defined, nonlinear decrease as operational distance increased (Figure 19 and 20). The initial maximum wave powers recorded for the Larson LXI 210, Malibu VLX, and Malibu MXZ were 860 J/m-s, 1,970 J/m-s, and 2,370 J/m-s, respectively, which occurred within an operational distance of 4-6 ft.

A comparison of all data and trendlines for each boat is presented in Figure 21. The Larson LXI 210 attenuated from an initial maximum wave power of 860 J/m-s to 50 J/m-s over the first 110 ft of operational distance. For operational distances greater than 210 ft, the maximum wave power for the Larson LXI 210 and Malibu Response LX were nearly identical, and by 600 ft they had decreased to roughly 10 J/m-s. The Malibu VLX had an initial maximum wave power of 1,970 J/m-s that attenuated to 100 J/m-s at an operational distance of 300 ft. By 600 ft, the maximum wave power decreased to roughly 40 J/m-s. Finally, the Malibu MXZ produced the greatest maximum wave powers at all operational distances, with an initial maximum wave power of 2,370 J/m-s that decreased to 100 J/m-s at approximately 400 ft, and 50 J/m-s by 600 ft of operational distance.

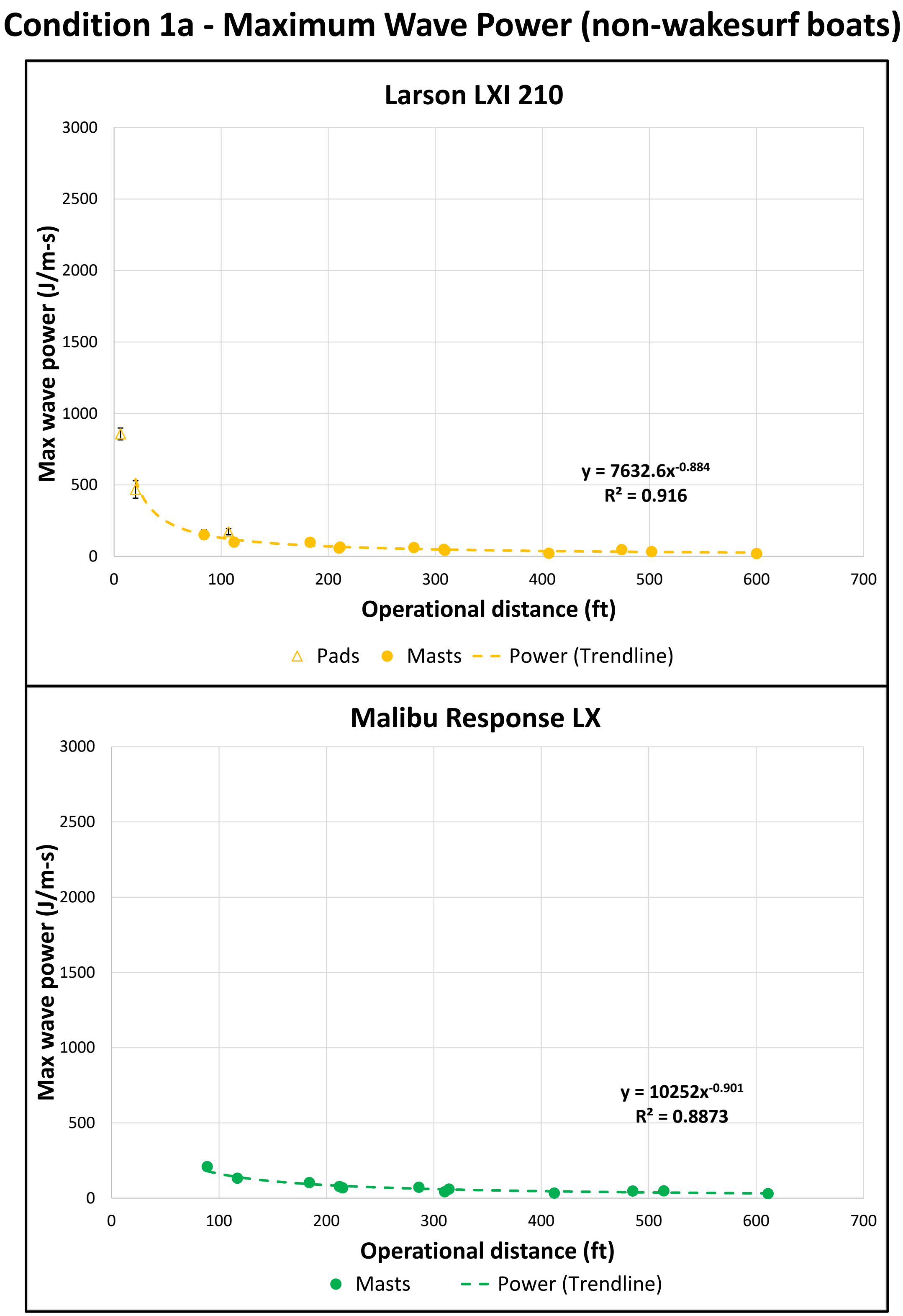


**Figure 19. Maximum wave power as a function of wave propagation distance for the two non-wakesurf boats tested under Condition 1a. There are no data for the Pads for the Malibu Response LX due to technical issues with the ADCP on test day. Data points less than one boat length from the track line were not included in the regression analysis.**

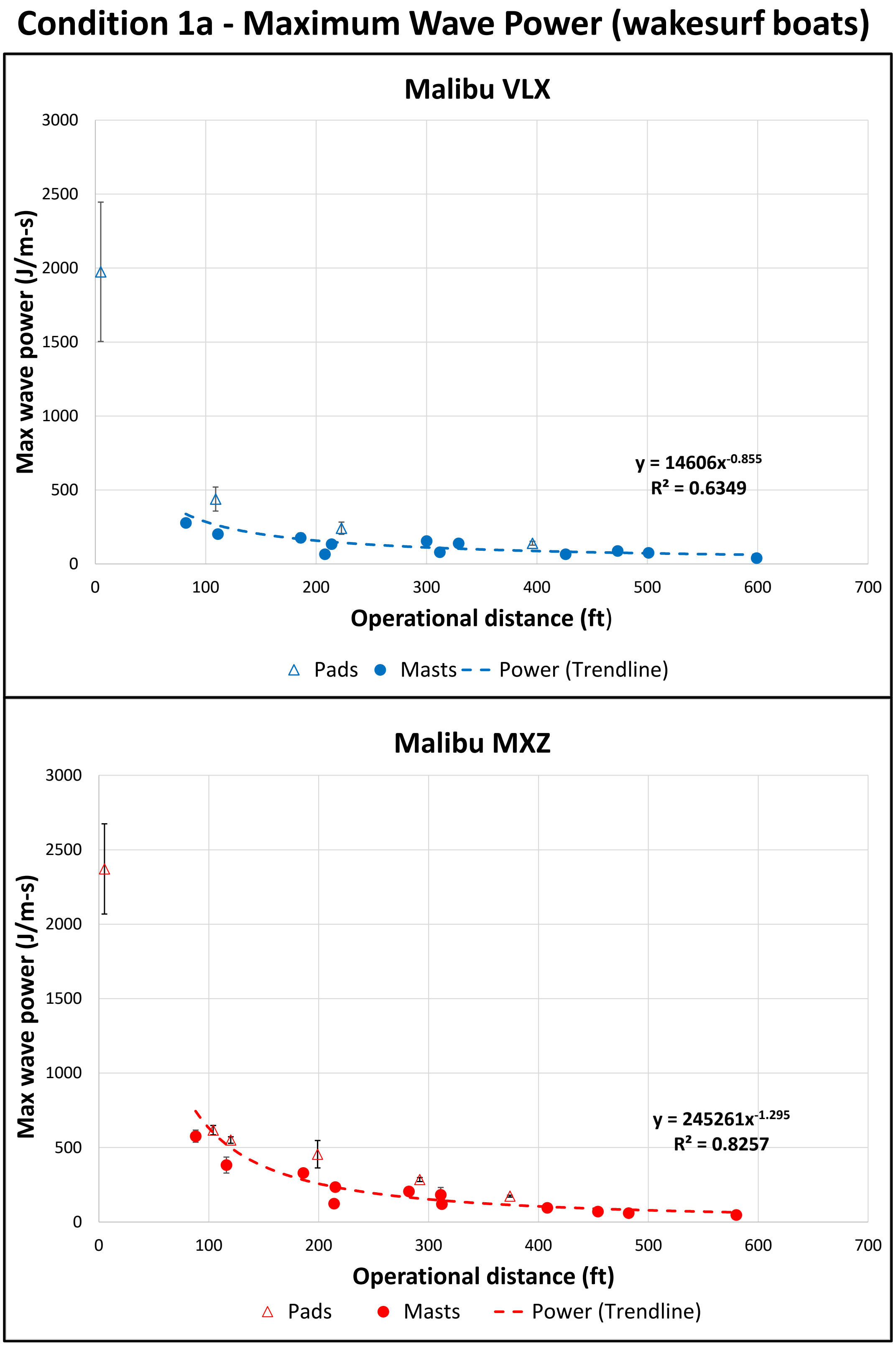


**Figure 20. Maximum wave power as a function of wave propagation distance for the two wakesurf boats tested under Condition 1a. Data points less than one boat length from the track line were not included in the regression analysis.**

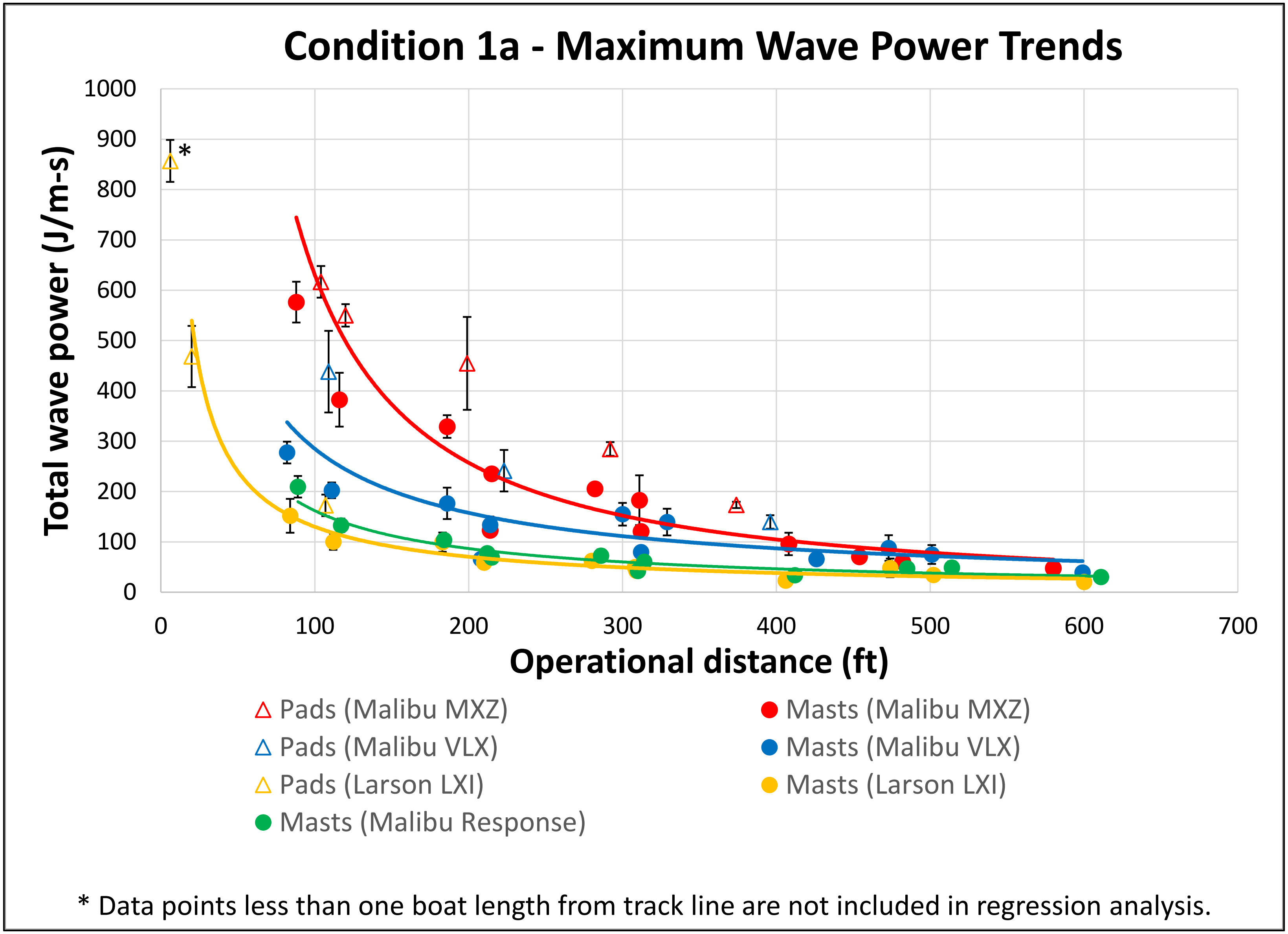


**Figure 21. Condition 1a trendlines for the four test boats showing maximum wave power over operational distance.**

## 5.2 Condition 2

This section discusses the results of the data analyses for maximum wave height, total wave energy, and maximum wave power for each of the four boats tested under operating Condition 2. Detailed descriptions of the boat operating conditions are provided in Section 3.6 and Table 3. It is important to note that the magnitudes of wave height, energy, and power were much smaller when the watercraft was planing. It is also important to note that the ADCP data at operational distances less than 100 ft for the Malibu MXZ under Condition 2 were noisy and thus eliminated from this analysis (see Section 6.2.1 for more details).

### 5.2.1 Maximum Wave Height

In general, all boats follow the same nonlinear decrease in maximum wave height with increasing operational distance (Figures 22, 23 and 24). The initial maximum wave height recorded for the Larson LXI 210 was 13 in at a distance of 9 ft. The maximum wave height was 6 in at roughly 150 ft, and continued decreasing to less than 4 in at operational distances greater than 600 ft. The Malibu Response LX recorded a maximum wave height of 8 in at 100 ft that attenuated to 6 in by 200 ft of propagation. At roughly 425 ft of operational distance, the maximum wave height had decreased to 4 in. The Malibu VLX produced an initial maximum wave height of 16 in at 10 ft, and attenuated to approximately 11 in at 100 ft of operational distance. By 500 ft of operational distance the maximum wave height decreased to 6 in. Like the Malibu VLX, the Malibu MXZ produced a maximum wave height of 11 in at roughly 100 ft. At 300 ft of operational distance, the maximum wave height was 6 in, and by 500 ft had decreased to 4 in.

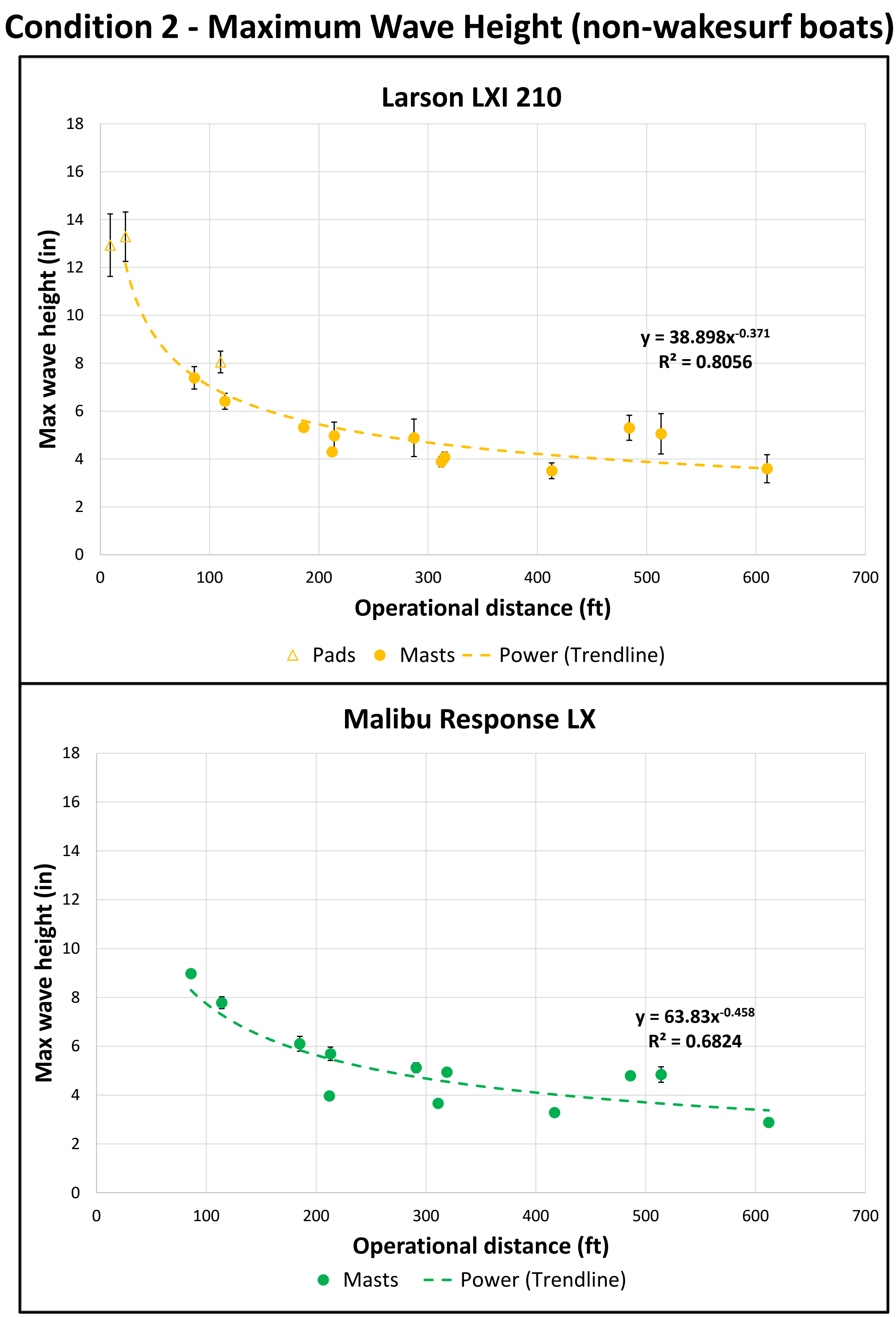


**Figure 22. Maximum wave height as a function of operational distance for the two non-wakesurf boats tested under Condition 2. There are no data for the Pads for the Malibu Response LX due to technical issues with the ADCP on test day. Data points less than one boat length from the track line were not included in the regression analysis.**

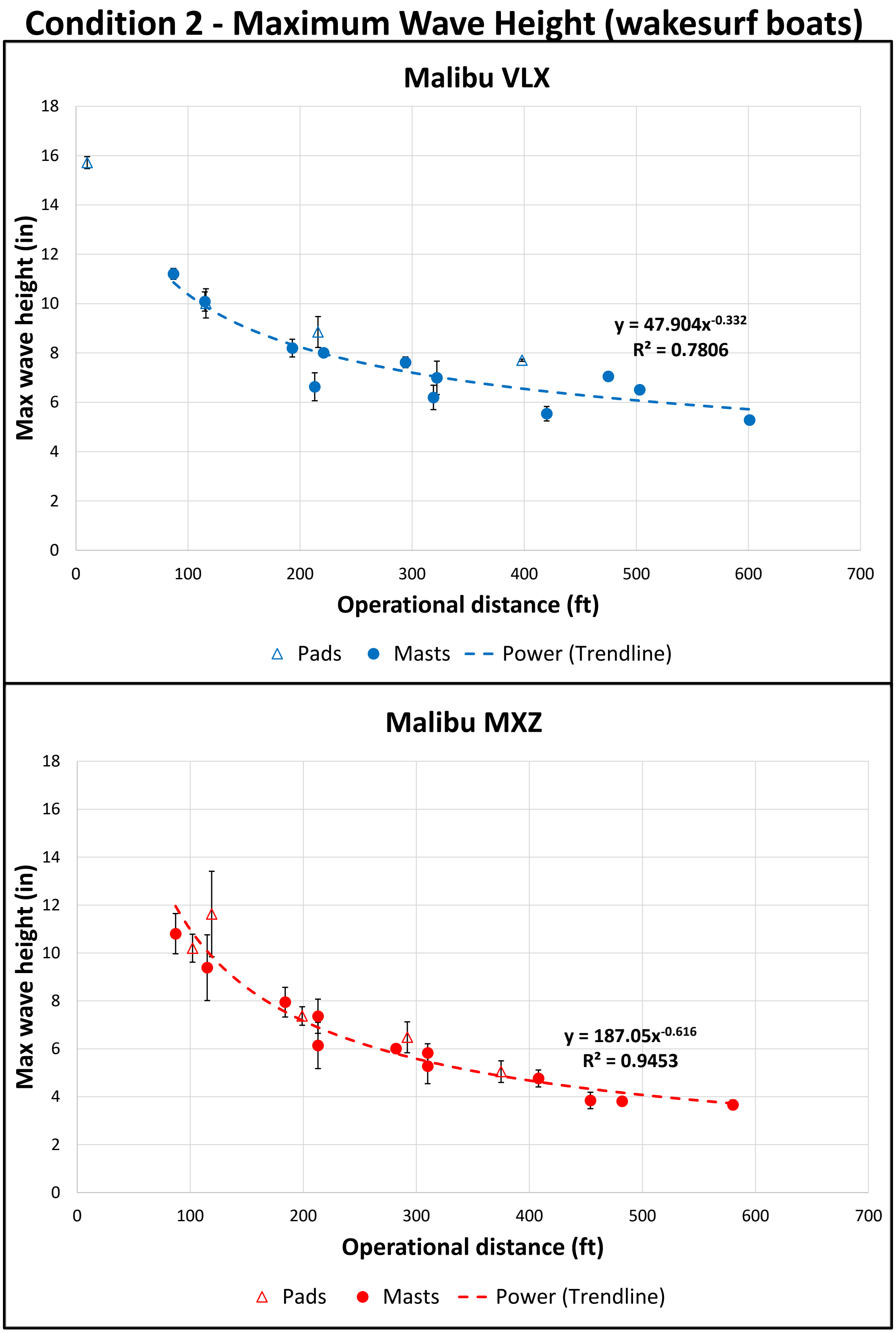


**Figure 23. Maximum wave height as a function of operational distance for the two wakesurf boats tested under Condition 2. The Pad data at distances less than 100 ft for the Malibu MXZ were noisy and thus eliminated from this analysis. Data points less than one boat length from the track line were not included in the regression analysis.**

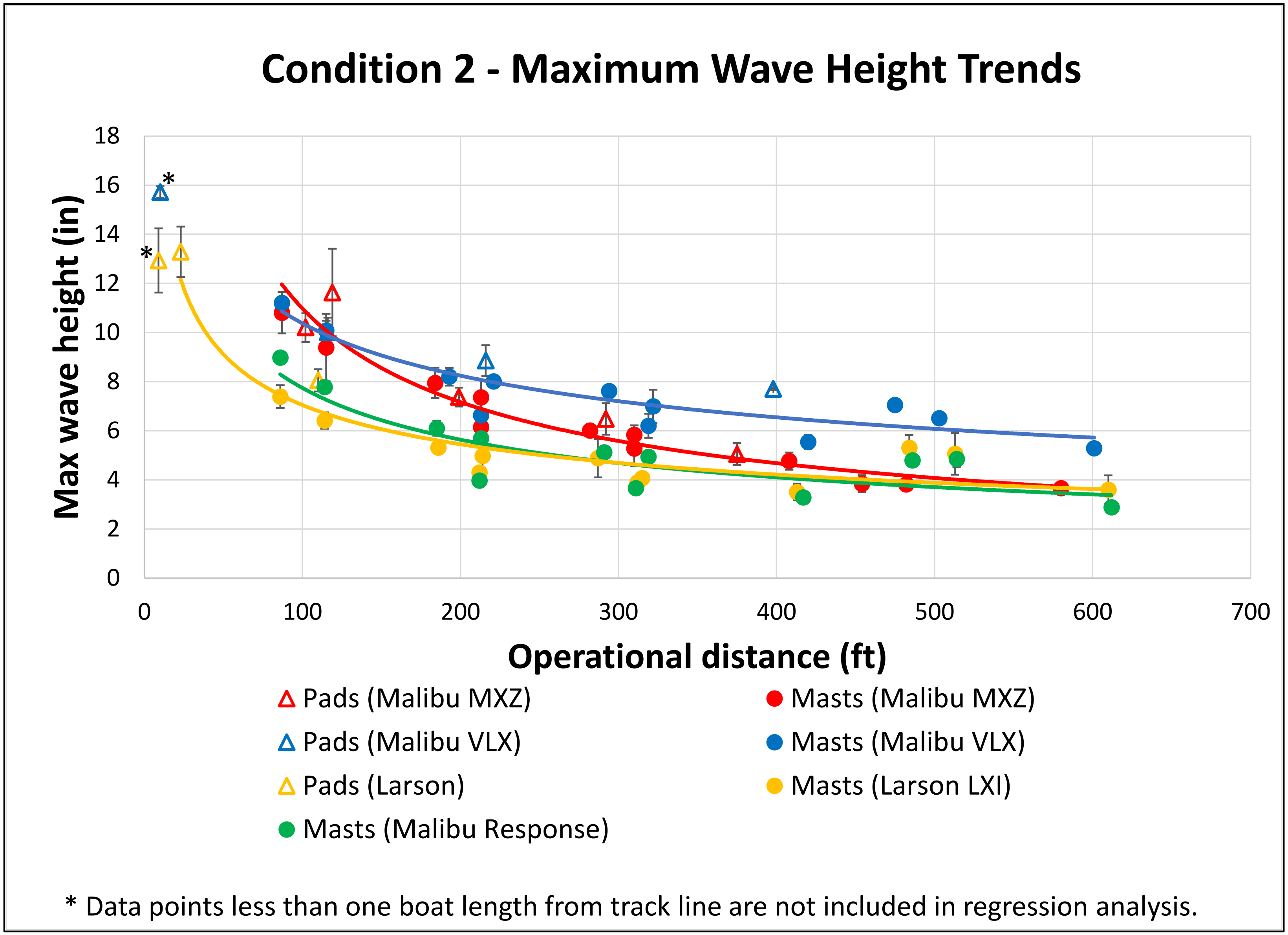


**Figure 24. Condition 2 trendlines of the four test boats showing maximum wave heights over operational distance.**

### 5.2.2 Total Wave Energy

The attenuation of the total wave energy as a function of operational distance shows a nonlinear decreasing trend for all test boats (Figures 25, 26 and 27). The Larson LXI 210 and Malibu Response LX had little change in total wave energy with operational distance, with the data only slightly varying between 1,500 J/m and 700 J/m. Likewise, the Malibu VLX had little change in total wave energy attenuation, as the magnitudes were between 2,500 J/m and 1,000 J/m over the full range of operational distances. The Malibu MXZ data show a wider range of total wave energies between 2,800 J/m and 900 J/m.

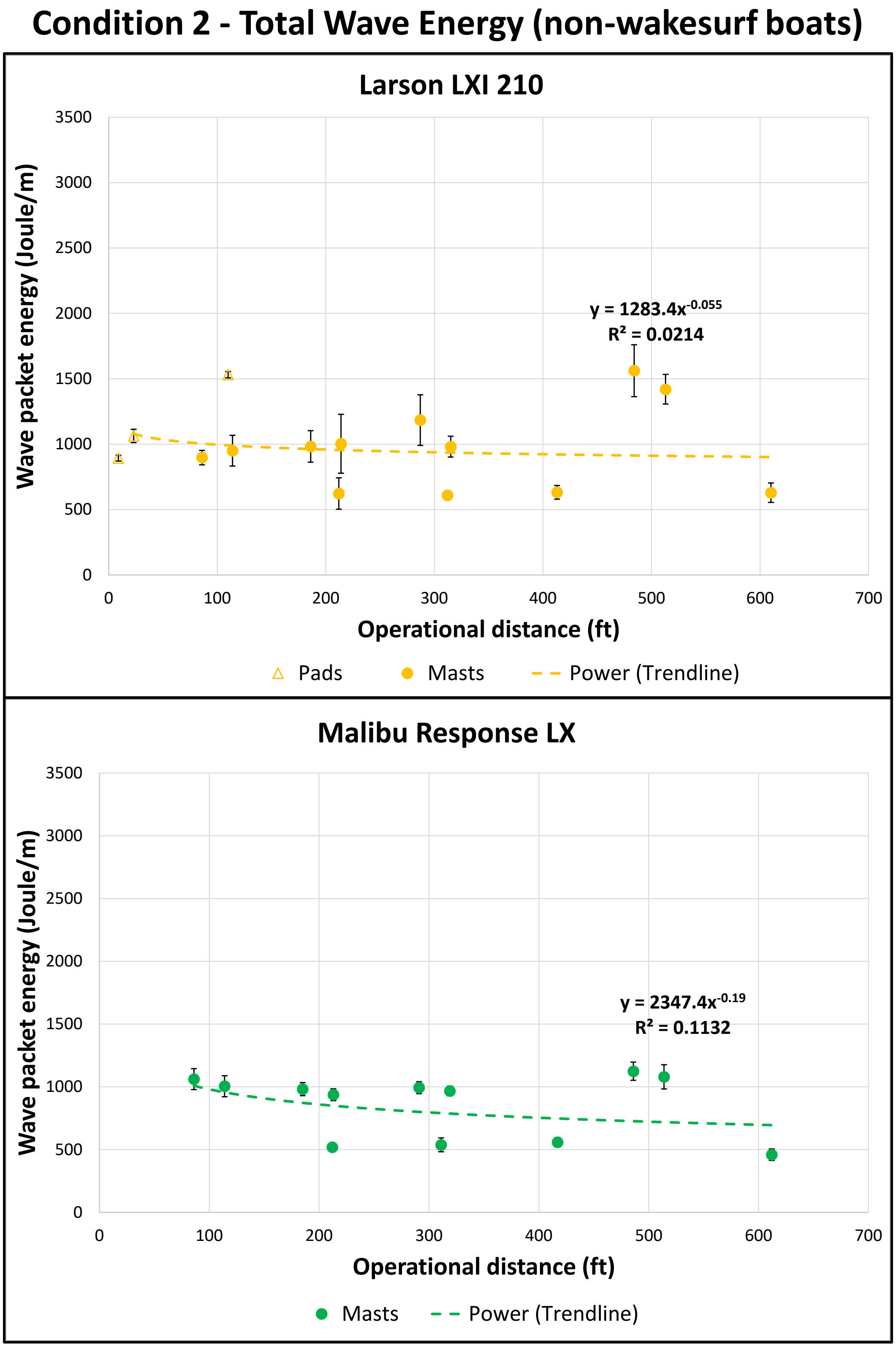


**Figure 25. Total wake packet energy as a function of operational distance for the two non-wakesurf boats tested under Condition 2. There are no data for the Pads for the Malibu Response LX due to technical issues with the ADCP on test day. Data points less than one boat length from the track line were not included in the regression analysis.**

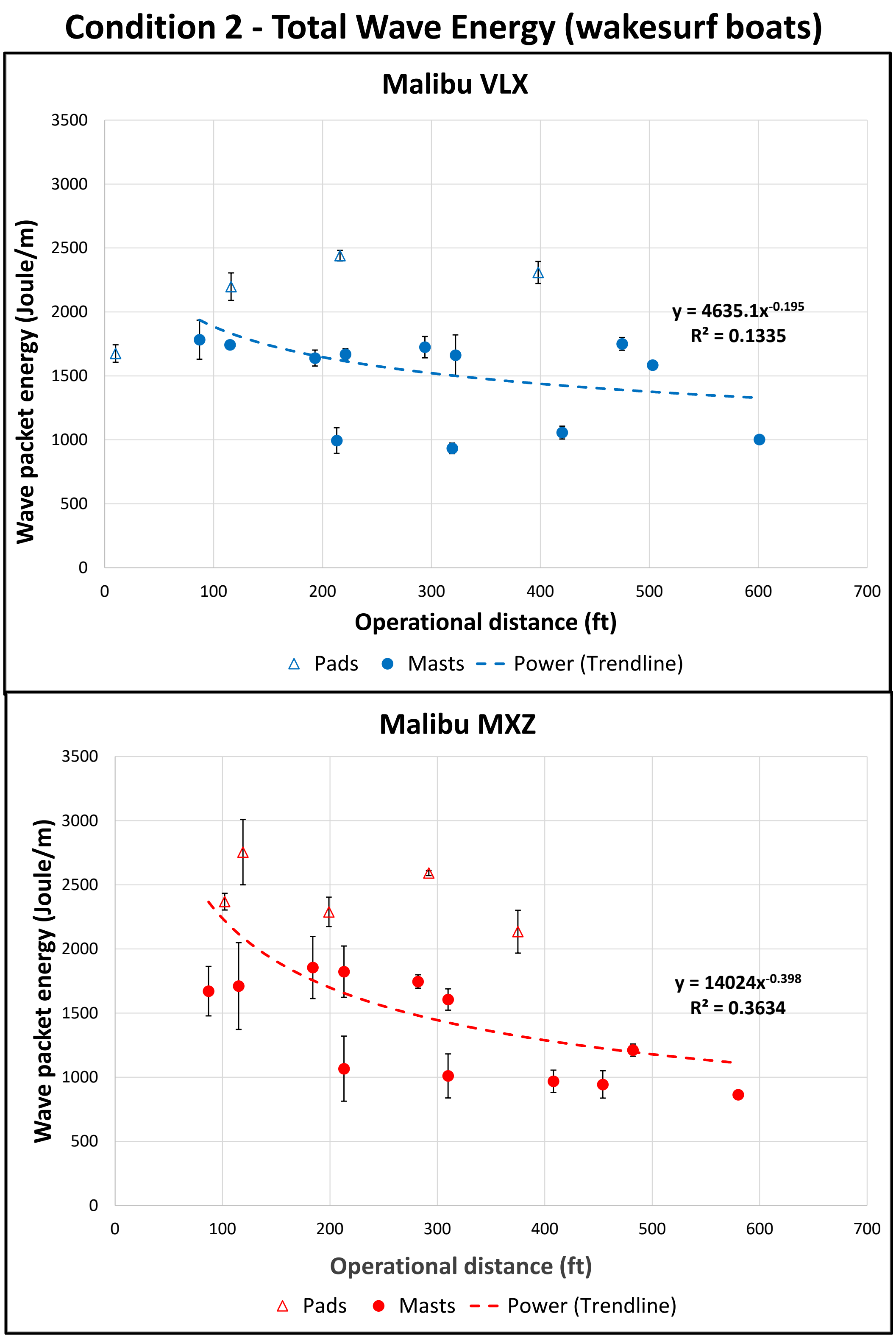


**Figure 26. Total wake packet energy as a function of operational distance for the two wakesurf boats tested under Condition 2. The Pad data at distances less than 100 ft for the Malibu MXZ were noisy and thus eliminated from this analysis. Data points less than one boat length from the track line were not included in the regression analysis.**

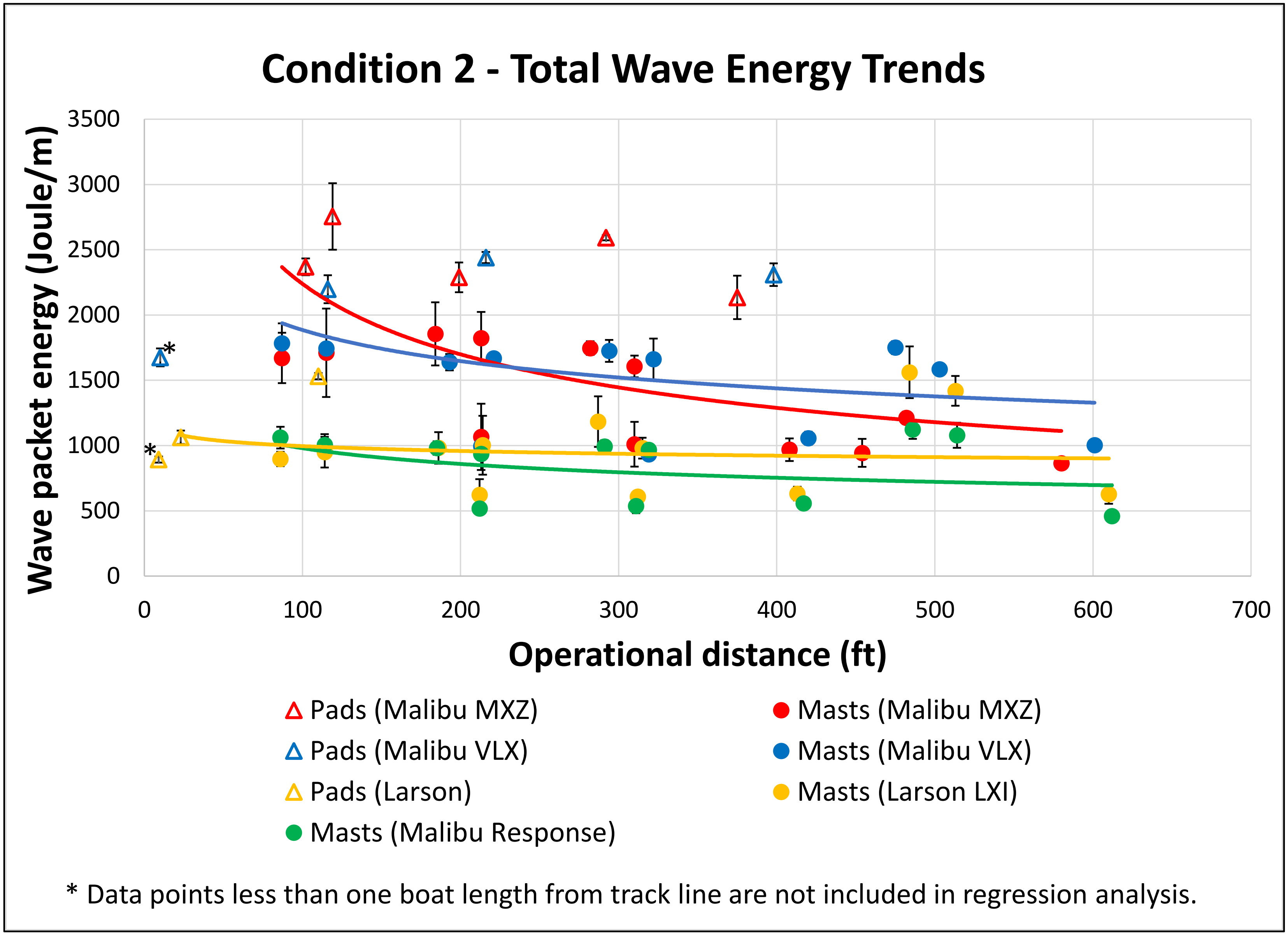


**Figure 27. Condition 2 trendlines for the four test boats showing total wave energy over operational distance.**

### 5.2.3 Maximum Wave Power

Attenuation of the maximum wave power with operational distance shows a decreasing nonlinear trend for all boats tested (Figures 28, 29 and 30). The initial maximum wave power for the Larson LXI 210 was roughly 180 J/m-s at a distance of 20 ft. The Malibu Response LX recorded a maximum wave power of approximately 80 J/m-s at 100 ft of operational distance. After a distance of roughly 300 ft, the maximum wave power for the Larson LXI 210 and Malibu Response LX were nearly identical at <25 J/m-s. The Malibu VLX produced an initial maximum wave power of about 270 J/m-s at 10 ft, which attenuated to approximately 30 J/m-s at 600 ft. The Malibu MXZ recorded a maximum wave power of 140 J/m-s at 100 ft, which decreased to roughly 40 J/m-s at 300 ft and 20 J/m-s at 600 ft.

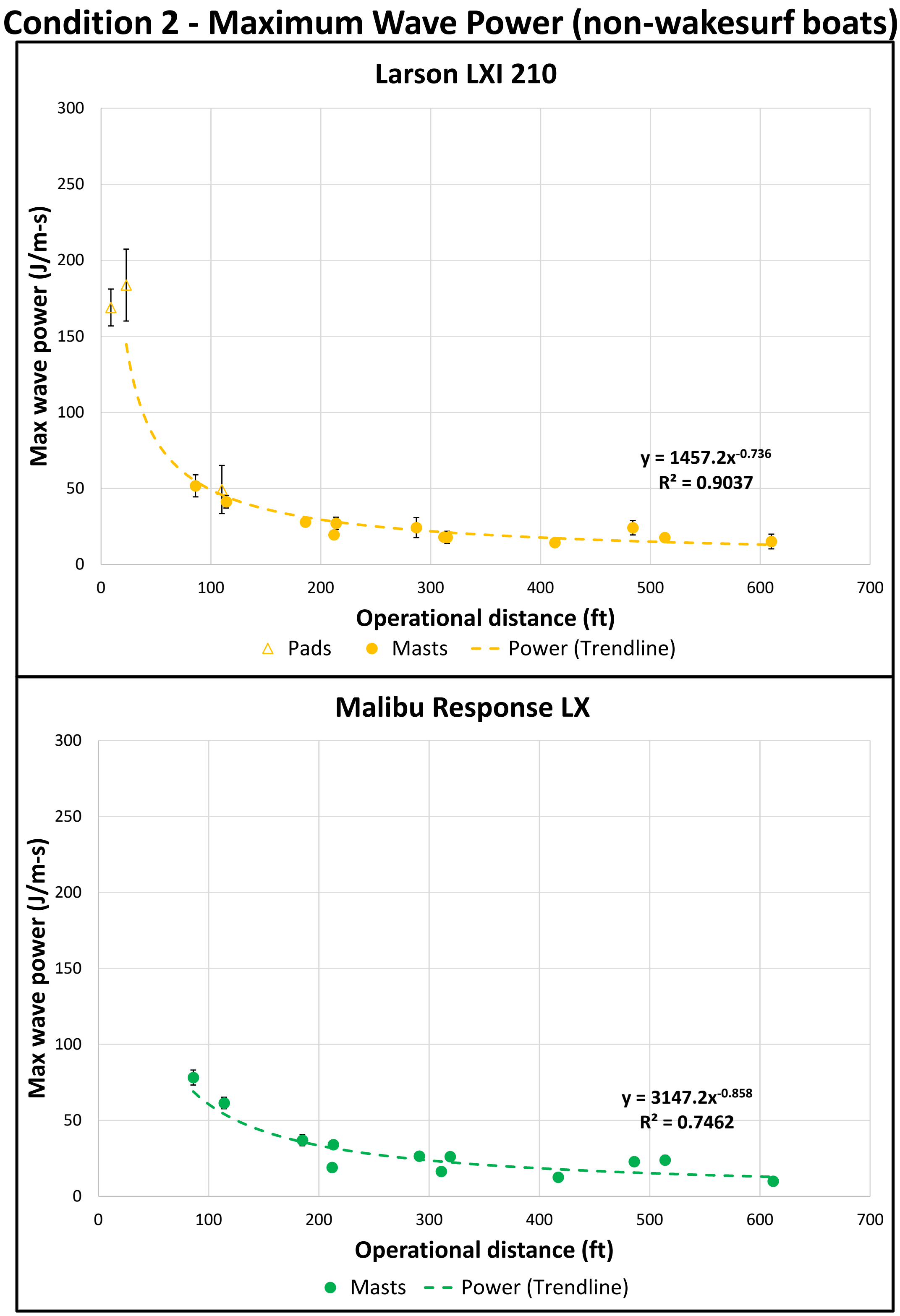


**Figure 28. Maximum wave power as a function of operational distance for the two non-wakesurf boats tested under Condition 2. There are no data for the Pads for the Malibu Response LX due to technical issues with the ADCP on test day. Data points less than one boat length from the track line were not included in the regression analysis.**

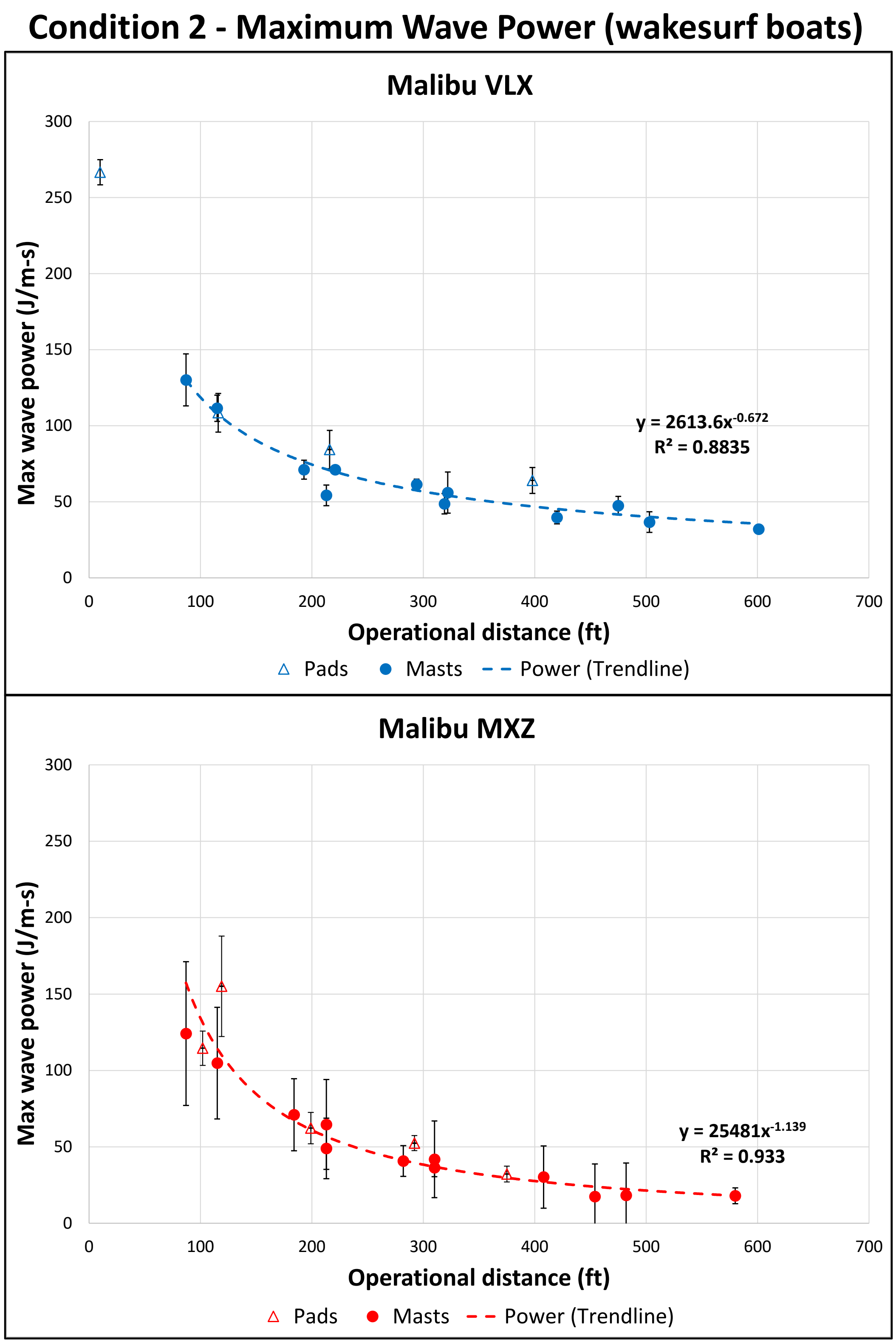


**Figure 29. Maximum wave power as a function of operational distance for the two wakesurf boats tested under Condition 2. The Pad data at distances less than 100 ft for the Malibu MXZ were noisy and thus eliminated from this analysis. Data points less than one boat length from the track line were not included in the regression analysis.**

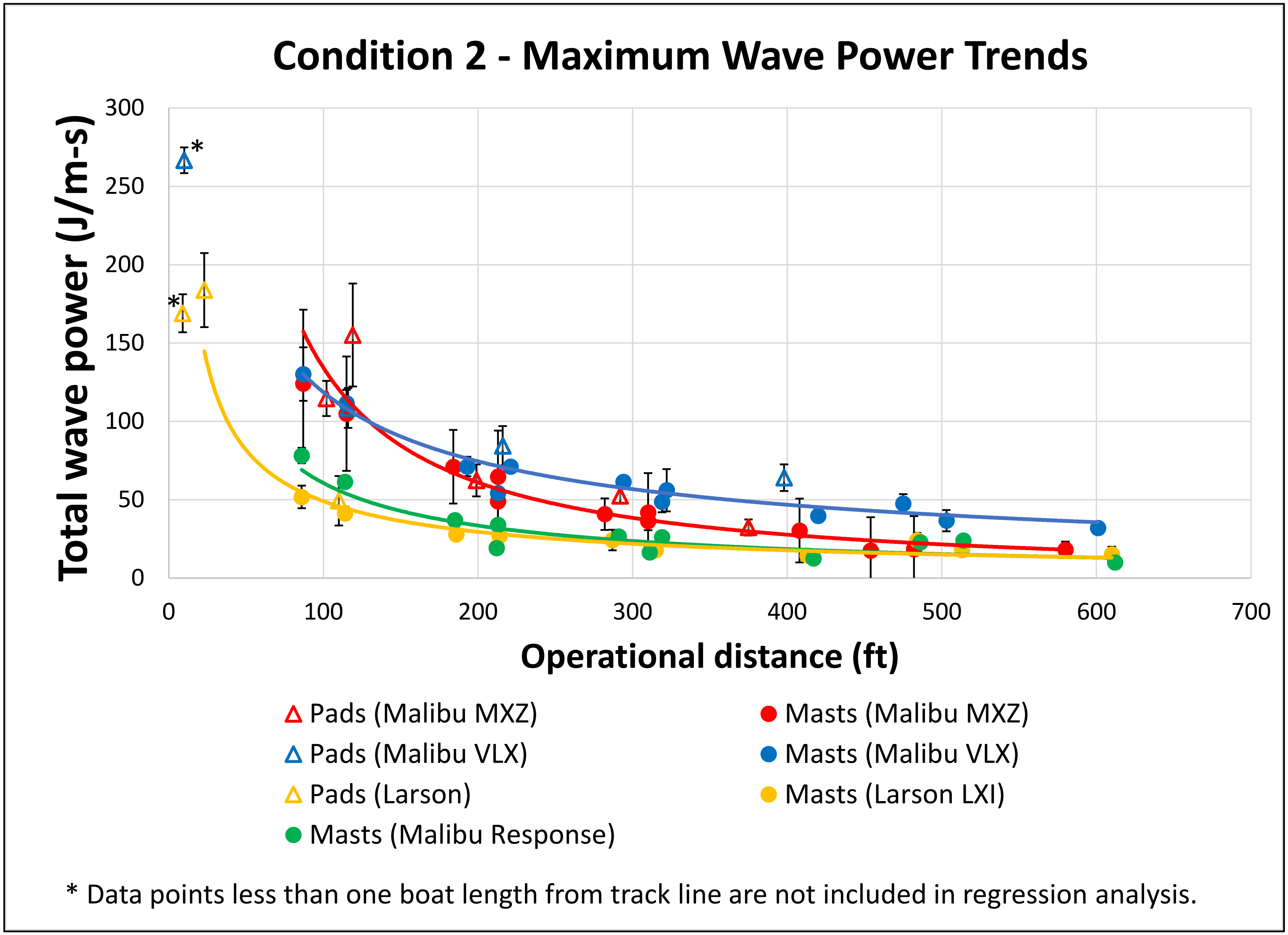


**Figure 30. Condition 2 trendlines for the four test boats showing maximum wave power over operational distance.**

## 5.3 Condition 1a (ballasts full) versus Condition 1b (ballasts empty)

Condition 1a for the Malibu VLX and Malibu MZX included operating with the ballast tanks completely full (results in Section 5.1). For Condition 1b, all variables remained the same except the ballast tanks were completely empty (Section 3.6.3, Table 3). Removing just the ballast water variable allowed for the comparison of its effects on measured wake wave characteristics (i.e., maximum wave height, total wave energy, and maximum wave power).

### 5.3.1 Malibu VLX

Overall, Condition 1a results (i.e., ballasts full) are very similar to Condition 1b results (i.e., ballasts empty) when maximum wave height, total wave energy, and maximum wave power are compared (Figures 31, 32 and 33). In the first 100 ft of operational distance, there appears to be an influence of the ballast weight on the measured wake wave characteristics. At a distance of 5 ft, the initial maximum wave heights were 34 in for ballasts full and 27 in for ballasts empty. However, by 100 ft the maximum wave height of both conditions had attenuated to approximately 14 in. At operational distances greater than 100 ft, the attenuating rates were very similar and had decreased to roughly 6 in by 600 ft. At an operational distance of 5 ft, the initial total wave energy was 12,200 J/m when the ballasts were full and 10,000 J/m when the ballasts were empty, however, it should be noted that the standard deviations for these data points were quite large. Again, by 100 ft of distance, the total wave energy of both conditions had attenuated to nearly identical values of approximately 3,900 J/m. Beyond this distance, the total wave energy continued to be very similar and eventually decreased to roughly 1,900 J/m at 600 ft. Finally, at 5 ft of operational distance, the initial maximum power was almost 2,000 J/m-s and 1,600 J/m-s for ballasts full and ballasts empty, respectively. Again, like initial total wave energy, the standard deviations for these data points were quite large. The maximum wave power for both conditions had attenuated to near identical values of roughly 250 J/m-s by 100 ft, and continued to attenuate to roughly 50 J/m-s at 600 ft.

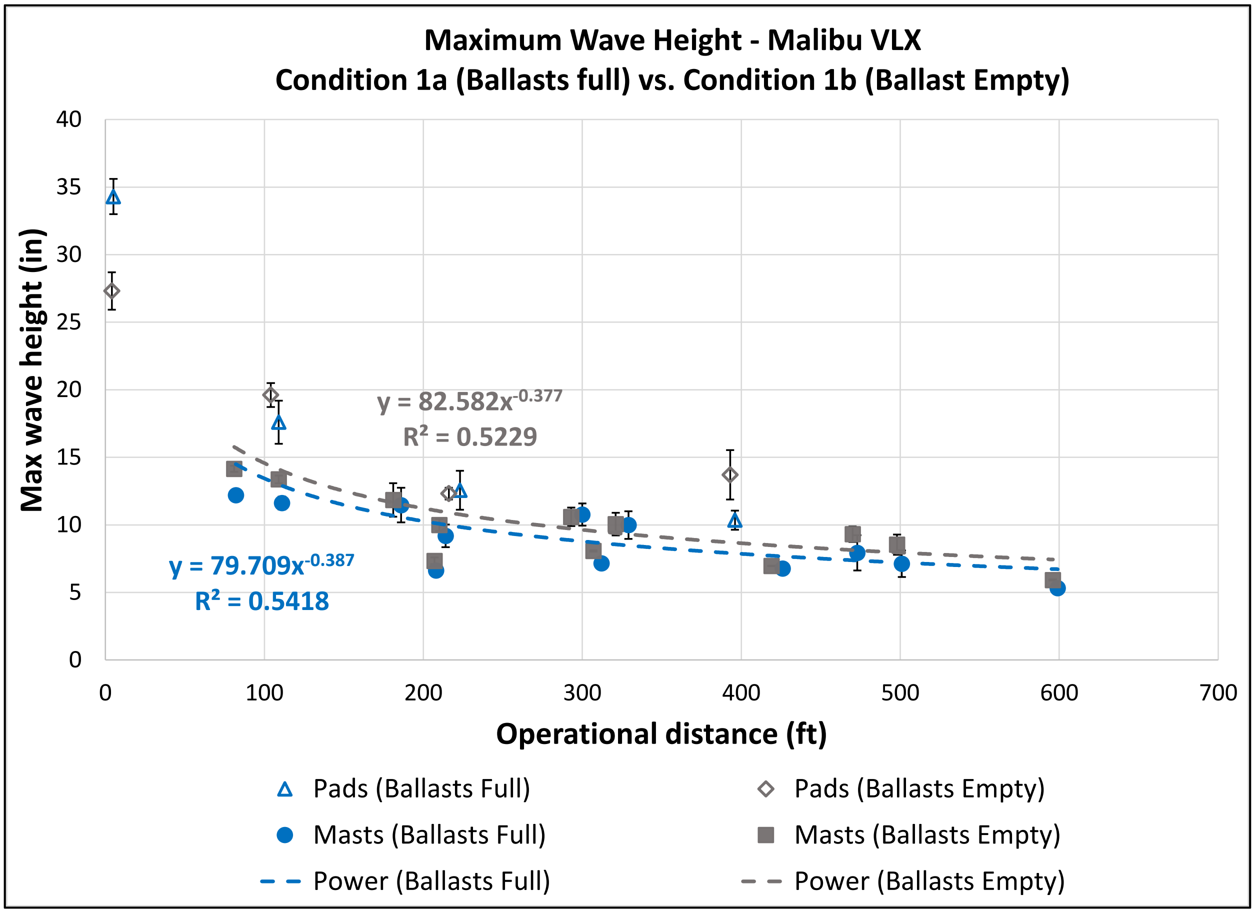


**Figure 31. Comparison of the maximum wave height of the Malibu VLX when the ballast tanks were full and empty. Data points less than one boat length from the track line were not included in the regression analysis.**

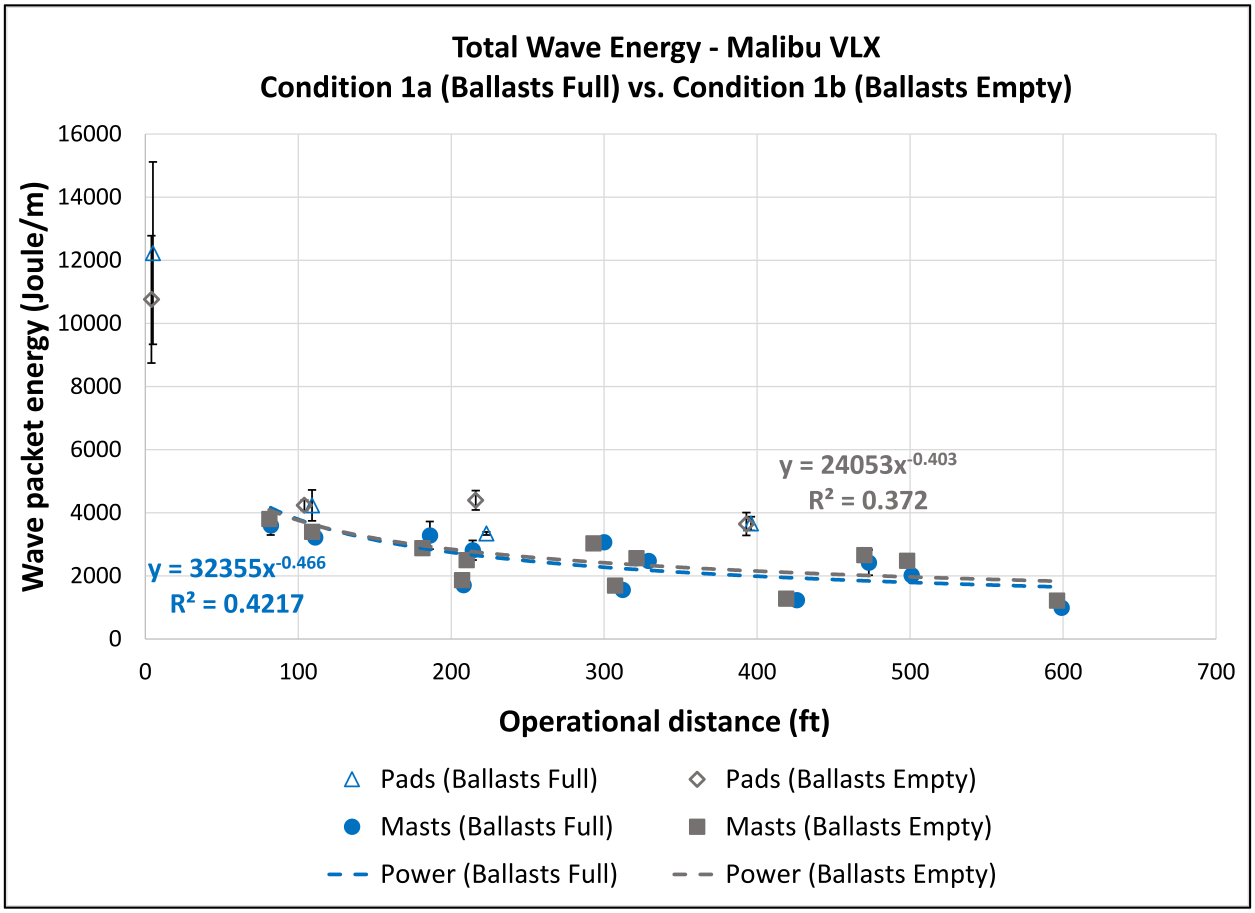


**Figure 32. Comparison of the total wave energy of the Malibu VLX when the ballast tanks were full and empty. Data points less than one boat length from the track line were not included in the regression analysis.**

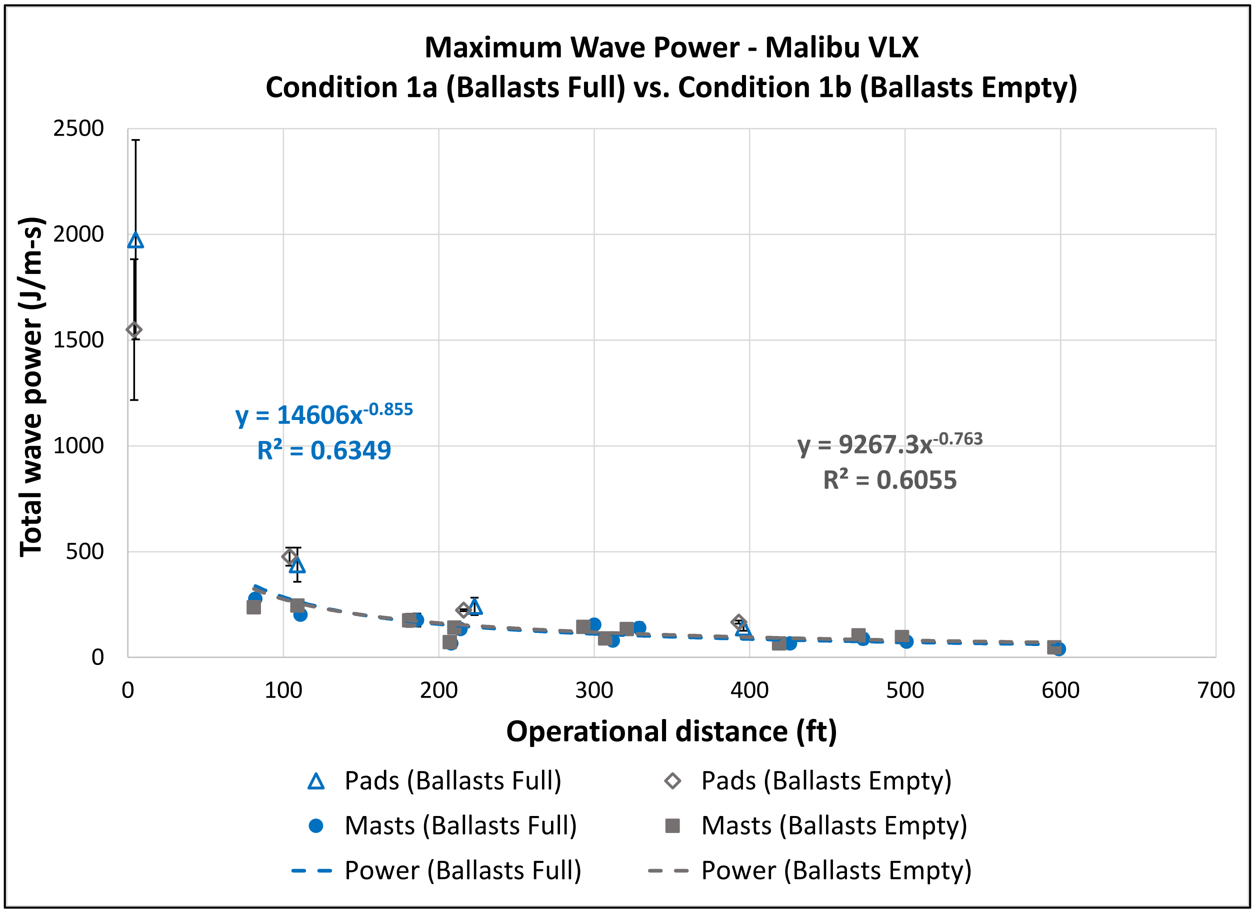


**Figure 33. Comparison of the maximum wave power of the Malibu VLX when the ballast tanks were full and empty. Data points less than one boat length from the track line were not included in the regression analysis.**

### 5.3.2 Malibu MXZ

Like the Malibu VLX, the Malibu MXZ has very similar results when Condition 1a (ballasts full) was compared to Condition 1b (ballasts empty) (Figures 34, 35 and 36). The data suggest there is an influence on the initial maximum wave height when the ballast tanks were full. At an operation distance of 5 ft, the initial maximum wave height was 39 in with the ballasts full and 31 in with the ballasts empty. However, the data and best-fit trendlines are nearly identical along the entire operational distance. By 590 ft the maximum wave heights attenuated to roughly 8 in. The total wave energy averaged roughly 1,000 J/m higher in the first 200 ft when the ballast tanks were full versus when they were empty. Between 200-400 ft, the influence of the ballast water could still be seen, however, the difference was less than ~500 J/m. After 400 ft, there was no discernable difference in total wave energy. Considering maximum wave power, the initial maximum measured at an operational distance of 5 ft was almost 2,400 J/m-s when the ballast tanks were full, and 1,900 J/m-s when the ballast tanks were empty. However, the standard deviations for these data points were quite large. By 100 ft the maximum wave power was approximately 500 J/m-s and this continued attenuating to about 40 J/m-s by 580 ft for both conditions.

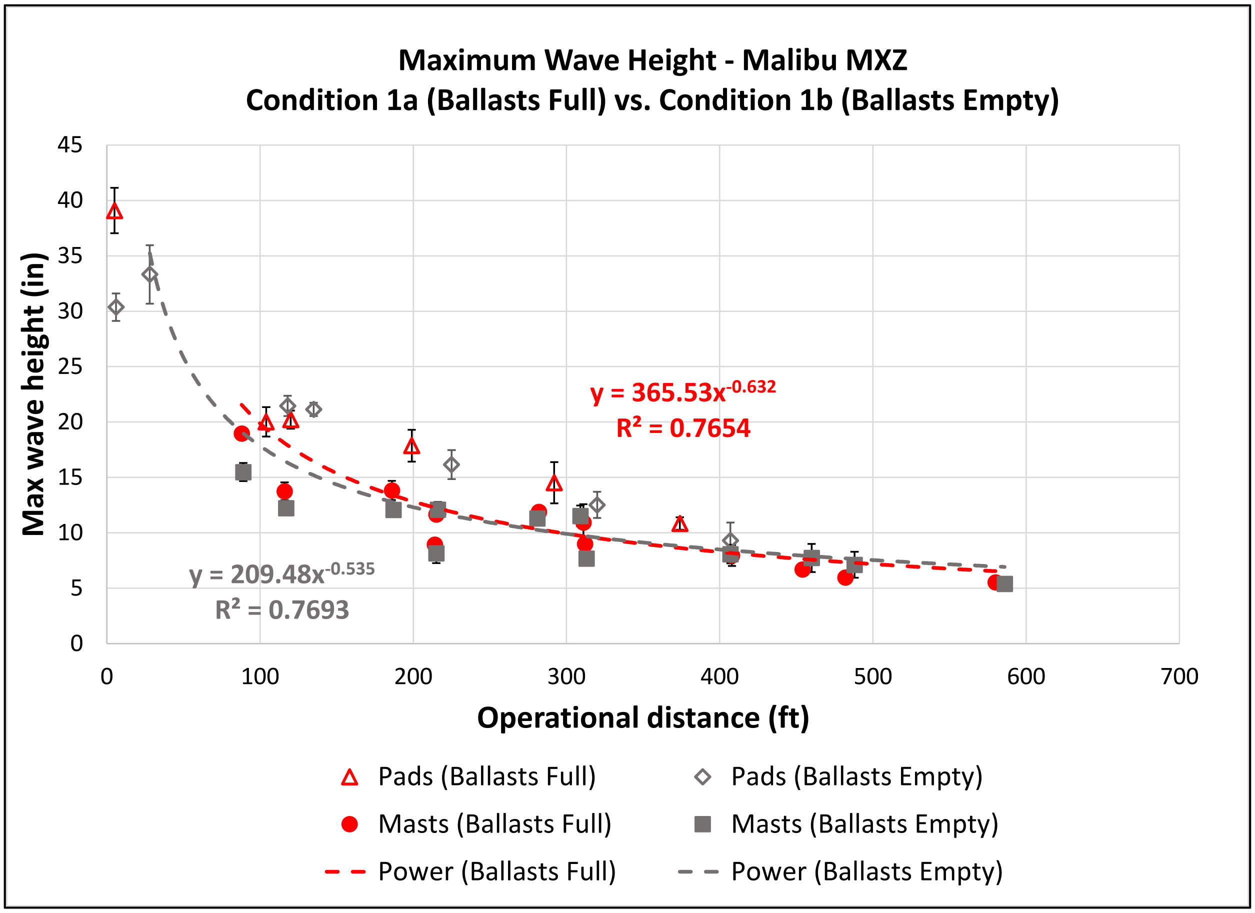


**Figure 34. Comparison of the maximum wave height of the Malibu MXZ when the ballast tanks were full and empty. Data points less than one boat length from the track line were not included in the regression analysis.**

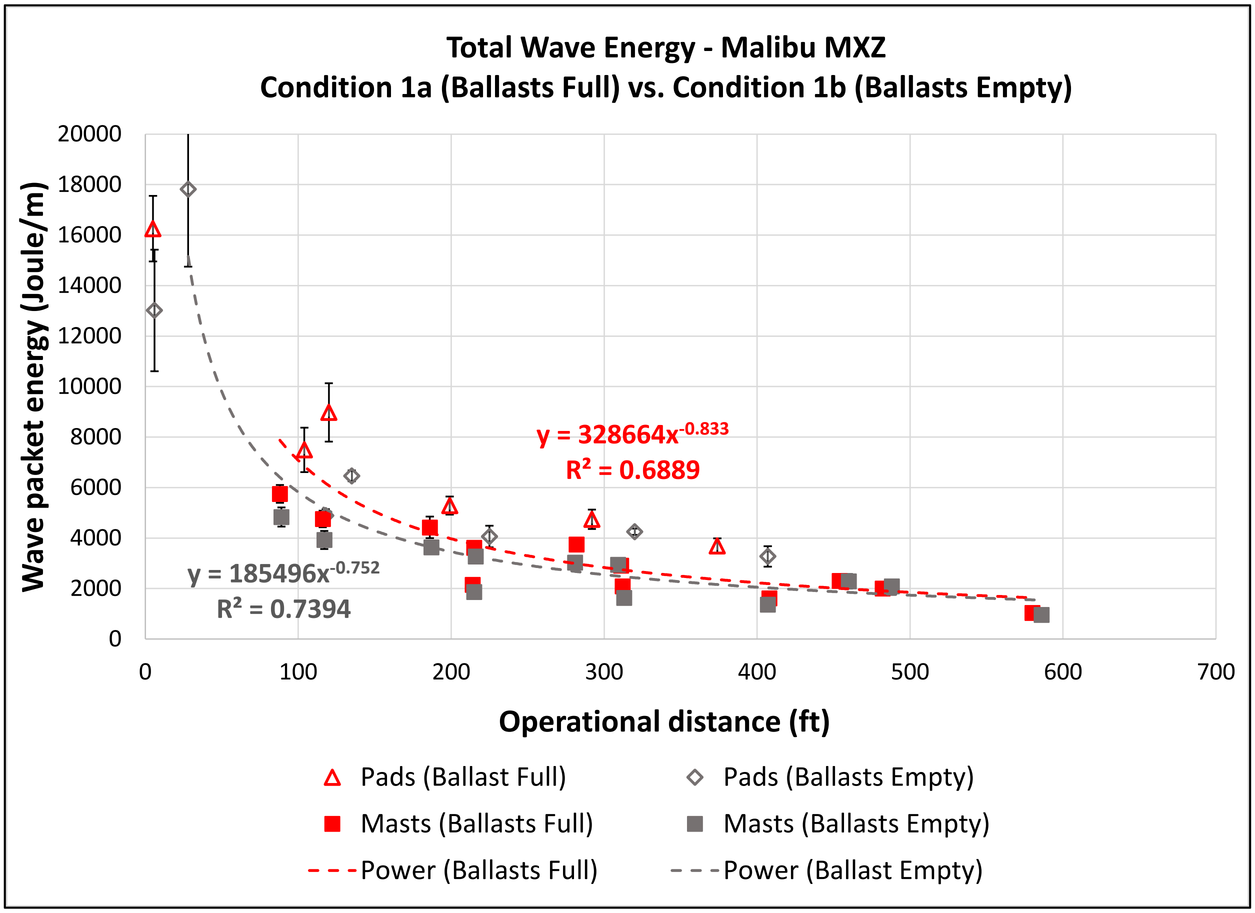


**Figure 35. Comparison of the total wave energy of the Malibu MXZ when the ballast tanks were full and empty. Data points less than one boat length from the track line were not included in the regression analysis.**

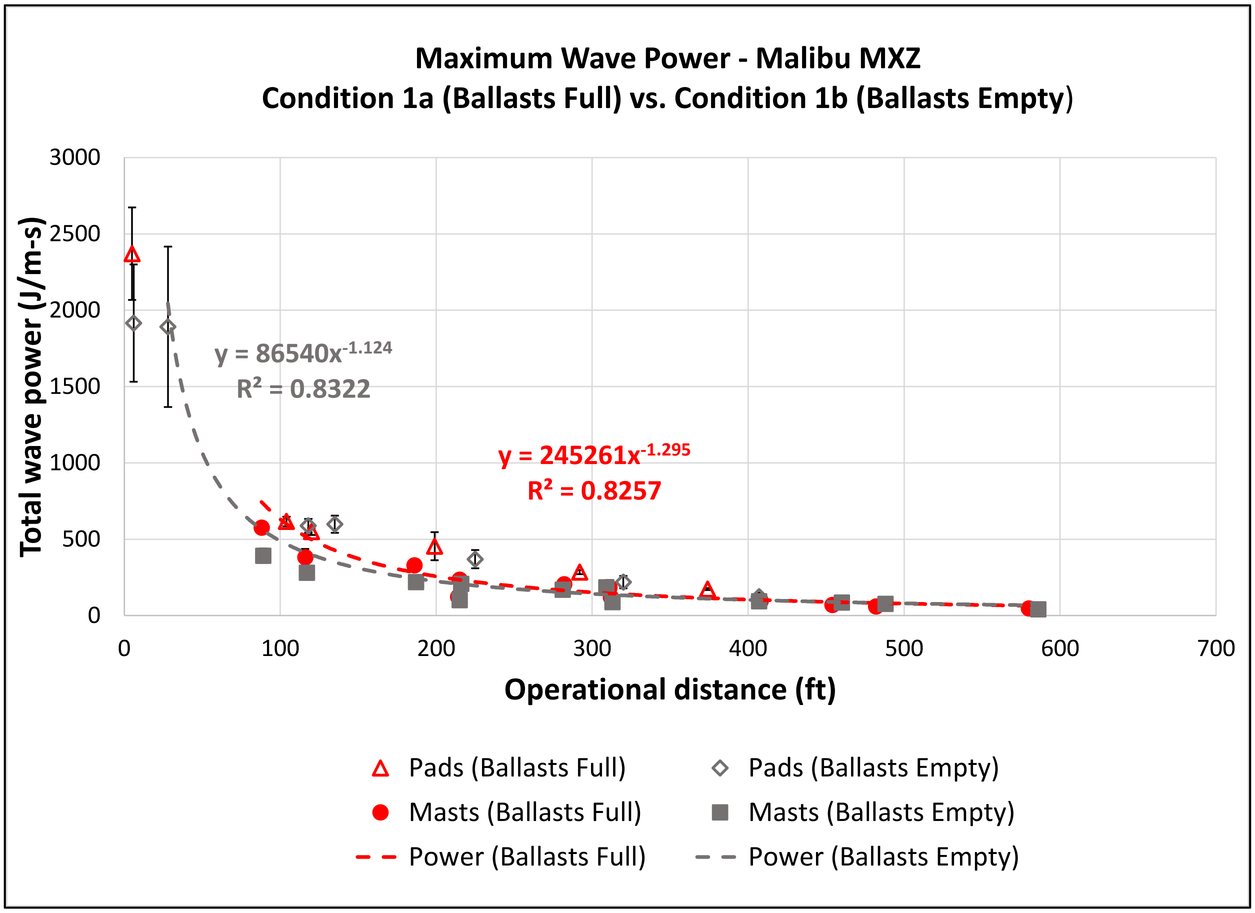


**Figure 36. Comparison of the maximum wave power of the Malibu MXZ when the ballast tanks were full and empty. Data points less than one boat length from the track line were not included in the regression analysis.**

## 5.4 Condition 1a (wake shaper on) versus Condition 1b (wake shaper off)

Condition 1a for the Malibu Response LX included an aftermarket wake shaper that was mounted just beneath the water surface on the port quarter of the hull (Section 3.6.2, Table 3). The wake shaper was removed from the boat during Condition 1b, while all other variables remained the same (Section 3.6.2, Table 3), allowing for the comparison of its influence on measured wake wave characteristics (Figures 37, 38 and 39).

The maximum wave height attenuation rates were similar for both conditions. However, the addition of the wake shaper resulted in a maximum wave height that was on the order of two inches higher over the entire operational distance. Just prior to 100 ft, the presence of the wake shaper created a maximum wave height of 12 in that attenuated to roughly 5 in after 600 ft. With the wake shaper removed, the maximum wave height was 10 in just prior 100 ft, and decreased to roughly 4 in after 600 ft. Like maximum wave height, the total wave energy attenuation rates were very similar between conditions. With the wake shaper attached, the total wave energy recorded over the entire operational distance was higher by roughly 200-500 J/m. The total wave energy was 2,300 J/m just prior to 100 ft and attenuated to approximately 650 J/m after 600 ft. With the wake shaper removed, the total wave energy was 1,900 J/m just prior to 100 ft, and by 600 ft it had decreased to roughly 430 J/m. Finally, attenuation rates for both conditions were nearly identical for maximum wave power. There was an increase in maximum wave power of around 20-40 J/m-s with the wake shaper attached. Just prior to 100 ft of operational distance, the maximum wave power was about 200 J/m-s, that attenuated to approximately 30 J/m-s at 600 ft. Without the wake shaper, the maximum wave power just prior to 100 ft was 160 J/m-s, which decreased to 10 J/m-s by 600ft.

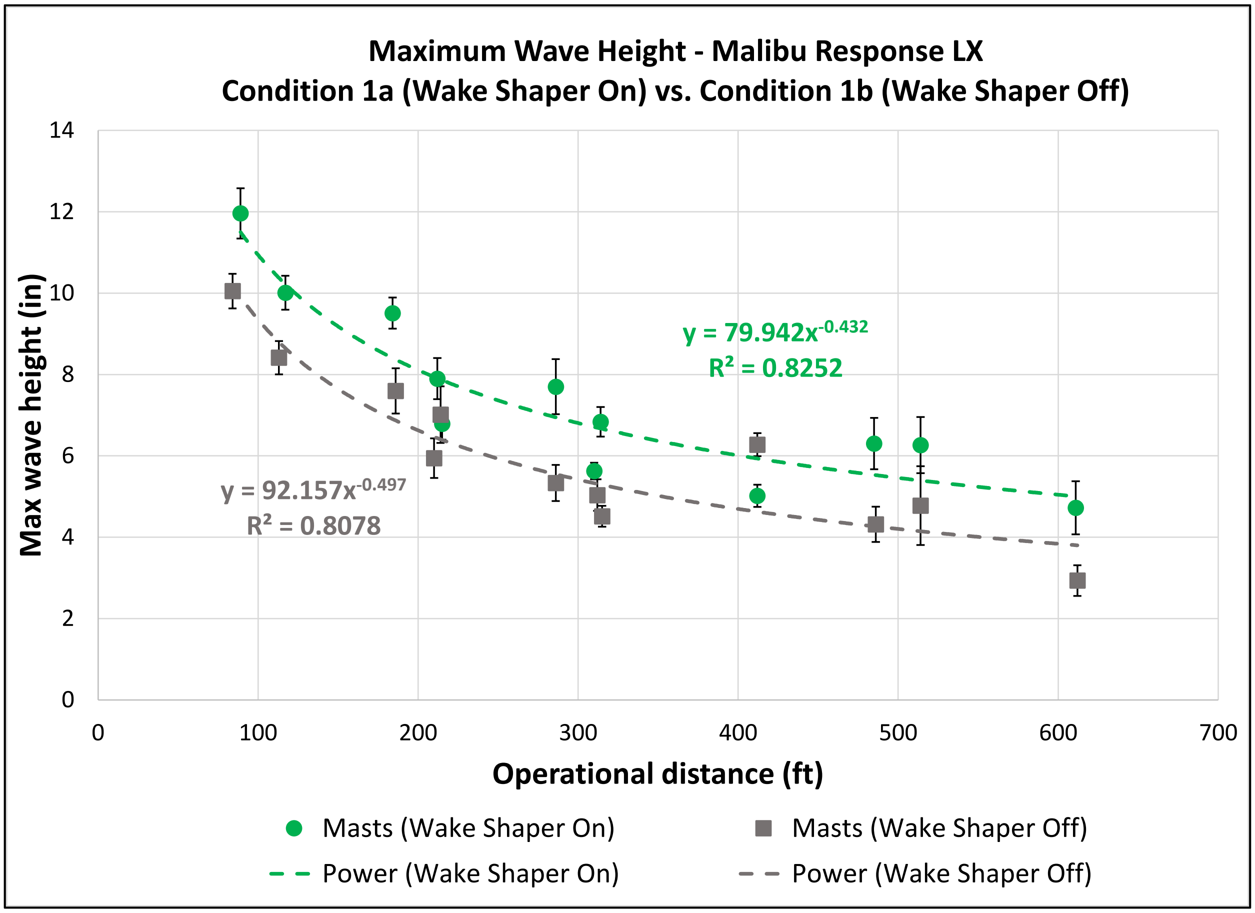


**Figure 37. Comparison of the maximum wave height of the Malibu Response LX when the wake shaper was on and off. There are no data for the Pads for the Malibu Response LX due to technical issues with the ADCP on test day.**

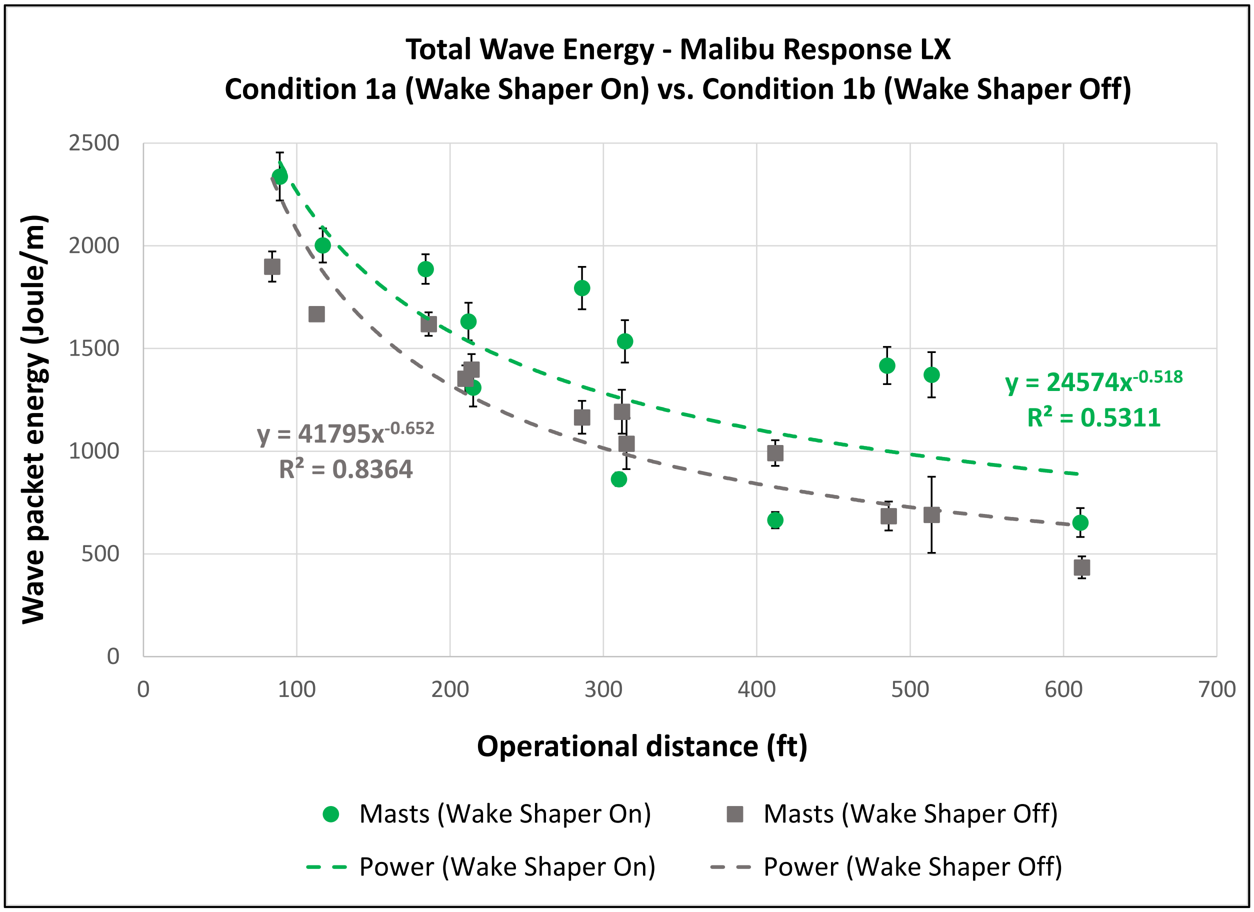


**Figure 38. Comparison of the total wave energy of the Malibu Response LX when the wake shaper was on and off. There are no data for the Pads for the Malibu Response LX due to technical issues with the ADCP on test day.**

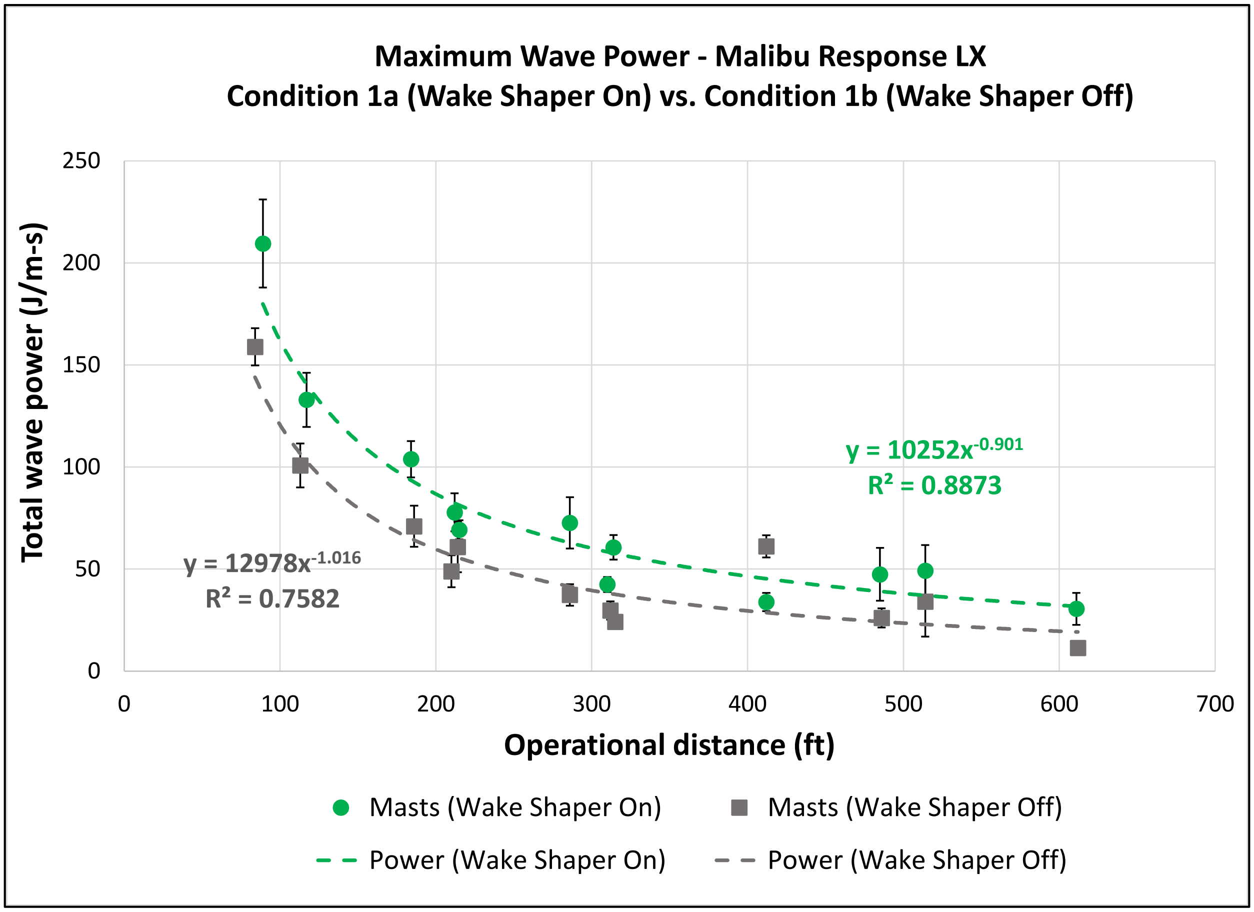


**Figure 39. Comparison of the maximum wave power of the Malibu Response LX when the wake shaper was on and off. There are no data for the Pads for the Malibu Response LX due to technical issues with the ADCP on test day.**

# 6.0 DISCUSSION

This section provides a discussion of the key observations and findings made in this study. We also provide guidance on how the information can be used by stakeholders in shaping future research efforts, managing lake and river resources, and providing education for boat operators. Finally, we end this section with a description of priority research needs related to boat-generated wake waves and their impacts.

## 6.1 Summary of observations

### 6.1.1 The maximum wave height, total wave energy, and maximum wave power produced by the four test boats were different between operational Condition 1a and Condition 2

The Larson LXI 210 is an all-purpose recreational boat that is typically operated at higher speeds where the boat is planing on the water surface. Typical usages include cruising or tow sports like tubing, waterskiing, and wakeboarding. Similarly, the Malibu Response LX is a recreational boat with a specialized design (e.g., D-Drive) for waterskiing and other tow sports that are performed at higher planing speeds. Figure 40 shows data for the Larson LXI 210 and Malibu Response LX comparing the total wave energy produced by Condition 1a (largest possible wake) and Condition 2 (planing). The data show a higher total wave energy under Condition 1a, which was also true for maximum wave height and maximum wave power. Although the Malibu Wakesetters can be operated on-plane for the same aforementioned tow sports, they are designed primarily to be operated at slow speeds that maximize water displacement and produce large wakes suitable for wakesurfing. Figure 41 shows the same data collected for the Malibu VLX and Malibu MXZ under Conditions 1a (wakesurfing) and Condition 2 (planing). Both boats showed significantly larger changes in total wave energy levels between Condition 1a and Condition 2. Again, the same trend was true for maximum wave height and power.

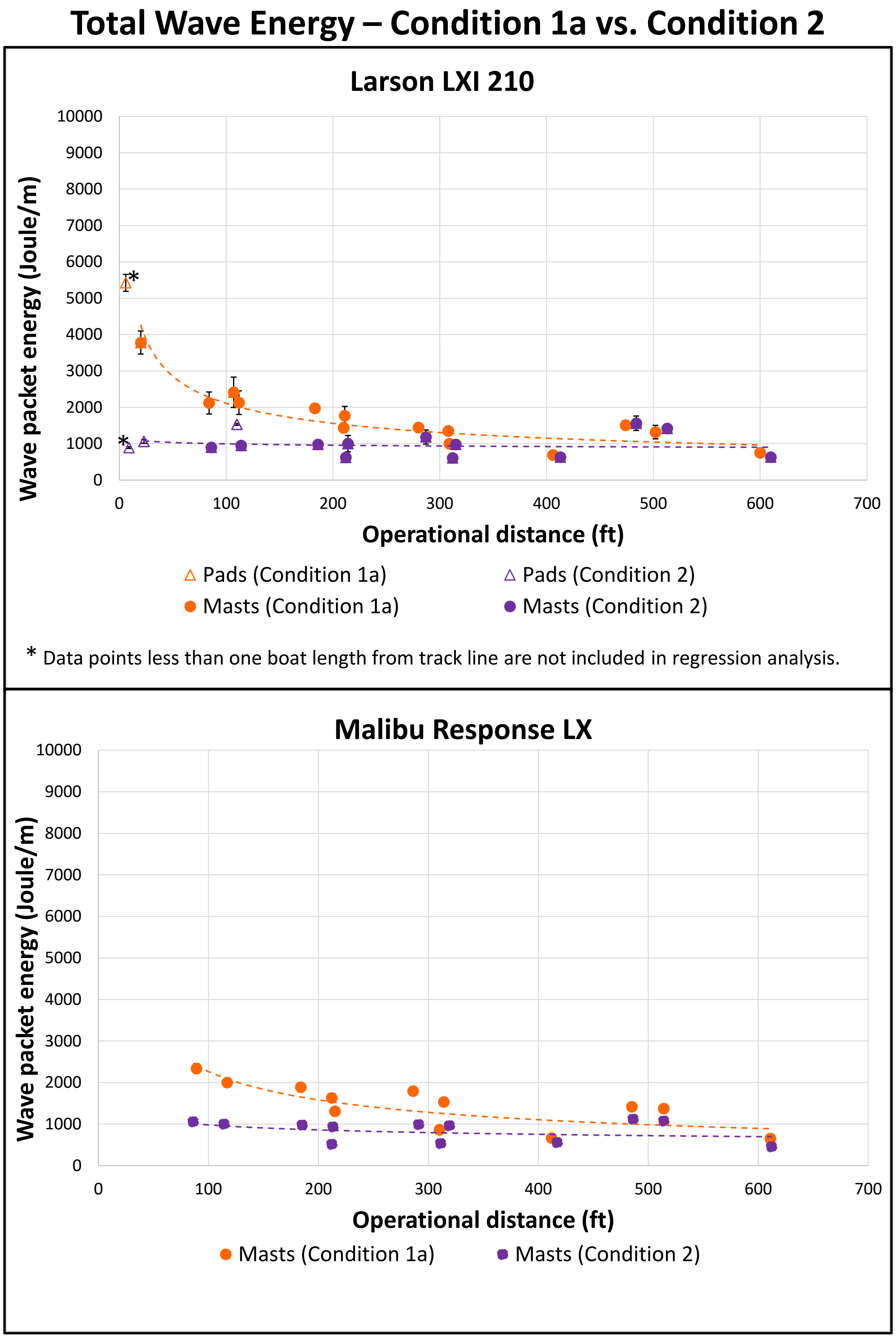


**Figure 40. Comparisons of the total wave energy for the Larson LXI 210, Malibu Response LX Condition 1a (largest wave/surfing) and Condition 2 (planing). There are no data for the Pads for the Malibu Response LX due to technical issues with the ADCP on test day. Note the maximum y-axis value is 10,000 J/m.**

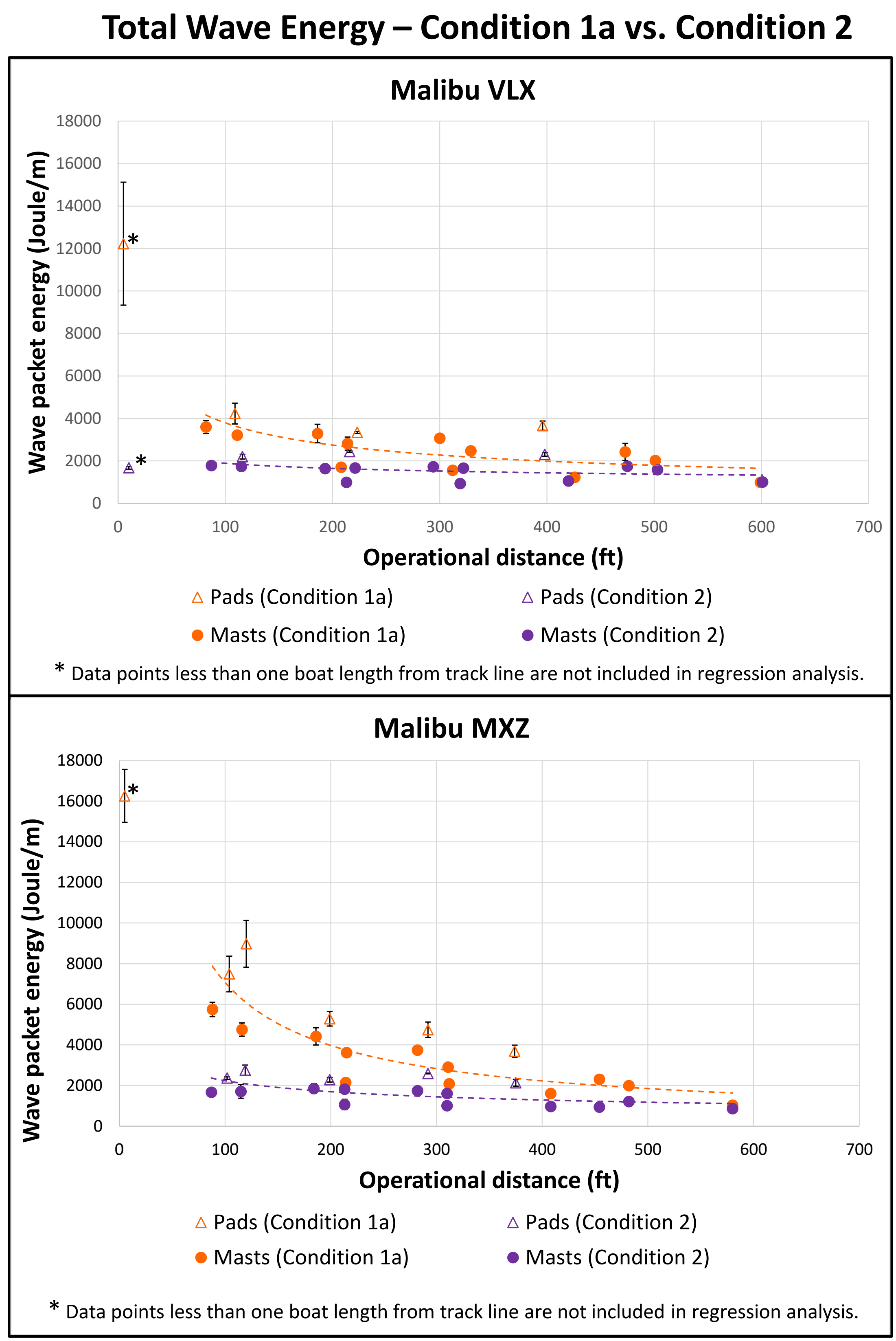


**Figure 41. Comparisons of the total wave energy for the Malibu VLX, and Malibu MXZ Condition 1a (wakesurfing) and Condition 2 (planing). Note the maximum y-axis value is 18,000 J/m.**

### 6.1.2 When operated under their most typical operating conditions, wakesurf boats were capable of producing larger wake waves that contain more energy and power than non-wakesurf boats

During boating water sports, the Larson LXI 210 and Malibu Response LX are typically operated in a planing mode (Condition 2), while the wakesurf boats studied here are engineered to operate, amongst other configurations, at Condition 1a. This is the condition associated with the sport of wakesurfing and it is safe to assume that this is the most common operational condition for these boats. Therefore, a useful comparison to consider is the maximum wave height, total wave energy, and maximum wave power under the conditions that are most common for the boat's operation (Figures 42, 43 and 44).

Under this comparison, the two wakesurf boats produced substantially higher (~2-3 times) maximum wave heights than the non-wakesurf boats at 100 ft and ~2 times higher after 600 ft. The wakesurf boats had maximum wave heights between 12-20 in at 100 ft of operational distance, that attenuated to 5-7 in around 600 ft. Maximum wave heights for non-wakesurf boats decreased from 7-9 in at 100 ft of distance to 4 in or less at 600 ft. Total wave energy showed a similar pattern, with the two wakesurf boats producing ~3 to 9 times more energy than the non-wakesurf boats after 100 ft of operational distance and ~3 times at 500 ft. At roughly 100 ft of operational distance, the wakesurf boats had total wave energies that ranged between 3,200-9,000 J/m, which attenuated to ~2,000 J/m by 450-550 ft. Both non-wakesurf boats had initial total energy levels of roughly 1,000 J/m with minimal attenuation over 600 ft of distance. Maximum power for the non-wakesurf boats was 50 J/m-s at 100 ft and attenuated to around 10 J/m-s at 600 ft of operational distance. The wakesurf boats had measured maximum powers that ranged from 280 to 620 J/m-s at 100 ft (~6 to 12 times more power) and attenuated to 40 J/m-s at 600 ft (4 times more power).

While Figures 42, 43 and 44 focus on assumed typical operations, it is important to note that wakesurf boats are multipurpose boats designed to also operate at Condition 2 where they can be used for cruising and other recreational tow sports. Similarly, with the addition of wake manipulating technology (e.g., hydrofoil and wake shaper), non-wakesurf boats like the Malibu Response LX can be operated as a wakesurf boat (i.e., Condition 1a). Finally, it is technically possible for the Larson LXI 210 to be operated in Condition 1a for long periods of time, however, it is our experience that boats of this type spend very little time in this condition; normally they would transition quickly through Condition 1a as they accelerate to planing operation.

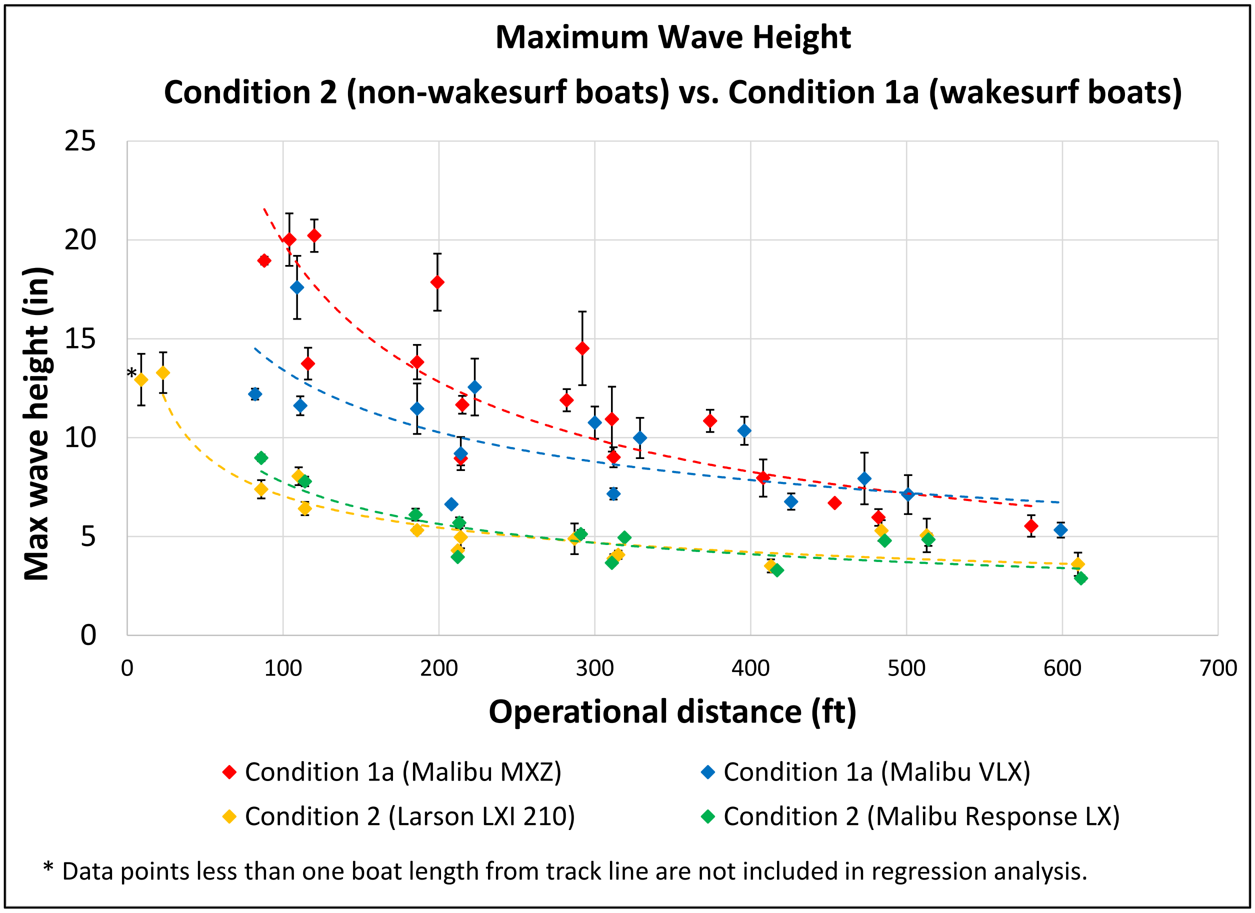


**Figure 42. Comparison of maximum wave height of the test boats under their typical operational conditions.**

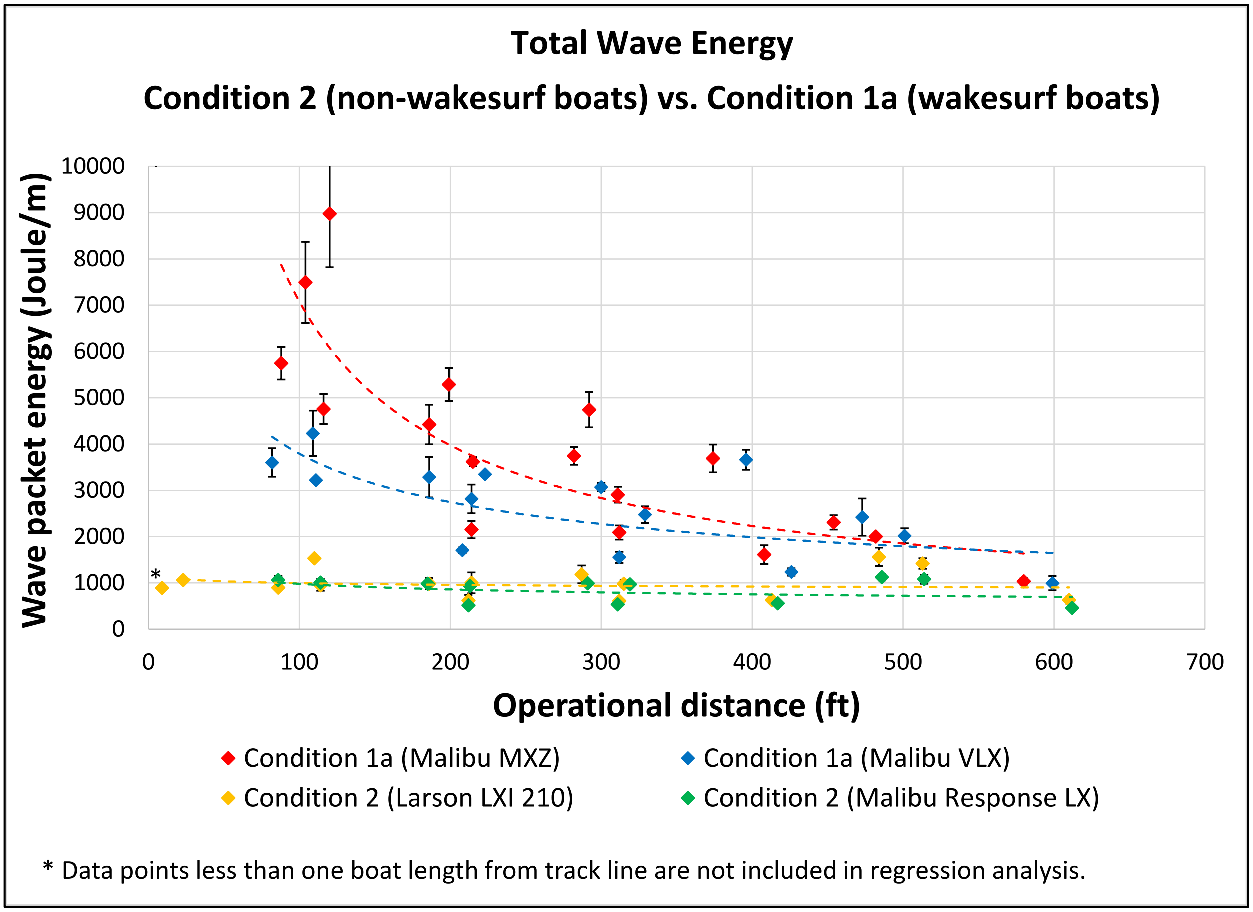


**Figure 43. Comparison of total wave energy of the test boats under their typical operational conditions.**

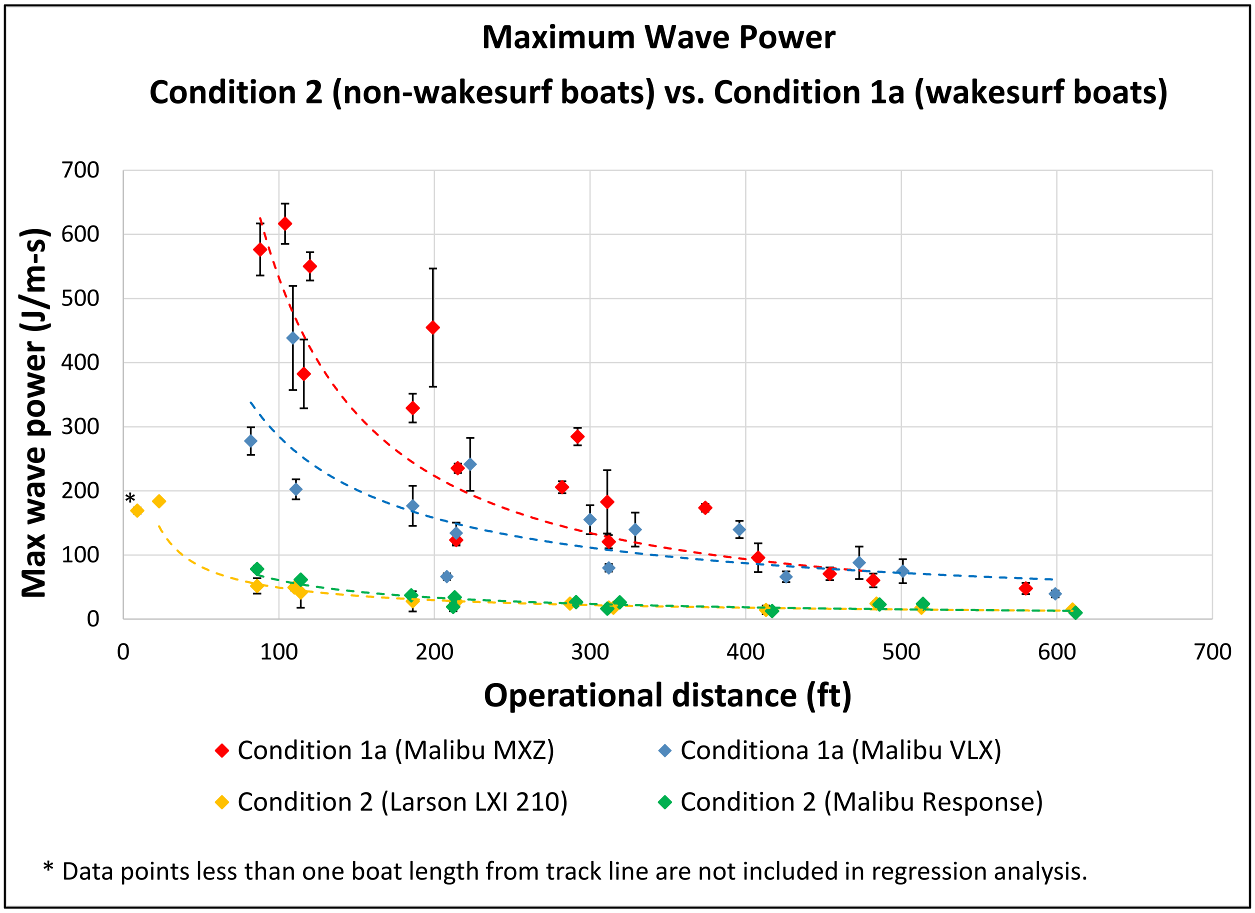


**Figure 44. Comparison of maximum wave power of the test boats under their typical operational conditions.**

### 6.1.3 Full ballast tanks had a minor impact on the wake wave characteristics of the Malibu Wakesetters at distances greater than 100 ft from the boat

An unexpected finding was the relatively small influence the added weight of the ballast water had on the maximum wave height, total wave energy, and maximum wave power for the Malibu Wakesetters. As shown in Table 2, completely full ballast tanks increased the total boat weight by 3,690 lbs (47% increase) and 4,885 lbs (47% increase) for the VLX and MXZ, respectively. Our expectation was that the increased water weight, and thus greater hull submergence equating to more water being displaced, would result in an increase in the magnitude of the measured wake wave characteristics over the entire operational distance. Although there were increases in the maximum wave height, total wave energy, and maximum wave power in the first 100 ft of operational distance for both boats when the ballast tanks were full, the differences quickly decreased with distance and were no longer discernible after approximately 200 ft (Figures 31-36). This observation motivates further investigations.

### 6.1.4 Addition of the aftermarket wake shaper to the Malibu Response LX resulted in larger maximum wave heights, increased total wave energy, and greater maximum wave power

The wake shaper attached to the Malibu Response LX altered the wake by creating an asymmetric wake that increased the measured maximum wave height, energy, and power. When compared to the Malibu Wakesetters, the wake wave characteristics were smaller (Figures 15, 18, and 21). Interestingly, when considering the Malibu Response LX individually, the aftermarket wake shaper resulted in notable increases in the wake wave characteristics, not only near the boat (i.e., first 100 ft), but at all operational distances (Figures 37, 38, and 39). This observation, along with those discussed in Section 6.1.3, suggest the wake shaper may have more influence on the measured wave characteristics than the addition of ballast water at greater operational distances. Nevertheless, the implications are that aftermarket products can effectively modify the wave characteristics of recreational boats.

### 6.1.5 A potential method for establishing guidance for boat operational distances based on measured wake wave characteristics (height, energy, power)

We conducted a review of the relevant laws, regulations, and recommendations for the state of Minnesota and the surrounding upper Midwest states regarding the operational distances that boats have to maintain between other watercrafts, shorelines, docks, etc. No consistent guidance has been adopted by these states (Table 4). Operational distances range between 100 ft and 300 ft, vary in the type of specification, and pertain to all types of motorboats. In Minnesota, for example, there is presently no law that prescribes an operational distance between boats, shorelines, docks, other watercraft, etc., rather there is a recommended distance of 200 ft. Iowa, Michigan, North Dakota, and Wisconsin have developed laws stating specific distances of 300 ft, 100 ft, and 100 ft, respectively. We could not locate operational distance criteria for South Dakota.

The data produced in this study can be used to inform boat operational distances necessary to attenuate maximum wave height, total wave energy, and maximum wave power to levels deemed acceptable. To illustrate this approach, we provide two examples below. In both examples, we select the Minnesota recommendation of 200 ft as the reference operational distance (Table 4). In principle, the point at which the various wake wave characteristic data cross a selected reference distance, defines the recommended threshold criteria for that characteristic.

In the first example (Figures 45, 46 and 47), we reference Figures 42, 43, and 44 from Section 6.1.2, where the boats were compared under their typical operational conditions: Condition 2 (planing) for the non-wakesurf boats and Condition 1a (wakesurfing) for the wakesurf boats (Section 3.6, Table 3). Because Condition 2 for the non-wakesurf boats are typical recreational operating conditions seen on Minnesota inland lakes, it was used as the reference condition. Moreover, the non-wakesurf boats produced the lowest overall values of wave height, energy, and power and were nearly identical to one another after 200 ft of distance. The results in Figures 45, 46 and 47 suggest, based on both the actual data points and best-fit power law regressions, that operational distances greater than 500 ft are needed to attenuate the wake wave characteristics of the wakesurf boats to the selected reference condition levels, which were roughly 6 in, 1,000 J/m, and 35 J/m-s for maximum wave height, total wave energy, and maximum wave power, respectively.

In the second example, (Figures 48, 49 and 50), we reference Figures 15, 18, and 21 from Section 5.0, where all boats were compared under Condition 1a (i.e., largest wave/surfing). Again, the non-wakesurf boats are the reference. The results in Figures 48, 49, and 50 suggest, based on the actual data points and best-fit regressions, that operational distances greater than 425 ft are needed to attenuate the wake wave characteristics of the wakesurf boats to the selected condition reference levels, which were approximately 7 in for maximum wave height, 1,600 J/m for total wave energy, and 80 J/m-s for maximum wave power. Table 5 summarizes the results from both examples.

**Table 4. Summary of state laws/recommendations regarding operational distances between recreational boats and shoreline, docks, other watercraft, etc.**

| State | Boats | Note | References |
|---|---|---|---|
| Iowa | speeds less than 10 mph at distances less than 300ft from shore | state law/ regulation | http://publications.iowa.gov/15950/1/ia_handbook_entire.pdf |
| Michigan | slow, no wake speed at distances less than 100 ft from shore (if < 3 ft deep), moored or anchored vessel, dock, raft, swimming area, or person(s) in the water | state law/ regulation | https://assets.kalkomey.com/boater/pdfs/handbook/michigan-handbook-entire.pdf |
| Minnesota | maintain greater than 200 ft between boat and shore/other structures | recommendation | http://files.dnr.state.mn.us/rlp/regulations/boatwater/boatingguide https://www.dnr.state.mn.us/safety/boatwater/own-your-wake.html |
| North Dakota | No operation within 100 ft of a person fishing from shore, swimmer, raft, or an occupied, anchored or nonmotorized vessel | state law/ regulation | https://gf.nd.gov/boating/safety-regulations |
| Wisconsin | slow, no wake speed at less than 100 ft from shore, dock, raft, pier, swimmer, or restricted area | state law/ regulation | https://dnr.wi.gov/files/pdf/pubs/le/le0301.pdf |

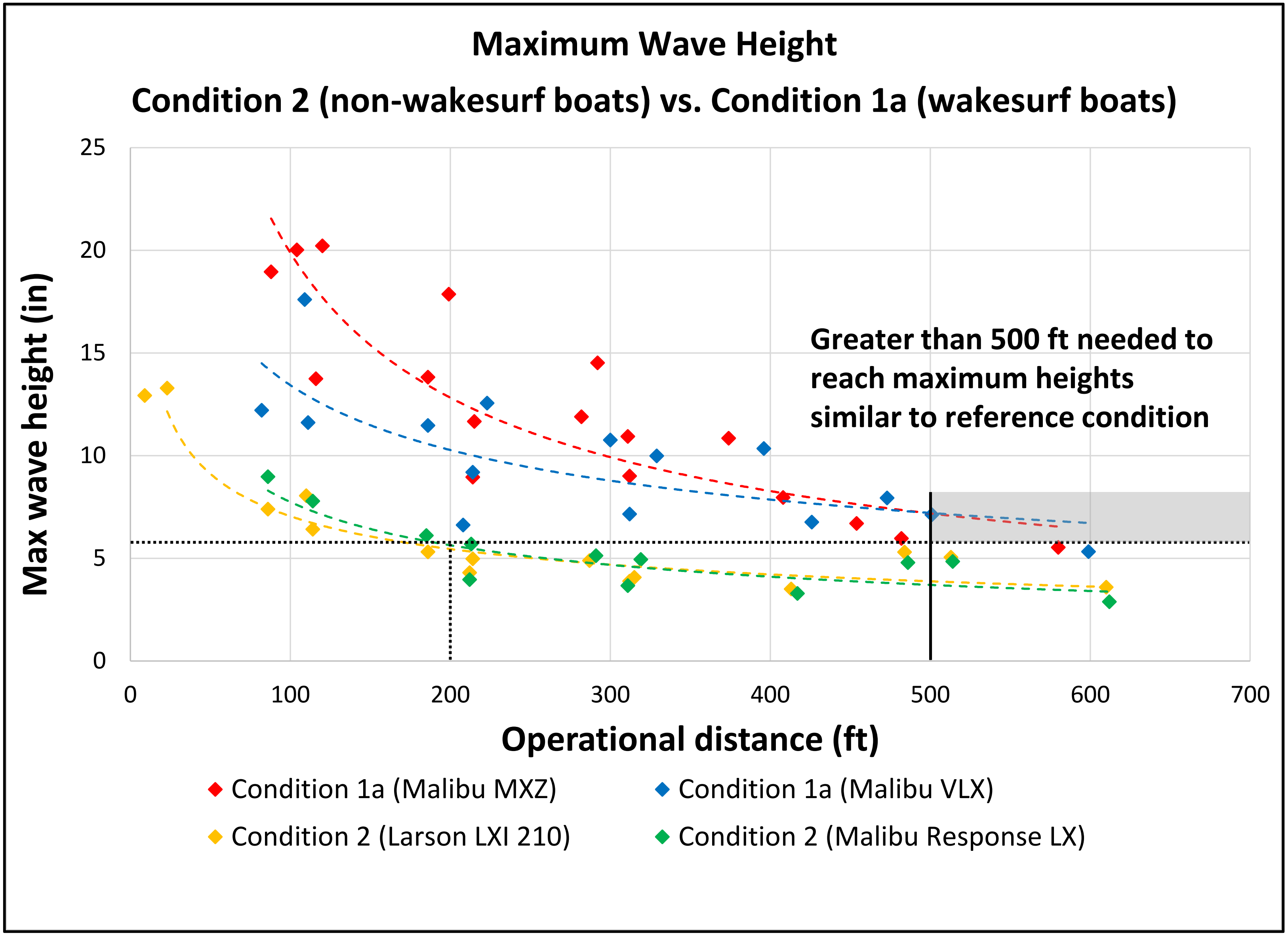


**Figure 45. Illustration of a potential method for estimating the operational distance needed to reduce the maximum wave height of the wakesurf boat to reference levels associated with Condition 2 (planing) of the non-wakesurf boats (black horizontal dashed line).**

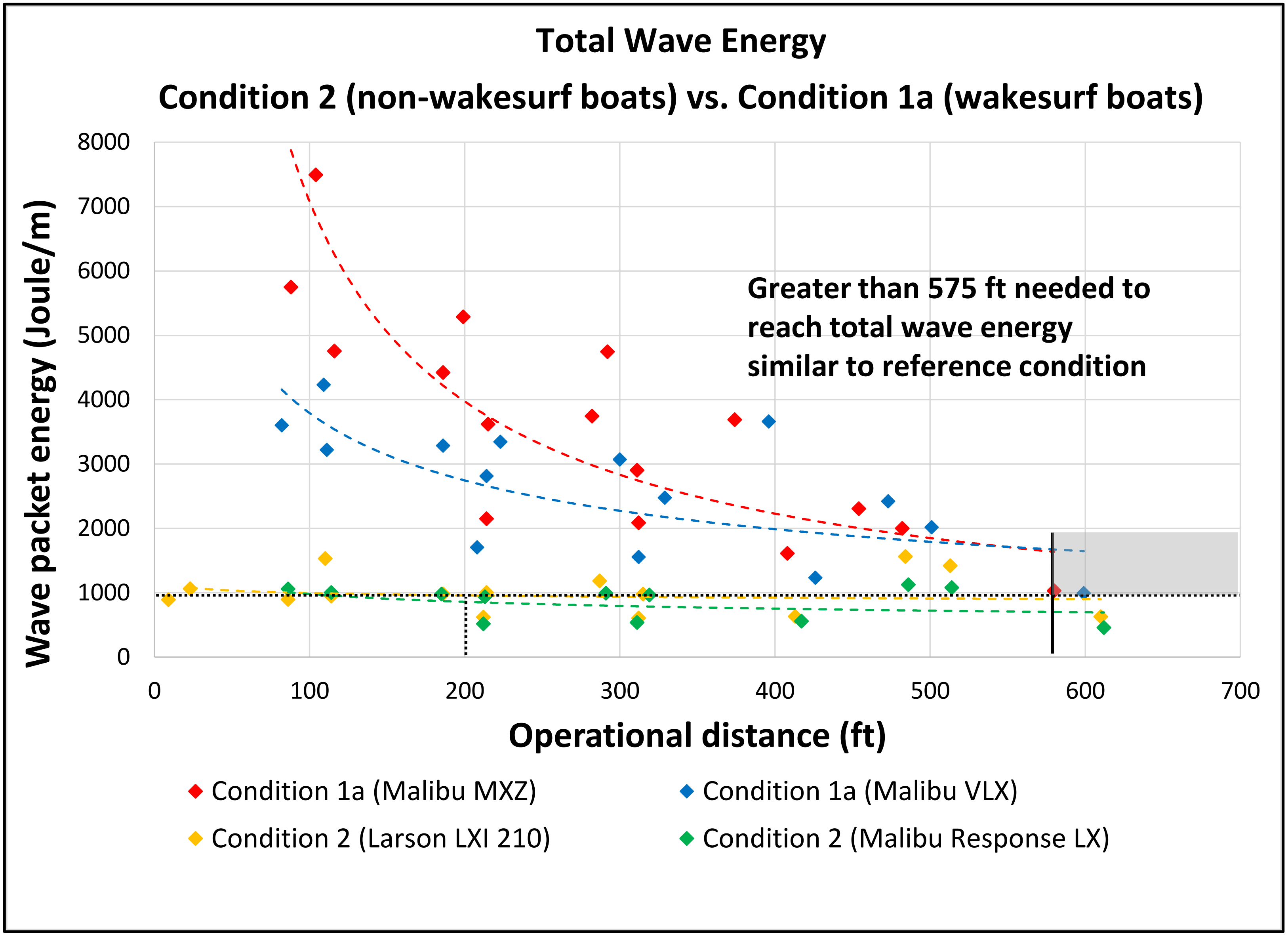


**Figure 46. Illustration of a potential method for estimating the operational distance needed to reduce the total wave energy of the wakesurf boat to reference levels associated with Condition 2 (planing) of the non-wakesurf boats (black horizontal dashed line).**

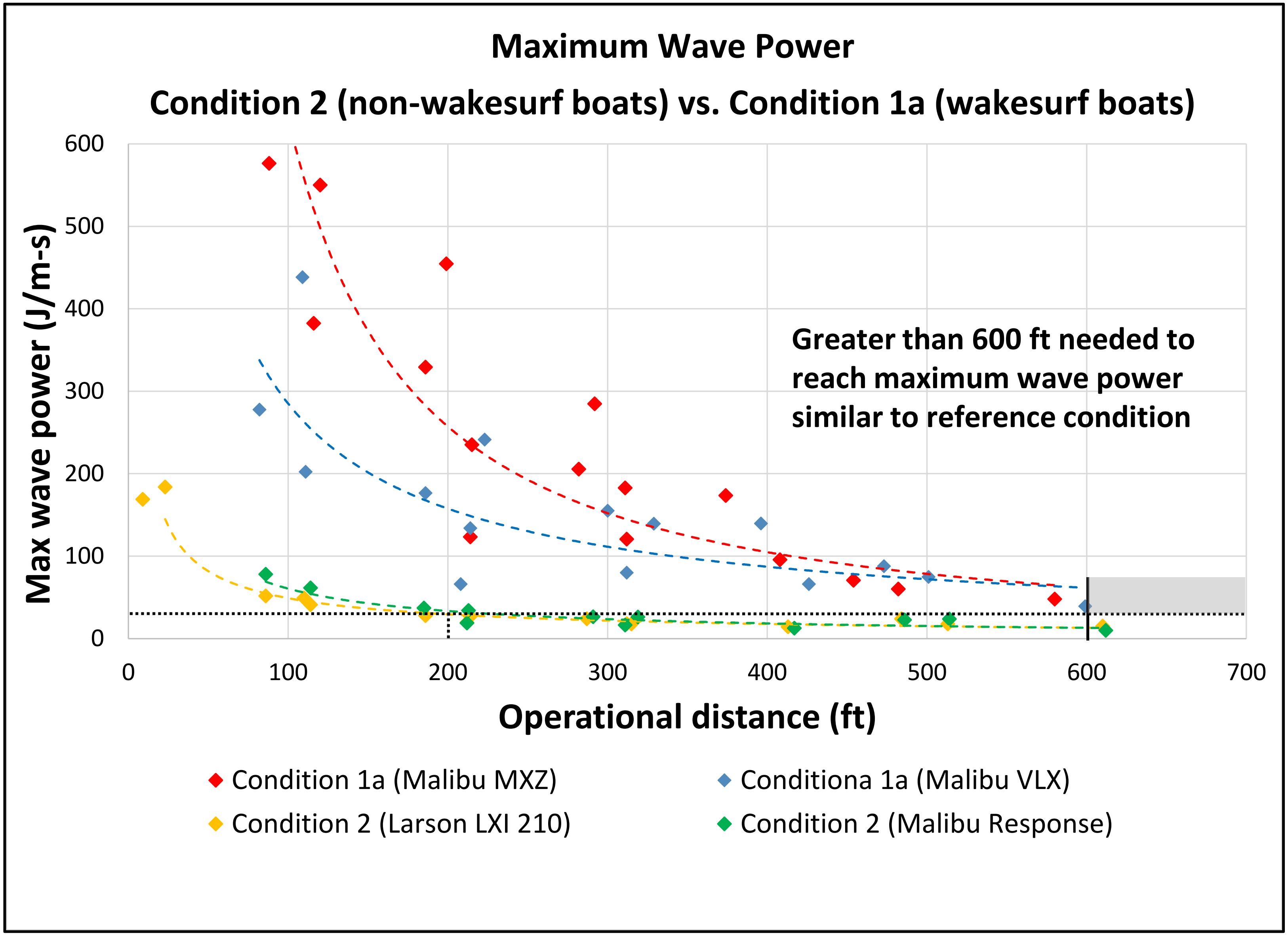


**Figure 47. Illustration of a potential method for estimating the operational distance needed to reduce the maximum wave power of the wakesurf boat to reference levels associated with Condition 2 (planing) of the non-wakesurf boats (black horizontal dashed line).**

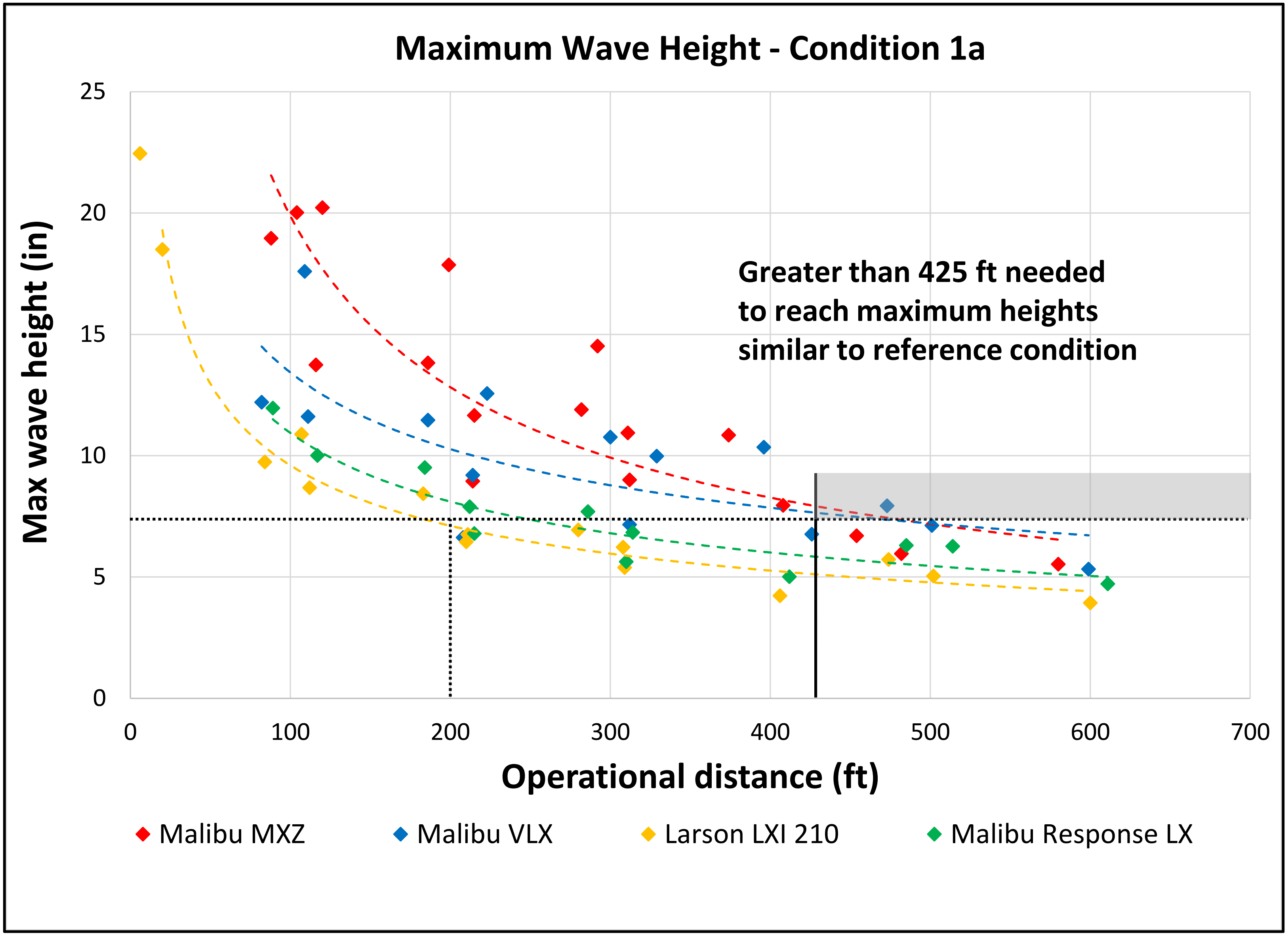


**Figure 48. Illustration of a potential method for estimating the operational distance needed to reduce the maximum wave height of the wakesurf boat to reference levels associated with Condition 1a (largest wave) of the non-wakesurf boats (black horizontal dashed line).**

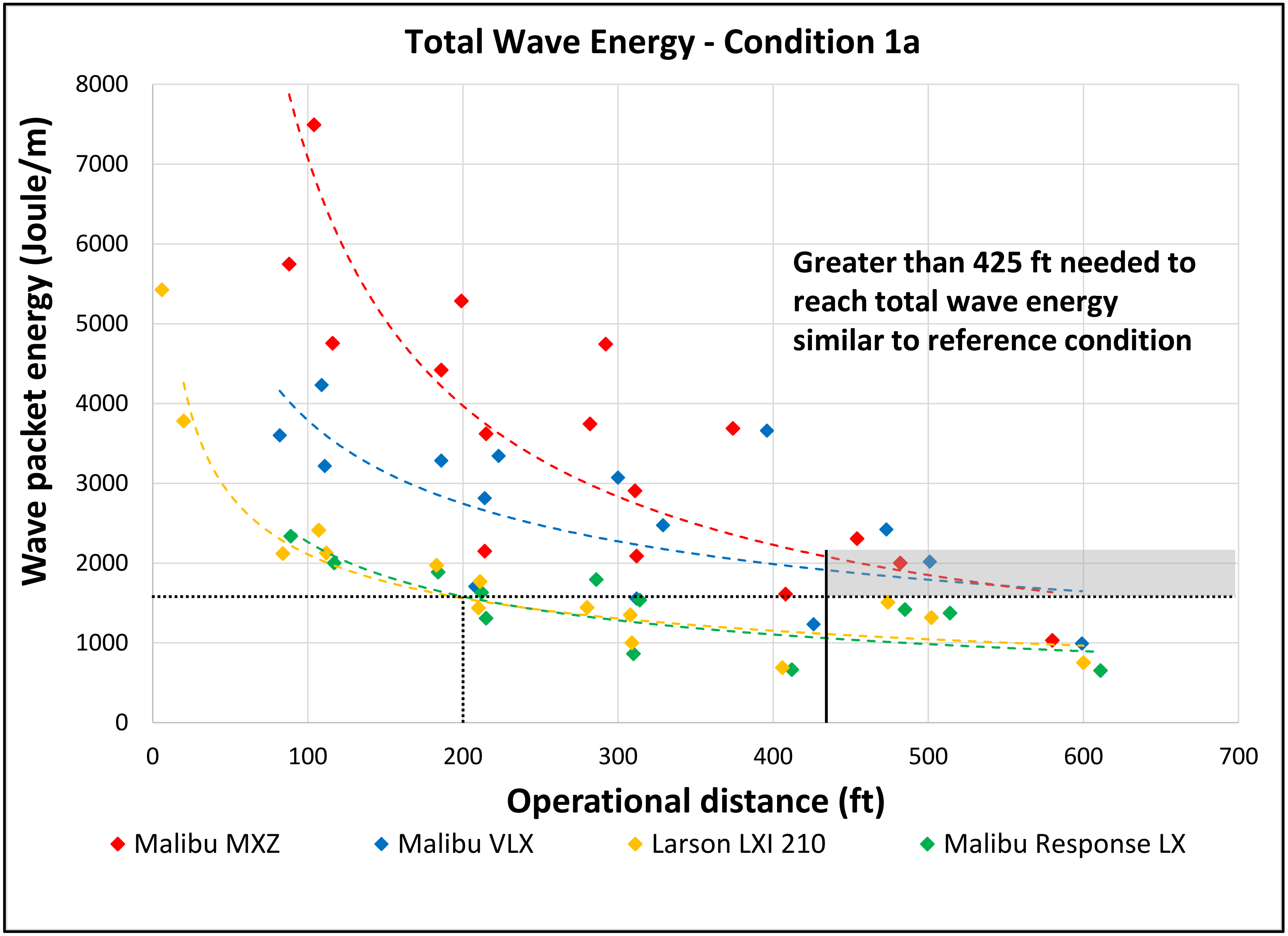


**Figure 49. Illustration of a potential method for estimating the operational distance needed to reduce the total wave energy of the wakesurf boat to reference levels associated with Condition 1a (largest wave) of the non-wakesurf boats (black horizontal dashed line).**

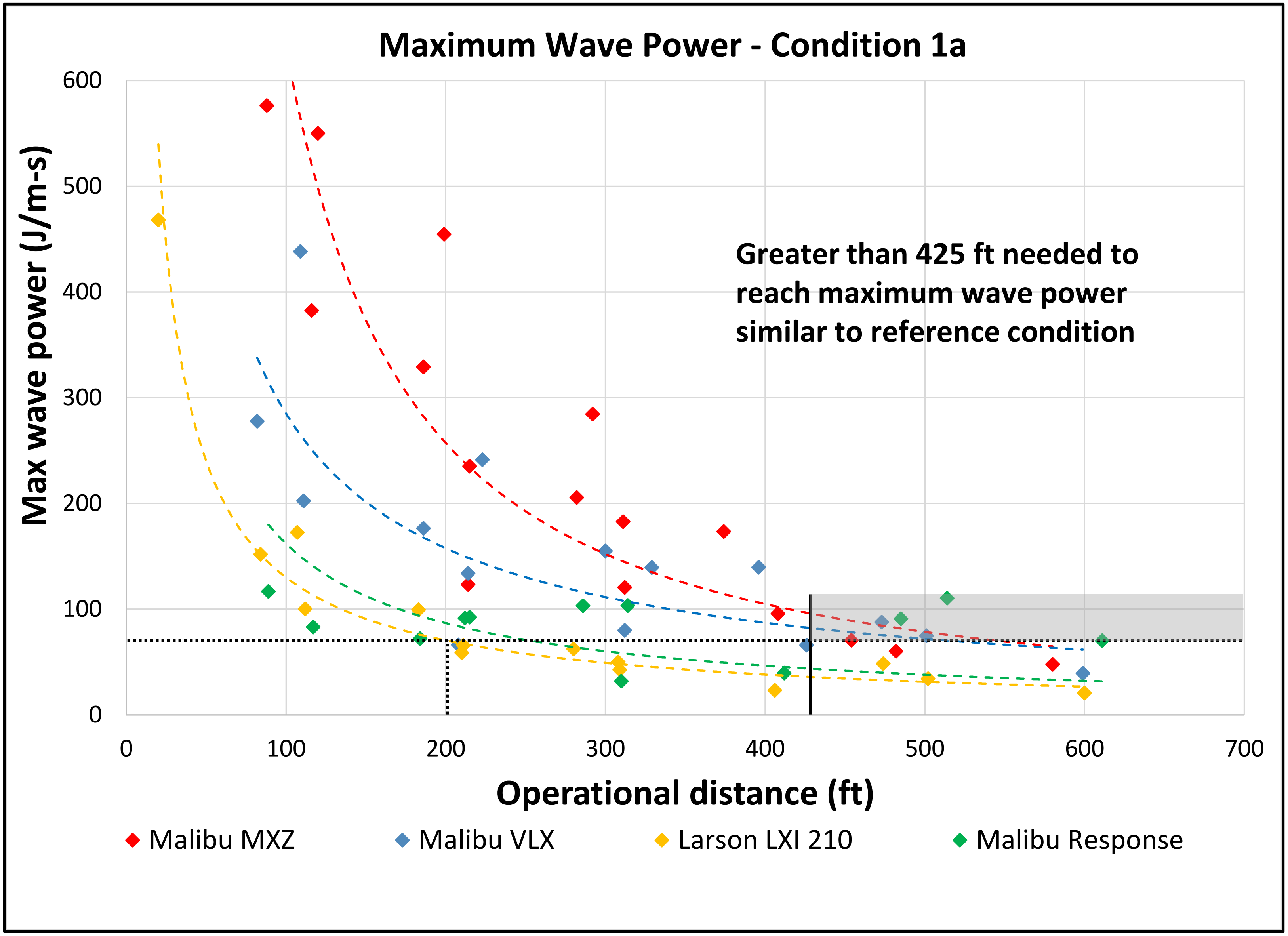


**Figure 50. Illustration of a potential method for estimating the operational distance needed to reduce the maximum wave power of the wakesurf boat to reference levels associated with Condition 1a (largest wave) of the non-wakesurf boats (black horizontal dashed line).**

**Table 5. Summary of the estimated operational distances needed to attenuate the wake wave characteristics (height, energy, and power) of the wakesurf boats to the reference condition levels selected in examples 1 and 2.**

| Reference condition | Operational distance required by wakesurf boat to attenuate to reference condition levels |
|---|---|
| Example 1<br>non-wakesurf boat planing at an operational distance of 200 ft (Condition 2 - planing) | Maximum Wave Height: >500 ft.<br>Total Wave Energy: >575 ft.<br>Maximum Wave Power: >600 ft. |
| Example 2<br>non-wakesurf boat transition to planing at an operational distance of 200 ft (Condition 1a - largest wave) | Maximum Wave Height: >425 ft.<br>Total Wave Energy: >425 ft.<br>Maximum Wave Power: >425 ft. |

### 6.1.6. Non-dimensionalization of operational conditions

It is common practice in the fields of fluid mechanics, naval architecture and other engineering disciplines to generalize the physics of a problem using dimensionless variables. For problems involving wake wave physics, the length Froude number (Equation 13) and depth Froude number (Equation 14) can be used. Transforming dimensional values like boat speed, boat length, and water depth into Froude number is a powerful tool for comparing the operational regime of different recreational and commercial vessels. The length Froude number can be used to describe whether the boat is displacing, transitioning to planing or planing. The depth Froude number is an indicator of the type of wake wave pattern that forms behind the boat. We recognize the power of dimensionless variables of the wake wave phenomena studied here, however because this report is focused on practical operational conditions and targets a general audience, we have chosen to present our results as dimensional values.

$$Fr_l = \frac{u}{\sqrt{gl}} \tag{13}$$

$$Fr_h = \frac{u}{\sqrt{gh}} \tag{14}$$

Where,

u = boat speed along the track line

g = gravitational acceleration coefficient

L = wetted length of the boat hull

h = the water depth under the boat.

## 6.2 Caveats, areas for improvement, and future research needs

### 6.2.1 Issues encountered with the Acoustic Doppler Current Profiler (ADCP)

The research involved deploying Nortek Signature 1000 ADCPs at Pad 1 and Pad 2. The instruments were used to capture wave height information and velocity profile information throughout the water column. The velocity profile data will be the focus of a second report that stems from this project. The ADCP is an acoustic device that uses the two-way travel time of short bursts of high frequency, narrow bandwidth sound to measure the velocity field and water surface elevation above the instruments. Some of our near-boat data were not usable because the boat passed too close to the sensor causing poor signal quality due to air entrainment and/or motor noise. For the Malibu Wakesetters, the wakesurf wave generated by the boat during these passes was also too steep for the sensor to capture the static water surface. In future tests, the boat should travel no closer than 20 ft (6.1 m) from the ADCP for water surface tracking measurements.

### 6.2.2 Boats and operational conditions tested

It is important to recognize that this study examined only four boats. We sought to pick watercraft that were representative of non-wakesurfing and wakesurfing boats; however, there are many other boat manufacturers and models that we were not able to study. Three of the test boats were from a single manufacturer (Malibu). The boat selection resulted from the boats that were available to us within the short window of field work for this study and the resulting research is not intended to represent a single manufacturer, but the operation conditions of recreational boats in general.

We also selected operational conditions that were representative of various tow sports for boats with different manufacturing characteristics (Section 3.6, Table 2), combined with the various wave manipulating technologies and settings; however, we recognize that the range of all possible operational conditions and data comparisons were larger than available time and resources.

### 6.2.3 Sample size of boat tracks

In this study, boats made passes along four track lines that were set at 225, 325, 425, and 625 ft from shore. In hindsight, adding a few more track lines at key distances would have increased the sample size, and thus narrowed the data variance (i.e., greater precision and less uncertainty). For example, few data points fell within the first 20-100 ft of operational distance where there was rapid attenuation of height, energy, and power. These near-field data are less important to informing boat operational distances, which will generally exceed 100 ft, but may be important for understanding processes of energy dissipation nearer the boat track. A similar data collection campaign within the first 100 ft where the wave heights, energy, and power are at their greatest would help to fill in these gaps.

### 6.2.4 Impacts of propeller wash on vertical mixing, sediment scour/suspension, and aquatic organisms

This project also involved collection of velocity and turbulence data associated with propeller wash from the four test boats. This data will be the subject of a future report. Boats of all sizes produce propeller wash and, at a certain depth the wash begins to interact with the thermocline, lake bottom, vegetation, and aquatic habitats. These complex interactions are not well-studied, and we believe this is a priority area for future research.

### 6.2.5 Linking wave height, energy and power to environmental impacts

This report only characterizes the wave height, energy, and power of a few recreational watercraft, and does not address potential environmental impacts such as shoreline/riparian erosion, water quality degradation, or alteration to aquatic habitats. Focus of future research will seek to understand the linkages between characteristics of boat-generated waves (e.g., wavelength, wave period, height, energy and power) and the nearshore environment. Future research will focus on: a) wave-induced sediment transport in the near-shore lake environment; b) interactions of wake waves with aquatic vegetation; c) impact of changing wave regimes on natural and armored shorelines. These topics are of great interest and concern to many stakeholders. For the benefit of finding solutions to the long-term protection and shared-used of recreational water resources, it is critical that researchers, funding agencies, and stakeholders prioritize coordinated, multi-year research in these areas.

### 6.2.6 Comparisons of boat wakes with wind waves for different lakes sizes

The sensitivity of a lake (or river) to boat wakes likely depends on the level of wind-wave energy that the lake experiences. For example, a small lake, with short fetches and relatively small wind-generated waves, is likely to be more sensitive to boat wakes than a large lake. Further work is needed, likely in the form of long-term monitoring, to compare the cumulative impacts of wind- and boat-generated waves on shoreline erosion, lake water quality, and nearshore habitat for different lake sizes, depths, and shoreline characteristics.

(This page intentionally left blank)

# 7.0 CONCLUSIONS

This report summarizes the data and results of a field-based assessment of wake wave characteristics (maximum height, total energy and maximum power) produced by four recreational boats operated under a range of conditions and at various distance from data sensors. Two of the boats, Larson LXI 210 and Malibu Response LX, were representative of typical boats used on Minnesota inland lakes over the last several decades. Two of the boats, Malibu Wakesetter VLX and Malibu Wakesetter MXZ, were representative of state-of-the-art wakesurf boats.

The main conclusions of the research are summarized below:

**The maximum wave height, total wave energy, and maximum wave power produced by the boats studied were substantially different between two operational conditions tested.** For all the test boats studied, the maximum wave heights, total wave packet energy and maximum wave power were greatest under Condition 1a (wakesurfing/largest possible wake) operation. These same wake wave parameters were smallest for all test boats under Condition 2 (planing). Most notably, we document a substantial increase in maximum wave height, total energy, and maximum power between Condition 1a and 2 for the wakesurf boats. This finding is not a surprise, but confirms that the design of wakesurf boats (i.e., weight, hull shape, powertrain, and wake enhancement technologies) enables the creation of large wake waves under wakesurfing conditions.

**When comparing the boats under their typical operational conditions, which was Condition 2 for the non-wakesurf boats and Condition 1a for the wakesurf boats, our data documents substantially larger maximum wave height, total wave energy, and maximum wave power for the wakesurf boats (Figures 42-44).** At 100 ft of operational distance, the wakesurf boats measured maximum wave heights that were roughly 5-13 in higher than the non-wakesurf boats, an increase of 2-3 times. The total wave energy was 2,200-7,000 J/m higher (~3-9 times higher) for the wakesurf boats at 100 ft. The maximum wave power at 100 ft was also higher for the wakesurf boats by 230-570 J/m-s, a 6-12 fold increase.

**Operating the Malibu Wakesetters with full ballast tanks (Condition 1a) appeared to have an observable but smaller than expected impact on maximum wave height, total wave energy and maximum wave power at operational distances less than 100 ft (Figures 31-36).** At distances greater than 100 ft, the measured wake wave characteristic values did not seem to be affected by the addition of ballast water. These results were unexpected as we anticipated that the additional ballast water weight and resulting water displacement during travel would generate higher waves with greater total energy; however, this observation was similar for both boats. Clearly, the role of ballast water weight on asymmetric wake wave characteristics is an area where more research is needed.

**The aftermarket wake shaper had an observable impact on the wake wave characteristics of the Malibu Response LX, resulting in increased maximum wave height, total wave energy, and maximum wave power (Figure 37-39).** With the wake shaper attached and at an operational distance of 200 ft, the data show an approximate increase in maximum wave height of 2 in (33%), total wave energy of 270 J/m (20%), and maximum wave power of 30 J/m-s (20%).

**We demonstrate how data collected in this study can be used to inform operational distance for wakesurf boats/wakesufing based on reference conditions derived from non-wakesurf boats.** In the first example provided (Figures 45-47) the boats were compared under their typical operational conditions, which was Condition 2 (planing) for the non-wakesurf boats and Condition 1a (wakesurfing) for the wakesurf boats. In this scenario, operational distances greater than 500 ft were needed to attenuate the measured wake wave characteristics of the wakesurf boats to levels equivalent to the non-wakesurf boats at 200 ft (Table 5). In the second example (Figures 48-50), the boats were all compared under Condition 1a (i.e., largest possible wake/wakesurfing). Here, operational distances greater than 425 ft were needed to decrease wave height, energy, and power of the wakesurf boats to levels similar to the non-wakesurf boats at operational distances of 200 ft.

## 8.0 REFERENCES


Bilkovic, D., Mitchell, M., Davis, J., Andrews, E., King, A., Mason, P., Herman, J., Tahvildari, N., Davis, J., 2017) Review of boat wake wave impacts on shoreline erosion and potential solutions for the Chesapeake Bay. STAC Publication Number 17-002, Edgewater, MD. 68 pp.

Bilkovic, D., Mitchell, M., Davis, J., Herman, J., Andrews, E., King, A., Mason, P., Tahvildari, N., Davis, J., Dixon, R., (2019) Defining boat wake impacts on shoreline stability toward management and policy solutions, Ocean & Coastal Management, Volume 182,

Cox, G.L. (2020) Vessel wave wakes: new perspectives on their generation, propagation and shoreline impacts', PhD thesis, University of Tasmania.

Dingemans, M.W. (1997) Water Wave Propagation Over Uneven Bottoms: Linear wave propagation, Part 1. World Scientific, Technology & Engineering.

Glamore, W.C. (2008). A decision support tool for assessing the impact of boat wake waves on inland waterways. In *International Conference on Coastal and Port Engineering in Developing Countries. 20p.*

Glamore, W.C., Badenhop, A.M., Davey, E.K. (2013) A Decision Support System to Assess the Impact of Boat Wake Wash on Riverbank Erosion, Water Research Laboratory, Research Report 245, University of New South Wales.

Glamore, W.C., Badenhop, A.M., Davey, E.K. (2013) Boat Wake Wash Decision Support System User's Manual, Water Research Laboratory, Research Report 246, University of New South Wales.

Gourlay, T., (2010) Full-scale Boat Wake and Wind Wave Trials on the Swan River, Centre for Marine Science and Technology. Final Report.

Kelpšaite, L., Parnell, K.E., and Soomere, T. (2009) Energy pollution: the relative influence of wind-wave and vessel-wake energy in Tallinn Bay, the Baltic Sea, Journal of Coastal Research, Special Issue No. 56. Proceedings of the 10th International Coastal Symposium ICS 2009, Vol. I, pp. 812-816.

Kurennoy, D., Soomere T., and Parnell, K.E. (2009) Variability in the Properties of Wakes Generated by High-Speed Ferries, Journal of Coastal Research, Special Issue No. 56. Proceedings of the 10th International Coastal Symposium ICS 2009, Vol. I, pp. 519-523.

Lighthill, J., (1978) Waves in fluids, Cambridge University Press.

Malibu Boat (2020) How to Make a Perfect Wake or Wave with Power Wedge III, website: https://www.malibuboats.com/news/2018-news/power-wedge, accessed June 2021.

MacFarlane, G., and Cox, G. (2003a) The development of vessel wave wake criteria for the Noosa and Brisbane Rivers in Southeast Queensland, Coastal Environment V, incorporating Oil Spill Studies, C. A. Brebbia, J. M. Saval Perez & L. Garcia Andion (Editors) © 2004 WIT Press, www.witpress.com, ISBN 1-85312-710-8

MacFarlane, G., and Cox, G. (2003b) Vessel Wash Impacts on Bank Erosion - Noosa River and Brisbane River - FINAL REPORT NO. 01/G/18, Moreton Bay Waterways and Catchments Partnership.

MacFarlane, G., and Cox, G. (2005) Vessel Wash Impacts on Bank Erosion – Maroochy River, FINAL REPORT NO. 04/G/18, Moreton Bay Waterways and Catchments Partnership.

MacFarlane, G.J. (2012) Marine vessel wave wake: Focus on vessel operations within sheltered waterways, PhD thesis, University of Tasmania.

Madsen, P.A., Fuhrman, D.R. and Wang, B., (2006) A Boussinesq-type method for fully non-linear waves interacting with a rapidly varying bathymetry, Coastal Engineering, vol. 53, pp. 487-504.

Maynord, S.T., Biedenharn, D.S., Fischenich, C.J., Zufelt, J.E. (2008) Boat-Wave-Induced Bank Erosion on the Kenai River, Alaska, Engineer Research and Development Center, ERDC TR-08-5, Final Report.

Mercier-Blaise, S., and Praire, Y., (2014) Project evaluation of the impact of the waves created by the type of boats wakeboat on the shore of Lake Memphremagog and Lovering, Final Project report, Memphremagog Conservation Inc and Université du Québec à Montréal.

McConchie, J. and Toleman, I.E.J. (2003) Boat wakes as a cause of riverbank erosion: A case study from the Waikato River, New Zealand. Journal of Hydrology New Zealand. 42. 163-179.

MN Department of Natural Resources (2021) Lakes, Rivers, and Wetland Facts, website: https://www.dnr.state.mn.us/faq/mnfacts/water.html. Accessed June 2021.

Neumeier, U., (2020) Processing of wave data from pressure sensors. http://neumeier.perso.ch/. Accessed December 2020.

Parnell, K.E., McDonald, S.C., and Burke, A.E., (2007) Shoreline effects of vessel wakes, Marlborough Sounds, New Zealand, Journal of Coastal Research, Special Issue 50: International Coastal Symposium (ICS 2007), pp. 502-506.

Parnell,K., Delpeche, N., Didenkulova, I., Dolphin, T., Erm, A., Kask, A., Kelpšaite, L., Kurennoy, D., Quak, E., Räämet, A., Soomere, T., Terentjeva, A., Torsvik, T. and Zaitseva-Pärnaste, I., (2008) Far-field vessel wakes in Tallinn Bay, Estonian Journal of Engineering, 2008, 14, 4, 273–302.

Raymond, S., and Galvez-Cloutier, R., (2015) Impact of Lake Navigation - Sediment Suspension Study: Lake Masson and Sand Lake Cases, Laval University. 30p. (Published in French, English translation)

Ruprecht, J.E., Glamore,W.C., Coghlan, I.R., and Flocard, F. (2015) Wakesurfing: Some Wakes are More Equal than Others, Australasian Coasts & Ports Conference 201, pg 15 – 18, September 2015, Auckland, New Zealand.

Stoker, J.J. (1957) Water Waves, the Mathematical Theory with Applications. Interscience Publishers Inc., New York.

Stumbo S, Fox, K., Dvorak F., & Elliot, L. (1999) The prediction, measurement and analysis of wake wash from marine vessels. Marine technology and SNAME news. Vol 36, Issue 4, pg 248-260.

Thomson W. (1887) On Ship Waves. Proceedings of the Institution of Mechanical Engineers. 1887;38(1):409-434. doi:10.1243/PIME_PROC_1887_038_028_0

Tucker M.J. & Pitt E.G. (2001) Waves in ocean engineering. Elsevier ocean engineering book series vol. 5, Elsevier, Amsterdam, 521 p.

USACE (2012) Coastal Engineering Manual – Part II – Coastal Hydrodynamics, Manual of the United States Army Corps of Engineers. EM 1110-2-1100.

USACE (1984) Shore Protection Manual Volume 1 and 2, Coastal Engineering Research Center, United States Army Corps of Engineers.

USACE (1994) Cumulative Impacts of Recreational Boating on the Fox River – Chain O' Lakes Area in Lake and McHenry Counties, Illinois. Final environmental statement. Chicago: Environmental and Social Analysis Branch, US Army Corps of Engineers.

Zabawa, C., and Ostrom, C. (editors) (1980) The role of boat wakes in shoreline erosion in Anne Arundel County, Maryland, Coastal Resources Division, Maryland Department of Natural Resources.